Earlier Phenology Associated With Spring Warming Will Help Offset Some of the Negative Impacts of Climate Change on Temperate Tree Seedling Recruitment

by

Benjamin Lee

A dissertation submitted in partial fulfillment
of the requirements for the degree of
Doctor of Philosophy
(Environment and Sustainability)
in the University of Michigan
2020

Doctoral Committee:

Associate Professor Inés Ibáñez, Chair
Professor William Currie
Professor Deborah Goldberg
Professor Donald Zak

Benjamin Lee

benrlee@umich.edu

ORCID iD: 0000-0002-5256-0515

Dedication

This dissertation is dedicated to all the seedlings that died to get me to where I am today.

Acknowledgements

This dissertation represents the culmination of six years of work that would have been impossible without the generosity, guidance, and friendship of so many people that I am deeply indebted to. First I would like to thank the current and past members of the Global Change Ecology Lab and the Plant Ecology Discussion Group for the incredible amount of feedback and support that helped me develop these ideas and experiments: Dan Katz, Ben Connor Barrie, Teegan McClung, Natalie Tonn, Kate Chapel, Chris Karounos, Kirk Acharya, Sam Schaeffer-Morrison, Caleb McCollum, Laís Petri, Deborah Goldberg, Chau Ho, Wes Bickford, John Guittar, Natalia Umáña, Monique Weemstra, and many others. Thank you to Leslie Decker for your friendship, advice, and occasional commiseration. I also want to acknowledge the staff at Li-COR Biosciences and John Sperry and his research lab at the University of Utah for teaching me how to measure gas exchange with my trusty 6400 and how to measure xylem conductivity. Thank you to Drew Peltier for your help in building and interpreting the photosynthesis model and for leaving me guidance and advice on how to use the IRGAs. Thank you to my field assistants, especially Caleb Fogel who helped me plant the hundreds of seedlings at the start of this experiment. Thank you to the greenhouse staff and volunteers at the Matthaei Botanical, most especially Mike Palmer without whom I would not have been able to complete my greenhouse experiment. Thank you to Sucila Fernandes for your help navigating the forests where I did my experiments and thank you to the staff at SNRE/SEAS for helping me keep track of all of the minutiae that goes into making experiments run successfully. Thank you to Don Zak for letting me use the equipment needed to complete this research (everything ranging from the

IRGA to the spectrophotometer) and thank you to Rima Upchurch for the lab support and guidance you generously provided that made the NSC extractions possible. Thank you to my family for the support they gave me and thank you to all the friends I made along the way, these six years would have been a lot longer without you. I particularly want to thank Elissa Mueller – your love and support helped me push through some of the toughest parts of this dissertation with a smile on my face. Lastly and most importantly, thank you to Inés Ibáñez. Your guidance, patience, and generosity have helped me develop the skills and passion that I have as a scientist, and I credit the immense amount of modeling that went into this dissertation to your advice and expertise.

This work was made possible primarily thanks to funding from the National Science Foundation (DEB 1252664). Additional funding was provided by the Shrank Summer Research Support Fund and by the Winifred B. Chase Fellowship.

Table of Contents

List of Tables

List of Figures

Abstract

The warming temperatures and increased drought predicted to occur over the course of the next century have the potential to profoundly impact the composition and structure of global plant communities. Because of the relevance of forest ecosystems in storing a large amount of the planet's carbon and thus in regulating the earth's climate, there is a major effort to forecast forest composition, structure, and functioning. Accurate predictions will require the application of studies that identify how climate drivers (and interactions between multiple drivers) affect physiological processes that underlie patterns of demography and assembly. In forest systems, community composition is strongly shaped by bottleneck effects that occur during recruitment at small size classes, size classes that are highly vulnerable to climate change. In this dissertation, I investigated how climate change will affect the seedling demography of two temperate tree species that commonly co-occur across eastern North America: *Acer saccharum* (sugar maple) and *Quercus rubra* (northern red oak). In chapter 2 I investigated how potential climate-driven shifts in seedling foliar phenology (in relation to shifts in canopy phenology) could affect the ability of seedlings to maintain positive net carbon assimilation over the growing season, a dynamic that is commonly referred to as phenological escape. I also modeled how environmental conditions drive photosynthetic rates and used that information to estimate the relative proportion of carbon that is assimilated in different seasons. In my third chapter I used the same photosynthesis models to estimate annual carbon assimilation for individual tree seedlings and then modeled the relationship between carbon assimilation and demographic performance (growth and survival). I used results from both chapters to project how climate change in my

study region could affect seedling demography directly (e.g., via changes in respiration rates associated with higher temperatures) and indirectly (e.g., via changes in access to light caused by different phenology shifts between seedlings and the canopy). In my last chapter I used a greenhouse study to investigate how seedlings of these two species respond to drought, specifically looking for differences in stomatal regulation of leaf water potential, reductions in photosynthetic capacity, reduction of non-structural carbohydrates, and loss of hydraulic conductivity.

My results suggest that climate change will primarily affect seedling recruitment via changes in annual carbon assimilation. Although I found evidence that seedlings are likely to gain access to light with warming spring temperatures (thereby increasing net carbon assimilation in spring), elevated leaf respiration rates in hotter and drier summers would outweigh these gains and lead to net reductions in annual assimilation. In turn, these reductions would reduce seedling demographic performance and lead to less growth and higher mortality rates. Access to water could affect plant performance via reductions in photosynthetic rates, but seedlings of both species are also highly vulnerable to hydraulic failure during severe drought events. In sum, my results indicate that seedlings of both species may experience steep reductions in performance under extreme climate change, but that phenological escape dynamics may be enough to compensate for these reductions under more conservative climate change scenarios.

Chapter 1 Introduction

Climate change is expected to affect the composition, structure, and health of plant communities across the world, including temperate forests, my study system. Globally, temperate forests cover 767 million hectares and account for ~29.9% of the world's carbon storage, accounting for 0.72 Pg C $year^{-1}$ (Pan et al. 2011), roughly equivalent to the CO_2 produced from the combustion of 81 billion gallons of gasoline[1]. Therefore, it is imperative that scientists understand the processes and mechanisms that underlie plant responses to environmental change and how these may shift within the context of global climate change.

One of the most effective ways to predict the structure and function of future forests is by measuring the demographic performance of tree seedlings under varying climate conditions. Tree seedlings are more likely than adult trees to experience directional mortality (Green et al. 2014), because of limited storage tissue and an inability to access critical resources (e.g., water via deep taproots or light via high canopies). Therefore, mortality that occurs during the seedling stage acts as a bottleneck that determines which species will eventually make it into the forest canopy (Harper 1977, Grubb 1977). Understanding recruitment dynamics and their relation to climate drivers will allow scientists to make more accurate predictions of likely dynamics and will allow forest managers to make more informed decisions to prepare for the future.

[1]https://www.epa.gov/energy/greenhouse-gases-equivalencies-calculator-calculations-and-references

Demographic performance of tree seedlings is affected by a combination of resource availability, biotic interactions, and interactions between the two, and one of the most important limiting resources for seedlings in temperate forests is light availability (Canham 1988). Light levels under closed tree canopies (i.e., once canopy trees have fully expanded their leaves) can be 2-3 orders of magnitude lower than in open canopy conditions (see Chapter 2) and are often insufficient to fulfill seedling carbon demands via photosynthesis. Although the role of canopy gaps in tree recruitment is well-established in the scientific literature (Canham 1988, Popma and Bongers 1988), tree seedlings must also be able to establish and survive in full shade conditions long enough to take advantage of gaps once they open.

To do so, seedlings of many temperate tree species make use of a strategy known as phenological escape (Jacques et al., 2015), where they expand their leaves in spring up to several weeks before the canopy closes in order to make use of high light availability (Augspurger 2008). Tree seedlings have been shown to assimilate ~80% of their net annual carbon budget during this period (Kwit et al. 2010), which is consistent with other studies which measured the contribution of early spring photosynthesis for herbaceous spring wildflower species (Heberling et al. 2019a, Heberling et al. 2019b). Furthermore, there is strong support in the literature for the relationship between plant carbon status and demographic performance (e.g., growth, fecundity, and survival; (Hlásny et al. 2011, Hoch et al. 2013, Lusk and Del Pozo 2002, Piper et al. 2009), so it is likely seedlings that leaf late in spring will experience reductions in performance associated with reduced access to high light availability during this critical period.

If this is true, climate change is likely to play an important role in determining demographic outcomes. Warmer springs have been extensively linked to earlier spring leaf-out phenology in temperate biomes (Piao et al. 2019), and there is evidence that the magnitude of

these shifts vary widely by species (Cleland et al. 2007), guild (Heberling et al. 2019b), and ontogeny (Cavender-Barres and Bazzaz 2000). For example, if tree seedling leaf-out is more sensitive to climate than canopy leaf-out is (i.e., if seedlings experience relatively earlier phenology in response to the same climate cues), the duration of high light access in spring would increase in the future. This would lead to greater spring carbon assimilation and, consequently, increased seedling demographic performance and recruitment. However, the opposite would also be true if seedling phenology is less sensitive to climate change compared to canopy tree phenology, as has been found for temperate wildflowers (Heberling et al. 2019a). Furthermore, the response of seedling leaf-out phenology to climate change may depend on species, which would result in increased performance for species that track climate and reduced performance for those that do not.

Although important, changes in spring carbon assimilation will only determine part of a seedling's annual carbon budget. Temperate forests in the U.S. Great Lakes region, my study region, are expected to experience increased growing season temperatures and more frequent drought events (particularly in summer) due to regional climate change (Handler et al. 2014) which could affect recruitment separately from changes in phenology. Hotter summers will lead to reductions in net carbon assimilation via increased respiration, which is more sensitive to temperature than photosynthesis (Caemmerer 2000), though this may be offset by increases in atmospheric CO_2 concentration or by plant acclimation to high temperatures (Larigauderie and Körner 1995, Smith and Dukes 2012). Drought associated with climate change could likewise affect seedling carbon assimilation and demography even if precipitation increases (as it is predicted to do in spring; Handler et al. 2014). Plant water availability has been shown to

decrease at high temperatures due to elevated evapotranspiration rates and increases in precipitation may not compensate for it (Sherwood and Fu 2014).

Plant drought tolerance is often characterized along a gradient of iso/anisohydry (McDowell et al. 2008), with drought-tolerant anisohydric species at one end and drought-intolerant isohydric species at the other. Species are sorted along this gradient by their stomatal response to drought. Isohydric ("same-water") species close their stomata during drought, reducing water lost to atmospheric evaporation and maintaining interior water pressures. This allows this group to limit the occurrence of xylem cavitation and damage to the water column, but it also prevents them from taking CO_2 into the plant, thereby limiting or stopping photosynthetic carbon assimilation. Anisohydric species keep their stomata open during drought events, allowing them to maintain photosynthetic rates but exposing them to increased risk of cavitation. Isohydric plants are more vulnerable to dying during long droughts from carbon starvation (i.e., when the plant exhausts labile carbon storage pools and is no longer able to maintain basic metabolic rates; Sala et al. 2010, Sala et al. 2012). Anisohydric plants are more vulnerable to dying from hydraulic failure during extreme droughts when catastrophic embolism cuts off water supply to aboveground tissues (Sperry et al. 2002).

Adults of temperate tree species vary widely along this gradient (Adams et al. 2017), but it is unclear whether tree seedlings follow the same categorization. For example, Cavender-Bares and Bazzaz (2000) found that *Quercus rubra* seedlings showed a more isohydric response to drought even though adults of that species fall on the anisohydric end of the gradient. This difference is likely partially due to seedlings' relative inability to access deep water resources, for which maintaining photosynthetic capacity would be better suited. The lack of light in the forest understory is also a potential factor, as shaded seedlings may be unable to photosynthesize

even with ample water availability (Piper and Fajardo 2016), making an isohydric response less costly overall. If seedlings tend toward isohydric responses to drought, a reduction in water availability could compound on the negative effects of shade and result in lower performance than would otherwise be expected.

Taken together, all of this suggests that accurate projections of seedling demographic performance under climate change will require the integration and synthesis of information pertaining to multiple ecological and ecophysiological processes. In this dissertation, I combine results from a field experiment and a glasshouse study to investigate how climate affects seedling phenology in relation to changes in canopy phenology, photosynthetic carbon assimilation in seedlings, drought response, and demography. I then use that information to forecast demographic performance for tree seedlings by combining it with climate change scenarios predicted for the Great Lakes region, where my study is based.

The climate change scenarios that I used in my predictions are based off projections made for the Great Lakes region by Handler et al. (2014), which are summarized in Table SI 2.2 in Chapter 2. The scenarios incorporate changes to average climate conditions predicted to occur by the end of the century, consistent with the Parallel Climate Model B1 (PCM B1; Washington et al. 2000) and Geophysical Fluid Dynamics Laboratory A1FI (GFDL A1FI; Delworth et al. 2005) climate change projections that are commonly used in ecological forecasting (IPCC, 2014). PCM B1 was developed to represent what future climate conditions might look like assuming the significant conservation and reduction of global CO_2 emissions and GFDL A1FI predicts the 'business-as-usual' climate conditions where emissions trends are assumed to continue into the future. We chose to use these two scenarios in particular because they bracket the scenarios used

by the Intergovernmental Panel on Climate Change and therefore represent a realistic range of possible climate conditions at the end of the century.

Phenological escape of temperate tree seedlings

The period of time between when understory plants leaf out and when temperate forest canopies close is critically important for the performance of understory plant species. Previous research has shown that plants ranging from herbaceous perennial wildflowers to deciduous tree seedlings rely on this window of high light availability to assimilate between 50-100% of their annual carbon budget (Kwit et al. 2010, Heberling et al. 2019a). Additionally, annual carbon assimilation has been linked to plant demographic performance metrics such as growth (Korol et al. 1991, Hlásny et al. 2011), fruiting (Hoch et al. 2013), and survival (Lusk and Del Pozo 2002, Piper et al. 2009), suggesting that changes to spring light availability will greatly affect the performance of understory plants in deciduous forests. The duration of this period depends on the relative phenology of both understory and canopy plants, and recent findings suggest that access to spring light may be changing for some species due to differences in climate change sensitivity relative to the canopy (Heberling et al. 2019b). However, this area of research has been understudied, particularly with respect to phenological escape of woody plant species.

In **Chapter 2**, I used a field experiment to investigate the climate drivers of phenological escape dynamics for seedlings of two temperate tree species commonly found co-occurring across eastern North America. Contrary to recent work investigating this dynamic in wildflowers (Heberling et al. 2019b), I found that seedling leaf-out in spring for both species was more sensitive to climate change than the timing of canopy closure was, suggesting that seedlings will gain access to light in spring in the future. I used gas exchange measurements to quantify

seasonal carbon assimilation for both species and to estimate the change in carbon associated with the projected increase in light in spring and the projected increases in temperature and reductions in precipitation in summer, relative to current climate conditions. My results suggest that years with greater spring light availability will lead to greater assimilation rates in spring for seedlings of both species, but that this increase will be offset by increased respiration rates in summer, especially under the extreme climate change scenario forecasted for the study region.

Climate change effects on seedling growth and survival

Phenological escape has been indirectly linked to understory plant survival, growth, and allocation to reproduction (Routhier and Lapointe 2002, Seiwa 2003, Augspurger 2008), and directly linked to the carbon assimilation of tree seedlings (Kwit et al. 2010) and herbaceous spring wildflowers (Heberling et al. 2019b). However, to the best of my knowledge, no study has yet combined these approaches to quantify how changes in spring phenology mechanistically affect understory plant demographic performance. In **Chapter 3,** I used the modeling approach developed in my second chapter to estimate annual carbon assimilation for individual seedlings in my field experiment and then modeled the relationship between carbon assimilation and seedling performance (growth and survival). I then used the same climate change scenarios described above to predict future demographic performance for seedlings of my two target species.

I found statistically significant relationships between annual carbon assimilation and demographic performance for both species (growth and survival for *Acer saccharum* and survival for *Quercus rubra*). The predicted decreases in carbon assimilation suggest that climate change will result in substantial decreases in performance of both species if global carbon

emissions are not reduced. Importantly, despite the overall reduction in annual carbon assimilation predicted in Chapter 2, the increases in spring carbon assimilation associated with phenological escape dynamics will allow both species to have better demographic performance than would otherwise be expected (Prasad et al. 2014).

Seedling physiological response to drought

Much of the forest drought response literature focuses on arid systems such as the Mediterranean or the American southwest where droughts are frequent and where many tree species are already near their physiological limits (Allen et al. 2015). Still, many other regions and biomes are expected to experience changes in precipitation patterns and increases in evapotranspiration that will result in prolonged, intensified, or more frequent drought (Dai 2011, Sherwood and Fu 2014). This includes the U.S. Great Lakes region where climate change is expected to result in increases Spring precipitation, but paradoxical increases in drought events during the summer due to both lower summer precipitation and increased temperature (Handler et al. 2014).

In **Chapter 4** I used a glasshouse dry-down experiment to quantify drought response for seedlings of the same two species I investigated in Chapters 2 and 3. Drought can affect tree seedling recruitment directly via hydraulic failure (i.e., catastrophic embolism of xylem) or indirectly via reduced photosynthetic capacity associated with isohydric stomatal behavior and subsequent carbon starvation (McDowell et al. 2008). I measured the effects of drought and shade (which can both exacerbate carbon starvation and ameliorate the effect of high temperature) on three metrics related to drought tolerance: nonstructural carbohydrate concentrations ([NSC]), photosynthetic capacity, and xylem conductivity. Despite adults of my

two study species being classified differently along the isohydric/anisohydric gradient (*A. saccharum* is considered isohydric while *Q. rubra* is anisohydric), seedlings of both species showed very similar responses to reduced water availability. Seedlings exhibited decreases in [NSC] and reductions in photosynthetic capacity characteristic of isohydric stomatal regulation. Isohydry was also supported by the relatively conservative internal water pressures maintained by both species (> -1 MPa), although there were a few instances where *Q. rubra* seedlings were able to withstand more negative pressures, suggesting they may have a slightly greater inclination for anisohydric behavior.

Tree recruitment under future climate change

The role of climate change in shaping future forests is complicated and nuanced, a fact that has been emphasized recently by studies showing that climate change responses are often non-linear and depend on combinations of climate drivers that have no present analog (Jackson and Williams 2005, Wolkovich et al. 2012). One solution for this problem is to prioritize studies that investigate the roles of multiple climate drivers on the physiological mechanisms that underlie the ecological phenomena of interest. In this dissertation I used such an approach to link shifts in phenology to tree seedling performance via changes in seasonal and annual carbon assimilation. As I conclude in **Chapter 5**, despite increases in early spring light availability and consequent increases in spring carbon assimilation, scenarios forecasting hotter and drier summers could result in elevated respiration costs for temperate tree seedlings that result in reduced performance projected under climate change if global CO_2 emissions are not reduced. Still, the increase in spring carbon assimilation results in higher projected performance than

would otherwise be expected, suggesting that phenological escape dynamics will play an important role in determining future forest communities.

REFERENCES

Adams, H. A., M. J. B. Zeppel, W. R. Anderegg, and 59 other authors. 2017. A multi-species synthesis of physiological mechanisms in drought-induced tree mortality. *Nature Ecology & Evolution*, 1: 1285-1291. https://doi.org/10.1038/s41559-017-0248-x

Allen, C. D., D. D. Breshears, and N. G. McDowell. 2015. On underestimation of global vulnerability to tree mortality and forest die-off from hotter drought in the Anthropocene. *Ecosphere*, 6: 1-55. https://doi.org/10.1890/ES15-00203.1

Augspurger, C. K. 2008. Early spring leaf out enhances growth and survival of saplings in a temperate deciduous forest. *Oecologia* 156: 281-286. http://doi.org/10.1007/s00442-008-1000-7

Caemmerer, S. 2000. Biochemical models of leaf photosynthesis. Techniques in Plant Sciences, 2. CSIRO Publishing, Collingwood, VIC, Australia.

Canham, C. D. 1988. Growth and canopy architecture of shade-tolerant trees: Response to canopy gaps. *Ecology*, 69: 786-795. https://doi.org/10.2307/1941027

Cavender-Bares, J., & Bazzaz, F. A. 2000. Changes in drought response strategies with ontogeny in *Quercus rubra*: Implications for scaling from seedlings to mature trees. *Oecologia, 124,* 8-18. https://doi.org/10.1007/PL00008865

Cleland, E. E., I. Chuine, A. Menzel, H. A. Mooney, and M. D. Schwartz. 2007. Shifting plant phenology in response to global change. *Trends in Ecology & Evolution*, 22: 357-365. https://doi.org/10.1016/j.tree.2007.04.003

Dai, A. 2011. Drought under global warming: A review. *WIREs Climate Change*, 2: 45-65. https://doi.org/10.1002/wcc.81

Delworth, T. L., A. J. Broccoli, A. Rosati, R. J. Stouffer, et al. 2006. GFDL's CM2 global coupled climate models Part 1 formulation and simulation characteristics. *Journal of Climate*, 19: 643-674. https://doi.org/10.1175/JCLI3629.1

Green, P. T., K. E. Harms, and J. H. Connell. 2014. Nonrandom, diversifying processes are disproportionately strong in the smallest size classes of a tropical forest. Proceedings of the National Academy of Sciences 111: 18649-18654. https://doi.org/10.1073/pnas.1321892112

Grubb, P. J. 1977. The maintenance of species-richness in plant communities: The importance of the regeneration niche. *Biological Reviews*, 52: 107-145. https://doi.org/10.1111/j.1469-185X.1977.tb01347.x

Handler, S., M. J. Duveneck, L. Iverson, and 42 other authors. 2014. Michigan forest ecosystem vulnerability assessment and synthesis: A report from the Northwoods Climate Change Response Framework. US Department of Agriculture, Forest Service, Northern Research Station, General Technical Report NRS-129, Newtown Square, PA. https://doi.org/10.2737/NRS-GTR-129

Harper, J. L. 1977. Population Biology of Plants. Academic Press. London, UK. ISBN 13: 9780123258502

Heberling, J. M., Cassidy, S. T., Fridley, J. D., & Kalisz, S. 2019a. Carbon gain phenologies of spring-flowering perennials in a deciduous forest indicate a novel niche for a widespread invader. *New Phytologist*, 221: 778-788. https://doi.org/10.1111/nph.15404

Heberling, J. M., McDonough MacKenzie, C., Fridley, J. D., Kalisz, S., & Primack, R. B. 2019b. Phenological mismatch with trees reduces wildflower carbon budgets. *Ecology Letters,* 22*:* 616-623. https://doi.org/10.1111/ele.13224

Hlásny, T., Z. Barcza, M. Fabrika, B. Balázs, G. Churkina, J. Pajtík, R. Sedmák, and M. Turˇáni. 2011. Climate change impacts on growth and carbon balance of forests in Central Europe. *Climate Research*, 47: 219-236. https://doi.org/10.3354/cr01024

Hoch, G., R. T. W. Siegwold, S. G. Keel, C. Körner, and Q. Han. 2013. Fruit production in three masting tree species does not rely on stored carbon reserves. *Oecologia,* 171: 653-662. https://doi.org/10.1007/s00442-012-2579-2

IPCC, 2014: Climate Change 2014: Synthesis Report. Contribution of Working Groups I, II and III to the Fifth Assessment Report of the Intergovernmental Panel on Climate Change [Core Writing Team, R.K. Pachauri and L.A. Meyer (eds.)]. IPCC, Geneva, Switzerland, 151 pp.

Jackson, S. T. and J. W. Williams. 2004. Modern analogs in quaternary paleoecology: Here today, gone yesterday, gone tomorrow? *Annual Review of Earth and Planetary Sciences,* 32: 495-537. https://doi.org/10.1146/annurev.earth.32.101802.120435

Jacques, M. -H., Lapointe, L., Rice, K., Montgomery, R. A., Stefanski, A., & Reich, P. B. 2015. Responses of two understory herbs, *Maianthemum canadense* and *Eurybia macrophylla*, to experimental forest warming: Early emergence is the key to enhanced reproductive output. *American Journal of Botany*, *102*, 1610-1624. https://doi.org/10.3732/ajb.1500046

Korol, R. L., S. W. Running, K. S. Milner, and E. R. Hunt, Jr. 1991. Testing a mechanistic carbon balance model against observed tree growth. *Canadian Journal of Forest Research*, 21: 1098-1105. https://doi.org/10.1139/x91-151

Kwit, M. C., L. S. Rigg, and D. Goldblum. 2010. Sugar maple seedling carbon assimilation at the northern limit of its range: The importance of seasonal light. *Canadian Journal of Forest Research,* 40: 385-393. https://doi.org/10.1139/X09-196

Lusk, C. H. and A. Del Pozo. 2008. Survival and growth of seedlings of 12 Chilean rainforest trees in two light environments: Gas exchange and biomass distribution correlates. *Austral Ecology*, 27: 173-182. https://doi.org/10.1046/j.1442-9993.2002.01168.x

Larigauderie, A. and C. Körner. 1995. Acclimation of leaf dark respiration to temperature in alpine and lowland plant species. *Annals of Botany*, 76: 245-252. https://doi.org/10.1006/anbo.1995.1093

McDowell, N., Pockman, W. T., Allen, C. D., Breshears, D. D., Cobb, N., Kolb, T., Plaut, J., Sperry, J., West, A., Williams, D. G., & Yepez, E. A. 2008. Mechanisms of plant survival and mortality during drought: Why do some plants survive while others succumb to drought? *New Phytologist, 178,* 719-739. https://doi.org/10.1111/j.1469-8137.2008.02436.x

Pan, Y., R. A. Birdsey, J. Fang, and 15 other authors. 2011. A large and persistent carbon sink in the world's forests. *Science*, 333: 988-993. https://doi.org/10.1126/science.1201609

Piao, S., Q. Liu, A. Chen, I. A. Janssens, Y. Fu, J. Dai, L. Liu, X. Lian, M. Shen, and X. Zhu. 2019. Plant phenology and global climate change: Current progresses and challenges. *Global Change Biology*, 25: 1922-1940. https://doi.org/10.1111/gcb/14619

Piper, F. I., M. Reyes-Díaz, L. J. Corcuera, and C. H. Lusk. 2009. Carbohydrate storage, survival, and growth of two evergreen *Nothofagus* species in two contrasting light environments. *Ecological Research*, 24: 1233-1241. https://doi.org/10.1007/s11284-009-0606-5

Piper, F. I., and A. Fajardo. 2016. Carbon dynamics of *Acer pseudoplatanus* seedlings under drought and complete darkness. *Tree Physiology*, 36: 1400-1408. https://doi.org/10.1093/treephys/tpw063

Popma, J. and F. Bongers. 1988. The effect of canopy gaps on growth and morphology of seedlings of rain forest species. *Oecologia*, 75: 625-632. https://doi.org/10.1007/BF00776429

Prasad, A. M., L. R. Iverson, M. P. Peters, and S. N. Matthews. 2014. Climate change tree atlas. Northern Research Station, U.S. Forest Service, Delaware, OH. http://www.nrs.fs.fed.us/atlas

Routhier, M. -C. and L. Lapointe. 2002. Impact of tree leaf phenology on growth rates and reproduction in the spring flowering species *Trillium erectum* (Liliaceae). *American Journal of Botany*, *89*, 500-505. https://doi.org/10.3732/ajb.89.3.500

Sala, A., Piper, F. I., & Hoch, G. 2010. Physiological mechanisms of drought-induced tree mortality are far from being resolved. *New Phytologist, 186,* 274-281. https://doi.org/10.1111/j.1469-8137.2009.03167.x

Sala, A., D. R. Woodruff, and F. C. Meinzer. 2012. Carbon dynamics in trees: Feast or famine? *Tree Physiology*, 32: 764-775. https://doi.org/10.1093/treephys/tpr143

Seiwa, K. 2003. Advantages of early germination for growth and survival of seedlings of *Acer mono* under different overstorey phenologies in deciduous broad-leaved forests. *Journal of Ecology, 86,* 219-228. https://doi.org/10.1046/j.1365-2745.1998.00245.x

Sherwood, S. and Q. Fu. 2014. A drier future? *Science*, 343: 737-739. https://doi.org/10.1126/science.1247620

Smith, N. G. and J. S. Dukes. 2012. Plant respiration and photosynthesis in global-scale models: Incorporating acclimation to temperature and CO_2. *Global Change Biology*, 19: 45-63. https://doi.org/10.1111/j.1365-2486.2012.02797.x

Sperry, J. S., U. G. Hacke, R. Oren, and J. P. Comstock. 2002. Water deficits and hydraulic limits to leaf water supply. *Plant, Cell & Environment*, 25: 251-263. https://doi.org/10.1046/j.0016-8025.2001.00799.x

Washington, W. M., J. W. Weatherly, G. A. Meehl, A. J. Semtner Jr., and 7 other authors. 2000. Parallel climate model (PCM) control and transient simulations. *Climate Dynamics*, 16: 755-74. https://doi.org/10.1007/s003820000079

Wolkovich, E. M., Cook, B. I., Allen, J. M., Crimmins, T. M., Betancourt, J. L., Travers, S. E., Pau, S., Regetz, J., Davies, T. J., Kraft, N. J. B., Ault, T. R., Bolmgren, K., Mazer, S. J., McCabe, G. J., McGill, B. J., Parmesan, C., Salamin, N., Schwartz, M. D., & Cleland, E. E. 2012. Warming experiments underpredict plant phenological responses to climate change. *Nature, 485,* 494-497. https://doi.org/10.1038/nature11014

Chapter 2 Tree Seedling Carbon Accumulation

ABSTRACT

Climate change is projected to impact plant performance in several ways. On one hand, warmer springs will increase the length of the growing season; on the other hand, warmer and drier summers will likely have a negative impact on plant carbon assimilation. In forests, understory plants heavily rely on high light availability early in spring for their annual carbon budget, thus it is important that their growing season is extended at the same rate or faster than that of the canopy. At the same time, although warmer temperatures could result in increased photosynthetic assimilation, they would also disproportionately increase plant respiration. This is especially true in summer when respiration costs are highest, and so it will be important that increases in summer respiration do not offset increases in spring assimilation.

In this study, we assessed the interactive impact of earlier springs and warmer summers on seedling performance of two dominant eastern North American tree species, *Acer saccharum* and *Quercus rubra*. We used photosynthetic parameters obtained from *in situ* gas exchange measurements to predict if the combined changes in spring phenology and summer temperature will result in significant shifts in seedling net annual carbon accumulation. Our results indicate that seedling leaf out is more sensitive to warming than the canopy and that seedlings will therefore gain access to light in spring, thereby increasing the amount of gross annual assimilated carbon by 39 to 50%. However, our results also indicate that this increase in gross assimilation will be largely offset by 71 to 124% increases in gross annual respiration costs due to higher temperatures. Finally, we found these responses were context dependent, with seedlings having

higher performance when planted under *A. saccharum* adult trees than when planted under *Q. rubra* adult trees. We simulated carbon budgets under climatic scenarios to assess future recruitment of these species. Overall, seedling carbon budgets are projected to decrease, and in some cases, especially under *Q. rubra* canopies, seedlings are not likely to sustain a positive carbon budget. This mechanistic approach of assessing future tree recruitment under climate change provided valuable insight into future tree demographic dynamics.

INTRODUCTION

With the onset of global warming, plant species are undergoing a variety of physiological changes triggered by their new environment. Plants in temperate forests are experiencing longer growing seasons due to warmer spring and fall seasons (Menzel and Fabian 1999, Chuine and Beaubien 2001, Chuine 2010, Fu et al. 2014, Piao et al. 2019), but also reduced photosynthetic performance due to hotter and drier summers (McDowell et al. 2008, Elliott et al. 2015). However, despite their potential impact, the synergistic consequences of changes in light and water availability on plant performance have rarely been quantified (but see Sack 2004, Niinemets 2010), thereby leaving an important gap in our ability to understand and anticipate plant performance within multiple climatic contexts.

Shifts in plant phenology have been one of the most widely reported responses of organisms to current climate change (Ibáñez et al. 2010, Menzel and Fabian 1999, Piao et al. 2019). However, few studies have addressed the implications that such phenological trends might have on individuals and the resulting implications for their populations and communities (but see Visser et al. 1998, Visser and Holleman 2001, Heberling et al. 2019). Climate change has led to a global advancement in the onset of spring in temperate biomes (Root et al. 2003,

Piao et al. 2019) and canopies are developing sooner (Richardson et al. 2006, Keenan et al. 2014), but it is unknown whether seedling phenology is adjusting at the same rate (Wolkovich et al. 2012, Heberling et al. 2019). Little is currently known about the biochemical pathways that link climatic drivers to plant phenology, and so it is difficult to identify a mechanism that fully explains the differences in phenology observed across ontogenetic stages. Still, such changes could occur as a result of differences in climatic cues (e.g., air temperature versus temperature buffered by snow (Chen et al. 2015), which would differently affect the development of foliar buds in canopy trees and seedlings, respectively) or potentially via differential gene expression (Wilczek et al. 2010).

In the case of temperate forest ecosystems, seedlings of deciduous trees experience leaf-out several days before their adult counterparts and some have been shown to rely on that period of high light availability before the canopy develops to fix most of that year's carbon (Kwit et al. 2010). If phenological shifts differ among species, and the time between seedling and canopy leaf-out increases for some but decreases for others (Fig. 2.1a), competitive abilities could shift and consequently alter species' relative performance (survival and growth). These changes could eventually affect the structure, diversity, and functioning of the future ecosystem (Green et al. 2014, Umaña et al. 2016).

Shifts in fall foliar phenology (i.e. the timing of leaf coloring and leaf senescence) will also alter the length of the growing season. Although less studied, it has also been suggested to play a significant role in determining net carbon budgets for deciduous plants in temperate systems (Gill et al. 1998, Fridley 2012). Seedlings of many temperate tree species retain their leaves until after the canopy has reopened in order to make use of a second peak in understory light availability (Gill et al. 1998, Augspurger 2008, Kwit et al. 2010). Autumn canopy

reopening (i.e., canopy leaf senescence) is projected to shift later with warming (Piao et al. 2019), and it is possible that seedling leaf senescence may shift at a different rate than the canopy, leading to a dynamic similar to the one in spring. Therefore, it is important that studies addressing the annual carbon budgets of understory plants take into account both leaf-expansion in spring and leaf senescence in fall.

Global warming is also likely to impact growing conditions (Pryor et al. 2014), and potentially affect photosynthetic activity of coexisting species differently (Oren et al. 1999). Net photosynthetic rates (Fig. 2.1b) are the sum of carbon gained from assimilation rates, which can be limited by water, light, and access to CO_2, and carbon lost from respiration, which is exacerbated by high temperatures. Annual carbon accumulation (also referred to as carbon budget or carbon balance) integrates net photosynthesis over the course of the growing season. Photosynthetic and respiration rates differ by species (Patrick et al. 2009), time (Baurle et al. 2012), and local climate environment (Peltier and Ibáñez 2015), but they are also strongly affected by how a plant responds to drought (Elliott et al. 2015, Marchin et al. 2015, Fahey 2016). Many drought-intolerant species follow an isohydric response to drought: they close their stomata to restrict water loss, which simultaneously restricts photosynthetic activity. After extended drought conditions, these plants may experience reduced photosynthetic performance, and even death, due to carbon starvation (i.e., depletion of the plant's carbon balance; McDowell and Sevanto 2010). In contrast, many drought-tolerant species are classified as anisohydric, meaning they keep stomata open during drought, maintain photosynthetic rates and growth, but increase their risk of death via hydraulic failure during intense droughts (McDowell et al. 2008).

Summers are projected to become drier in many forest ecosystems, and vegetation forecasts subsequently predict an increase in drought-tolerant anisohydric species (Gustafson and

Sturtevant 2013). However, such studies largely ignore the potential for temperate plants to offset the increased carbon costs associated with summer drought and warming by increasing their access to high light availability (and therefore increasing carbon assimilation) at either end of the growing season. Although drought-tolerant species are likely to outperform intolerant species in the long term, seedling performance over years to decades will depend on the combined response to both earlier spring growth and summer drought, and of that we know little (Sack and Grubb 2002, Sack 2004, Niinemets 2010, Hartmann 2011). For instance, increased spring light availability may mitigate the effects of summer shade- and drought-induced carbon starvation in seedlings of isohydric species.

These species are already photosynthetically limited by water in the summer and so drier summers might not have a large impact in their carbon budgets. Concurrently, changes in spring light availability may not affect late-leafing seedlings of anisohydric species, but, even if they are drought-tolerant, drier summers would likely have a negative effect on their growth as they are photosynthetically active during the whole growing season. These scenarios, although plausible, contradict most predictions made of forest responses to global warming. Thus, a considerable knowledge gap must be filled as to how these varying responses to climate change interact to affect overall plant carbon assimilation and performance.

To gain a better understanding of how the multifaceted effects of climate change may affect seedling performance under projected scenarios, we measured foliar phenology and growing season photosynthesis in seedlings of two temperate tree species with contrasting spring phenologies and hydraulic strategies. We asked the following questions: 1) Could warming temperatures lead to tree seedlings increasing, maintaining, or losing access to light in spring and fall? 2) How might projections of increasing temperatures and decreasing water availability

affect seedling carbon assimilation? 3) What are the combined effects of these two processes on net annual carbon assimilation and how might carbon assimilation change under forecasted conditions? Answering these questions will inform ecologists how tree seedling carbon budgets are affected by their environment and will yield important insight into how temperate tree recruitment may change in the future.

METHODS

Experimental Design

Study Locations

Our study took place at three locations in southeast Michigan, USA: Saginaw Forest (42.270977 N, 83.806022 W), Radrick Forest (42.287083 N, 83.658056 W), and the E. S. George Reserve (42.457104 N, 84.020226 W). All three locations have similar climates, averaging 22 °C in summer (June-August) and -6 °C in winter (December-February); annual precipitation is 925 mm and is evenly distributed throughout the year. Radrick Forest and E. S. George Reserve are mesic temperate hardwood forests dominated by *Acer, Prunus,* and *Quercus* species whereas plots at Saginaw Forest are former monocultures of *Acer saccharum* and *Quercus rubra* planted in the early 1900's.

Study Species

We chose to use two species for this study that would allow us to generate hypotheses about roles of phenological and hydraulic traits: *Acer saccharum* (Marsh.) and *Quercus rubra* (L.). *A. saccharum* is late-successional, *Q. rubra* is mid-successional, and both species are common across our study region and regularly co-occur. *A. saccharum* is one of the earliest

species in temperate hardwood forests to expand its leaves in spring, whereas *Q. rubra* is typically one of the last (Augspurger and Bartlett 2003). The opposite is true at the end of the growing season where *A. saccharum* undergoes color change and leaf senescence much earlier than *Q. rubra*. These differences suggest that *A. saccharum* and *Q. rubra* may differ in sensitivity to the climate cues that trigger their foliar phenology. With respect to hydraulic features, *A. saccharum* has diffuse-porous xylem (narrow conduits) and demonstrates isohydric stomatal behavior in response to drought (Roman et al. 2015), both of which help this species avoid catastrophic xylem embolism (i.e. hydraulic failure). In contrast, *Q. rubra* is ring-porous (wider xylem conduits) and anisohydric (Roman et al. 2015), traits which allow the species to maintain photosynthetic activity during drought but leaving them more vulnerable to hydraulic failure. This is beneficial to *Q.* rubra in extended drought periods that are moderate in intensity, whereas *A. saccharum* runs the risk of succumbing to carbon starvation. *A. saccharum* and *Q. rubra* are both predicted to decrease in importance value across eastern North America under climate change (Iverson et al. 2008), but the former is expected to experience a stronger decline, particularly in the location of this study (southeastern Michigan).

Field experimental set up

We transplanted seedlings of the study species at all three sites in three cohorts (2014-2016). Seeds of each species (for seed sources see Table SI 2.1) were cold stratified over winter according to published protocol before being germinated in large tubs containing potting soil (Sun Gro Horticulture; Agawam, MA, USA) in a greenhouse. Approximately four weeks after germination, we gently removed them from the soil and transplanted them bare root in the field. Because seedling survival and growth may be additionally modified by biotic interactions

associated with neighboring adult trees via soil mechanisms such as plant-soil feedbacks (McCarthy-Neumann and Ibáñez 2012), allelopathy (Pellissier and Souto 1999, Gómez-Aparicio and Canham 2008, Ruan et al. 2016), and nutrient availability (Phillips and Fahey 2006, Classen et al. 2015), at each site seedlings were planted under both *A. saccharum* and *Q. rubra* trees. There were three replicate canopy trees per canopy species and site. Depending on seedling availability in each year, five to ten seedlings per target species were transplanted in separate rows extending from the base of each adult canopy tree (for detailed number of seedlings planted see Table SI 2.1).

Data collection

Environmental data

We established environmental data stations at each site that measured temperature (°C), relative humidity (%), soil moisture (%), and photosynthetically active radiation (PAR; μmol photons m^{-2} s^{-1}) at hourly intervals. Temperature and relative humidity were measured using HOBO U23 Pro v2 data loggers (Onset Computer Corporation; Bourne, MA, USA) placed at central locations at each site. Soil moisture and PAR were measured using Smart Sensors in combination with HOBO Micro Stations (Onset Computer Corporation).

Leaf Phenology

Canopy phenology was measured as the change in light availability in the understory measured by the PAR sensor. Day of canopy closure in the spring was defined as the day in which the average daytime PAR (between 1000-1700 hours) dropped below 100 μmol m^{-2} s^{-1} and then did not increase above that threshold for one week (in order to rule out the possibility of low

light resulting from cloudy days). We estimated the day of canopy reopening in the fall as the day at which average daytime PAR (between 1000-1700 hours) increased above 20 μmol m^{-2} s^{-1} without then decreasing below that value for more than a day (to account for cloudy weather). This value is much lower than the threshold we used to estimate canopy closure in spring because there is significantly less radiation in fall due to the angle the sunlight passes through the atmosphere (Fig. SI 2.6).

Seedling foliar phenology was measured on a weekly basis in spring and fall beginning the year following transplantation (e.g., 2015 for the first cohort). We recorded the date of leaf expansion in spring and leaf color change and senescence in fall for each individual at weekly intervals. We used standardized initial leaf expansion, autumnal leaf color change, and leaf senescence (i.e., "initial leaf occurrence", "colored leaves", and "falling leaves" *sensu* Denny et al. [2014]). A previous study noted a significant drop in net carbon assimilation associated with high respiration rates during the breakdown and resorption of photosynthetic machinery in fall (Collier and Thibodeau 1995). In order to account for this elevated respiration early in fall, we recorded two fall phenophases that differ in the total amount of leaf area that has undergone color change associated with nutrient resorption. Fall1 was defined as the period of time beginning with the onset of leaf color change and ending when 50% of leaf area had changed color. Fall2 was defined as the period between the end of Fall1 and when all leaves had fully senesced. Leaf coloration was measured visually and did not include discoloration caused by foliar pathogens. We measured foliar phenology for four years (2015-2018) and canopy phenology for 9 years (2010-2018).

Photosynthesis and Carbon Assimilation Data Collection

We used a LI-6400 Portable Photosynthesis System equipped with a CO_2 mixer assembly, LI-02B LED red/blue light source and LI-06 PAR sensor (Li-COR Biosciences, Lincoln, NE, USA) to measure *in situ* gas exchange for a subset of transplanted seedlings following spring leaf expansion and continuing through the growing season. Gas exchange measurements were taken once every two weeks in spring and fall and approximately monthly during the summer for the 2015-2017 growing seasons. We constructed *A-Ci* (at 400, 300, 200, 100, 50, 400, 400, 600, 800, 1000, 1250, and 1500 ppm CO_2) and *A-Q* curves (at 1500, 1000, 750, 500, 250, 125, 60, 30, 20, 10, and 0 μmol photon m^{-2} s^{-1}) for each seedling, maintaining ambient humidity and temperature. Leaves smaller than the cuvette were traced in the field and leaf area was measured using ImageJ software (Schneider et al. 2012). Soil moisture was measured at the individual seedling level during each measurement using a Fieldscout TDR300 Soil Moisture Meter (Spectrum Technologies, Aurora, IL, USA).

Analyses

Projecting the effects that climate change will have on seedling phenology and carbon assimilation involves great uncertainty. This includes both the uncertainty surrounding what future climates will look like as well as the uncertainty entailed in making long-term predictions using data collected across random variability of climate drivers. The climate change scenarios we use here to project the possible changes in phenology and carbon assimilation of temperate tree seedlings represent the best- and worst-case climate scenarios developed by the IPCC (2014). Therefore, although it is unlikely that either of the two scenarios accurately portrays environmental conditions in 2100 in their entirety (Hausfather and Peters 2020), they can still

serve to bound our expectations for what seedling performance could look like at the end of the century.

The second source of uncertainty, associated with using random variability to make long-term predictions, arises from two main sources. First, climate change is projected to result in no-analog environmental conditions (Jackson and Williams 2005) that include combinations of drivers that are not represented in field experiments without direct manipulation (e.g., Sendall et al. 2014). Second, climate change relationships are often nonlinear, and it can therefore be difficult to predict the effects of climate change past the limits of observed variability (Wolkovich et al. 2012). Still, capitalizing on natural variability to infer potential future performance is currently one of the best tools we have to forecast ecological change (Ibáñez et al. 2013).

Phenology

Day of canopy closure (spring) and canopy reopening (fall) was analyzed for as far back as we had been taking these measurements (2011 for E. S. George Reserve, 2012 for Radrick Forest, and 2015 for Saginaw Forest; n = 20 because of occasional missing data). Canopy tree leaf-out is tightly linked to climate cues such as temperature forcing (Ibáñez et al. 2010), winter vernalization (Roberts et al. 2015), and frost occurrence (Vitasse et al. 2014) as well as photoperiod (Way and Montgomery 2015), which varies latitudinally rather than temporally. We tested the effects of monthly and seasonal average, minimum, and maximum temperatures and frost occurrence (number of days per month or week with average daytime temperature < 0 °C) on day of canopy closure and seedling leaf expansion and chose the models with the best fit to

use in this analysis (Fig. SI 2.7ii). We analyzed day of canopy closure for each site *s*, and year *y*, using a normal likelihood distribution:

$$CanopyClosure_{s,y} \sim N(\mu_{s,y}, \sigma^2)$$

The mean, μ, is modeled with linear relationships to different climatic factors (*n*) and site random effects (α):

$$\mu_{s,y} = \alpha_s + \beta_n \times ClimateFactor_{n,y}$$

$$\alpha_{site} \sim N(\rho_\alpha, {\sigma^2}_\alpha)$$

Seedling spring foliar phenology was modeled similarly, but in this case included individual random effects (since we have individual level phenology across years). Additional analysis did not reveal a significant effect of canopy species, seed source, or planting cohort on seedling phenology, so they were not included in the final models. For all three analyses (canopy closure and seedling phenology for two species), we used non-informative prior distributions in our estimation of parameters, β_n ~ N(0, 1000), ρ_α ~ logN(1, 1000), and $1/{\sigma^2}_\alpha$ ~ Gamma(0.001, 0.001).

For seedling fall phenology we estimated the timing of the three events that defined the end of Summer through the end of Fall: 1) Fall 1: onset of leaf color change, 2) Fall 2: greater than 50% leaf coloring, and 3) leaf senescence. As with spring phenology, we evaluated the relationship between fall phenology and canopy reopening and several climate variables including monthly and seasonal average, minimum, and maximum temperature; monthly and seasonal average, minimum, and maximum soil moisture; and monthly and weekly frost occurrence (number of days with average daytime temperature < 0 °C). Similarly, we included individual random effects in the seedling models and site random effects in the canopy reopening models.

Seedling phenology models included data for all seedlings that successfully established and survived for at least one year. Because of growing season mortality in the year following planting, sample size was higher in spring (n = 43, 24, 47, and 23 for *A. saccharum* in 2015, 2016, 2017, and 2018, respectively, and n = 23, 17, 95, and 46 for *Q. rubra*) than in fall (n = 25, 15, 30, and 18 for *A. saccharum* and n = 15, 11, 59, and 36 for *Q. rubra*). The photosynthetic model used data collected from a subset of these seedlings (n = 35 and 37 for *A. saccharum* and *Q. rubra*, respectively).

Photosynthesis and Carbon

We analyzed our gas exchange data using an adaptation of the Farquhar et al. (1980) model of C3 photosynthesis originally developed by Patrick et al. (2009) and then further modified by Peltier and Ibáñez (2015). Patrick et al. (2009) adapted the Farquhar et al. (1980) model into a Bayesian framework and incorporated light dependency of potential electron transport according to Farquhar and Wong (1984) and mesophyll conductance according to Caemmerer and Evans (1991), Caemmerer (2000), and Niinemets et al. (2009). Peltier and Ibáñez (2015) then included linear relationships with additional explanatory variables (i.e., soil moisture and vapor pressure deficit; VPD) and allowed seasonal variation of certain parameters. A detailed description of the model (Fig. SI 2.7i) can be found in Supporting Information 2.2 along with tables of associated parameter definitions (Table SI 2.5) and parameter posterior estimates (Table SI 2.6).

Because we were interested in the role of phenology in these parameters, we estimated photosynthesis model parameters for each of the following phenophases : 1) spring period between leaf-out and the day of canopy closure; 2) summer, defined as the time between canopy

closure and the beginning of leaf coloration; 3) Fall 1, the time between the onset of coloration and when a specific leaf had surpassed 50% of coloration; and 4) Fall 2, measurement taken between 50% coloration and leaf senescence. Preliminary data analysis did not indicate differences in photosynthetic rates based on seed source or cohort (age), so these variables were not included in the analysis.

Predicting photosynthetic performance over the growing season

We simulated current average climate conditions by averaging hourly temperature, soil moisture, and relative humidity data collected from our environmental sensors across all three sites between 2014-2018 (Fig. SI 2.7iii). VPD was calculated from relative humidity and temperature and then both VPD and soil moisture data were centered around their respective annual means. Climate conditions were then estimated for two climate change scenarios in the year 2100 (Table SI 2.2, Handler et al. 2014) that assume either a global reduction in carbon emissions (Scenario 1) or maintained levels of carbon emissions (Scenario 2). We transformed 'current climate' temperature, soil moisture, and VPD simulated data by applying climate projections for our study region (Table SI 2.2; Handler et al. 2014). Spring and fall light availability were accounted for by using the posterior estimates of canopy close and reopening from the canopy phenology models and shifting simulated light data under current conditions to match projected phenology dates. We then used parameter estimates (mean and variances) from our photosynthesis and phenology models combined with the simulated climate data to estimate annual carbon assimilation, respiration, and accumulation for seedlings of each species (Fig. SI 2.7iv). A full description of simulated data generation, including the approximation of summer light availability, can be found in Supporting Information 2.3.

All models were run using OpenBUGS 3.2.3 (Lunn et al. 2009). Model code and associated data for phenology and photosynthesis models are available (see Data Availability). Phenology models were run for 50,000 iterations and posterior densities were calculated following a 10,000-iteration burn-in period. Photosynthesis models were run for 8,000 iterations following a 2,000-iteration burn-in. Convergence for parameters in both sets of models was assessed visually and by using the Brooks-Gelman-Rubin statistic from two independent chains (Gelman and Rubin 1992). Parameter values (means, variances, and covariances) were estimated from their posterior distributions. Climate effects (β in phenology models) were considered significant if the 95% confidence intervals of their posterior distributions did not overlap zero.

RESULTS

Spring Canopy and Seedling Phenology

The variation in average spring, February, and August temperatures that were observed over the course of our experiment was of the same order of magnitude as the projected changes in seasonal temperature (see Table SI 2.2) made by Handler et al. (2014). Average observed February temperature in our study ranged from -11.1 to 1.3 °C (expected change in Scenario 1 is + 1.4 °C from a baseline temperature of -6.4 °C and is + 4.1 °C for Scenario 2), average March-April temperature ranged from 2.5 to 6.5 °C (projected Scenario 1 change + 0.9 °C from a baseline temperature of 5.1 °C, projected Scenario 2 change + 3.3 °C), and average August temperature ranged from 18.7 to 22.4 °C (projected Scenario 1 change + 1.2 °C from a baseline temperature of 18.3 °C, projected Scenario 2 change + 6.2 °C).

The best model predicting spring phenology included average February temperature and average Spring (March-April) temperature for both canopy and seedlings (based on deviance

information criterion, DIC; Spiegelhalter et al. 2002; Fig. 2.2a). Fits (R^2, predicted vs observed values) for our spring phenology models were 0.55 for *A. saccharum* seedlings, 0.39 for *Q. rubra* seedlings, and 0.38 for canopy closure. Average spring temperature (SpT) was negatively and significantly associated with spring leaf-out (leaf-out took place earlier in years with warmer springs) in all three models (Fig. 2.2b). However, average February temperature (FebT) was positively and significantly associated with *A. saccharum* seedling leaf-out, negatively and significantly associated with *Q. rubra* seedling leaf-out, and positively, but non-significantly, associated with canopy closure (Fig. 2.2b).

Modeled canopy closure shifted 1.6 and 5.4 days earlier in Scenarios 1 and 2, respectively, relative to current climate conditions (Fig. 2.2c). *A. saccharum* seedling leaf-out shifted 2.4 and 9 days earlier in the two climate change scenarios, leading to increased differences between seedling leaf-out and canopy close from 18.4 days in current conditions to 19.2 days in Scenario 1 and 21.5 days in Scenario 2. *Q. rubra* seedlings shifted leaf-out 2.3 and 8 days earlier in the two climate change scenarios, leading to increased difference between leaf-out and canopy close from 12.2 days in current conditions to 12.9 days in Scenario 1 and 14.3 days in Scenario 2.

Fall Canopy and Seedling Senescence Phenology

The best model predicting fall phenology for both canopy reopening and seedling phenophases included August average temperature (based on DIC). Leaf senescence model fit (Fig. 2.2d; R^2, predicted vs. observed values) was 0.87 and 0.39 for *A. saccharum* and *Q. rubra* seedlings, respectively, and 0.64 for the canopy closure model. The timing of all three events shifted later with increases in average August temperature; the association was significant for *Q.*

rubra senescence and canopy reopening but not for *A. saccharum* (Fig. 2.2e). Senescence in *A. saccharum* seedlings was projected to occur prior to canopy reopening under current conditions and both future climate scenarios, resulting in no net change to fall light availability for this species (Fig. 2.2f). In contrast, *Q. rubra* seedlings are projected to experience a decrease in access to light prior to leaf senescence from 14.2 days under current climate conditions to 11.9 days in Scenario 1 and 2.3 days in Scenario 2. Information for other Fall events is provided in Figures SI 2.8 and 2.9.

Photosynthesis analysis

Model fits for the seedling carbon assimilation models (R^2, predicted vs. observed) were 0.72 for *A. saccharum* seedlings and 0.76 for *Q. rubra* seedlings. Photosynthetic parameter estimates (Fig. SI 2.10; Table SI 2.6) were largely consistent with previous research published for these two species (Peltier and Ibáñez 2015). Soil moisture had significant positive effects on net photosynthesis, whereas negative effects of VPD were more apparent in fall (Fig. SI 2.11). Projected daily rates of net carbon assimilation peaked in spring (i.e., carbon assimilation rates were much higher than respiration rates; Tables SI 2.3 and 2.4) for seedlings of both species, in both canopy treatments, and in all three climate simulations (Fig. 2.3a-b and 2.4a-b). Projected daily net assimilation rates decreased as the canopy closed and were relatively constant throughout the remainder of the growing season, although there was a consistent drop in net assimilation rates at the beginning of fall associated with the onset of leaf color change (Fig. 2.3a-b and 2.4a-b).

Acer saccharum seedlings planted under *A. saccharum* adults were predicted to maintain positive net assimilation rates throughout the summer under current climate conditions and in

climate Scenario 1 (Fig. 2.3a). In Scenario 2, projected net assimilation rates became negative for a large portion of summer before becoming positive again in late summer, associated with increased water availability from increased rainfall. In contrast, when planted under *Q. rubra* adults, *A. saccharum* seedlings are predicted to have net negative assimilation rates for most of the growing season in all three climate simulations (Fig. 2.3b). Projected net assimilation rates were particularly negative in Scenario 2, which was the only species-canopy-scenario combination to have days where all hours were projected to have negative carbon assimilation rates.

Quercus rubra seedlings in current climate conditions are predicted to have similar responses between the two canopy treatments (Fig. 2.4a-b), with net positive daily assimilation rates in spring as well as in late summer, again corresponding to periods of increased water availability. This pattern was maintained under Scenario 1, but seedlings in both treatments suffered under Scenario 2 with long periods of time in summer with consistently negative carbon assimilation rates (Fig. 2.4a-b). Projected net carbon assimilation rates were negatively affected when planted under *Q. rubra* canopies (Fig. 2.4b).

Carbon accumulation simulation

When integrated over the growing season, modeled carbon accumulation reflected the trends in net carbon assimilation rates. Seedlings of both species were predicted to constructpositive carbon budgets in spring across both canopy treatments and in all three climate simulations (Fig. 2.3c-d and 2.4c-d). By the end of summer, estimated carbon accumulation ranges from strongly positive (e.g., seedlings of both species under *A. saccharum* in current climate conditions and in Scenario 1; Fig. 2.3c and 2.4c), to neutral (e.g, *Q. rubra* under *A.*

saccharum in Scenario 2; Fig. 2.4c), to strongly negative (e.g., *A. saccharum* seedlings under *Q. rubra* in Scenario 2; Fig. 2.3d). Projected carbon accumulation changed little in fall, with seedlings of both species and in all climate scenario-canopy combinations tending to maintain carbon levels from the end of the summer. Climate scenario played a large and obvious effect on carbon accumulation. Projected net carbon accumulation in summer declined more sharply in Scenario 2 than in current conditions or Scenario 1, reaching negative values in three out of the four species-treatment combinations (Fig. 2.3c-d and 2.4c-d). Only *A. saccharum* seedlings under conspecific canopy trees are projected to maintain positive carbon budgets across the entire growing season under the most extreme scenarios (Fig. 2.3c), and then only because of the sharp increase in projected spring assimilation. *Q. rubra* seedlings under *A. saccharum* canopy trees in Scenario 2 are also projected finish the growing season with positive carbon accumulation, but only after a short period in fall with net negative accumulation (Fig. 2.4c).

Growing season respiration was projected to increase more in the two climate change scenarios compared to projected assimilation from photosynthesis (Fig. 2.5, Tables SI 2.3 and 2.4). Differences in canopy treatment effects were primarily driven by differences in projected respiration costs, with consistently greater respiration for both species of seedling when growing below *Q.* rubra adults (Fig. 2.5b) than when planted below *A. saccharum* adults (Fig. 2.5a). Carbon lost to respiration was estimated to increase by 71-124% (across both species) in the more extreme climate change scenario (Scenario 2) whereas carbon gain from photosynthesis would only increase by 39-50% under the same conditions. Projected increases in gross carbon gain were strongest in spring, where predicted increases in access to light led to 75-167% increases in carbon gained, and projected increases in respiration costs were strongest in summer (79-163% increases). Although across all three climate simulations the spring seasonal bin

represented only 11% or 7% of the total length of the growing season (*A. saccharum* and *Q. rubra*, respectively), estimated spring gross carbon assimilation accounted for 18-22% of annual gross assimilation under current climate conditions and 24-33% in Scenario 2. Seasonal values can be found in Tables SI 2.3 and 2.4.

DISCUSSION

Climate change is projected to simultaneously affect growing season length (Piao et al. 2019) and summer water availability (Choat et al. 2012); however, few studies account for both effects when making predictions of future tree recruitment. In this study, we investigated the combined effects of temperature and water availability on seedling phenology, i.e., growing season length, and carbon assimilation for two species dominant in North America eastern temperate deciduous forests. We found that tree seedling phenology is more sensitive to warming than canopy tree phenology in spring, resulting in an increase in high light availability and consequently in seedling net carbon accumulation. When extrapolating our results to projecte changes in climate conditions, we found that this increase in spring carbon assimilation could allow *A. saccharum* to escape negative summer carbon balances and to increase performance under the more moderate climate scenario. *Quercus rubra* seedlings may also benefit from extending growing seasons but not to the same extent that *A. saccharum* did. The differences in projected performance between the two species favor future performance of *A. saccharum*. However, we also found this effect was not homogeneous under the forest canopy; the tree species under which the seedlings were growing mattered. Seedling performance of the two species was higher under *A. saccharum* adults than under *Q. rubra* adults. Together, these results suggest that under the moderate climate scenario, and despite drier summers, the effects of

earlier springs will benefit isohydric *A. saccharum* seedlings more relative to anisohydric *Q. rubra* seedlings. This unexpected result points out the importance of considering the multifaceted effects of global warming on tree seedling performance.

1) Could warming temperatures lead to tree seedlings increasing, maintaining, or losing access to light in spring and fall?

Light availability is often a limiting factor for understory plants growing in temperate forests (Canham et al. 1999, Kobe et al. 1995), in which nutrients and water are often abundant relative to light. Access to light has strong implications for carbon assimilation (Kwit et al. 2010, Heberling et al. 2019) and can also indirectly affect plant performance by altering the direction and magnitude of plant-soil feedbacks (McCarthy-Neuman and Ibáñez 2012). Tree seedlings in temperate forests expand their leaves up to several weeks prior to canopy closure in order to increase access to high light availability (Augspurger 2008, Kwit et al. 2010) and will also maintain leaves later into fall (Gill et al. 1998). However, growing season length is expanding at both ends of the season for canopy trees, and it was previously uncertain if tree seedling phenology is shifting at the same rate (Heberling et al. 2019).

The phenology of leaf color change and senescence is also well-documented for canopy trees in the northern hemisphere (Gill et al. 2015) and deciduous plants across Europe and Asia (Piao et al. 2019). However, differential responses among tree seedlings and the canopy has received relatively little attention, and no study we are aware of has assessed the impact of these differences in seedling performance. Furthermore, we also accounted for impact of fall phenology on seedlings ability to accumulate carbon. Even if light availability is much less in

fall than it is in spring, seedlings are still photosynthetically active and may rely on that period of time to maintain a positive carbon balances (Gill et al. 1998).

Our results suggest that seedling access to light will increase in spring and will either decrease (for *Q. rubra* seedlings) or remain at zero (for *A. saccharum* seedlings) in fall. This stands in contrast to previous work which found that shifts in spring canopy phenology were outpacing shifts in spring leaf out phenology of wildflower species (Heberling et al. 2019) and suggests that tree seedling performance will not be as affected as herbaceous plant performance under future climate conditions. Furthermore, *A. saccharum* spring phenology was found to be shifting at a faster rate than *Q. rubra* spring phenology, suggesting that climate change will have different effects between the two species, potentially leading to different photosynthetic performance.

2) How will increasing temperatures and decreasing water availability affect seedling carbon assimilation?

Warmer temperatures associated with climate change are projected to reduce tree performance (Zhao and Running 2010, Williams et al. 2012) and increase tree mortality if precipitation is insufficient (McDowell et al. 2008, Allen et al. 2010). In plants, carbon assimilation can be limited by water availability (Niinemets 2010) and VPD (Oren et al. 1999) via plant stomatal regulation (Wilson et al. 2000). Summer carbon assimilation rates for both species in this study were positively associated with soil moisture and VPD (Fig. SI 2.11). Projected reductions in water availability, coupled with higher respiration demand driven by increased temperatures (Table SI 2.4), led to sharp declines in net carbon assimilation rates and net accumulation following canopy closure (Fig. 2.3 and 2.4). Negative carbon accumulation is

shown in the bottom panels of both figures but is potentially unrealistic given that seedlings are likely to die shortly after reaching negative accumulation due to a limited capacity to store carbon from previous years. This agrees with previous research that found that, although respiration and photosynthesis rates are both positively associated with increases in temperature, respiration has a stronger dependency on temperature than photosynthetic rates (Caemmerer 2000), and therefore increases in respiration costs are likely to outweigh increasing photosynthetic gains under future warming.

Our findings echoed results from previous research which suggested that access to light in fall is far less important than access to spring light when considering plant performance and carbon dynamics (Gill et al. 1998, Kwit et al. 2010). Our projections show relatively little difference in fall carbon accumulation across climate scenarios (Tables SI 2.3 and 2.4), despite substantial losses in light availability for seedlings of one of the species (*Q. rubra*, Fig. 2.2f). The other species, *A. saccharum*, was also less sensitive to fall temperatures compared to the canopy. However, leaves of this species senesce prior to canopy reopening (Fig. 2.2f), so there we did not predict any net loss in light availability under climate change scenarios. Importantly, even if seedlings were able to significantly add to their carbon budgets in fall, it would likely be irrelevant for three out of the four species-treatment combinations in the more extreme climate scenario because they would have run out of carbon (e.g. reached negative carbon accumulation) prior to canopy reopening. Only *A. saccharum* seedlings planted under conspecific canopy trees are predicted to be able to maintain positive carbon balances over the entire growing season under the more extreme climate scenario. *Q. rubra* seedlings planted under *A. saccharum* trees are also predicted to finish with a slightly positive carbon balance, but only after first reaching

negative carbon accumulation early in fall, suggesting that these seedlings will need to rely on stored carbon in order to survive long-term.

Changes in estimated net carbon assimilation and respiration were strongly modulated by the species of canopy tree the seedlings were planted under. Seedlings of both species experienced significant reductions in net annual carbon accumulation when planted under *Q. rubra* canopy trees compared to when planted under *A. saccharum* canopy trees (Fig. 2.6c-d and 2.7c-d), despite no significant difference in water or light availability between the two treatments (data not shown). This reduction in carbon accumulation was attributable to more negative respiration rates for both species in the *Q. rubra* canopy treatment (Fig. 2.5b). The cause of this difference is likely not attributable to abiotic factors because canopy phenology, summer canopy openness, and soil moisture did not significantly differ between treatments (data not shown), however the underlying cause for this difference deserves further study.

Tree seedling performance may be affected by biotic interactions with neighboring canopy trees, as previous studies have found that temperate tree seedling survival is significantly affected by plant-soil feedback effects (McCarthy-Neumann and Ibáñez 2012, 2013), allelopathy (Pellissier and Souto 1999, Gómez-Aparicio and Canham 2008), composition of mycorrhizal communities associated with neighboring canopy trees (Phillips and Fahey 2006), and nutrient availability (Classen et al. 2015). Differences in canopy structure and composition have also been shown to create diverse microclimates that may differentially mitigate the effects of climate change on seedling performance (Dobrowski et al. 2015). Furthermore, tree seedling photosynthetic performance has been shown to be directly affected by soil nitrogen content (Reich et al. 1998, Cannell and Thornley 2000), which can be strongly associated with neighboring canopy species (Finzi et al. 1998, Phillips and Fahey 2006), and by increases in the

production of secondary metabolites in response to damage from foliar herbivores (Zangerl et al. 1997). Together, this evidence suggests that interactions with neighboring canopy trees may modulate photosynthetic performance of tree seedlings.

We posit that our observations on higher respiration rates when planted under *Q. rubra* canopy trees may be due to increased levels of leaf nitrogen for seedlings in that canopy treatment. Leaf respiration rates have been found to correlate with leaf nitrogen concentration (Reich et al. 1998, Cannell and Thornley 2000), and although we did not measure the availability of mineral nitrogen as part of this study, previous studies working in similar systems have found higher rates of nitrogen mineralization (Finzi et al. 1998, Phillips and Fahey 2006) and higher amounts of organic nitrogen (McCarthy-Neumann and Ibáñez 2012) in soils associated with *Q. rubra* compared to soils collected from beneath *A. saccharum*. Soil nitrogen has recently been demonstrated to affect leaf nitrogen content (Tang et al. 2019), so it is possible that this mechanism is leading to higher respiration in our tree seedlings when they are planted below *Q. rubra* canopy trees.

A second possible explanation could be if pressure from natural enemies (e.g., herbivores) was higher under one canopy compared to the other, we might expect to see an associated increase in the production of plant secondary metabolites (Zangerl et al. 1997), and a consequent increase in respiration. However, we measured leaf damage as a part of a concurrent study and found no significant difference in leaf herbivory or pathogen damage between species of seedlings or between canopy treatments (data not shown), suggesting that this is not the underlying cause here.

3) What are the combined effects of these two processes on net annual carbon assimilation and how might carbon assimilation change under forecasted conditions?

We found that the projected increase in access to light in spring allowed seedlings to increase net carbon assimilation enough to offset rising respiration costs associated with warmer and drier summers, but only when planted near *A. saccharum* canopy trees. Seedlings of both species in the more extreme climate scenario are projected to be able to maintain positive annual carbon budgets in this planting treatment (Fig. 2.5a), whereas both species had strongly negative carbon accumulation when planted under *Q. rubra* canopy trees (Fig. 2.5b). Importantly, *A. saccharum* seedlings currently perform better than *Q. rubra* seedlings under *A. saccharum* canopy trees and are projected to continue to do so, suggesting *A. saccharum* seedlings may outcompete *Q. rubra* seedlings under climate change when establishing under conspecific trees. However, although *Q. rubra* seedlings currently outperform *A. saccharum* seedlings when growing under *Q. rubra* canopy trees, this advantage disappears in the more extreme climate scenario as seedlings of both species are projected to reach negative carbon balances. This suggests that, unless global carbon emissions are reduced, *Q. rubra* seedlings will not outperform *A. saccharum* seedlings in either of these two canopy treatments.

Still, earlier leaf out and later leaf senescence may lead to an increased risk of frost damage from late spring and early fall frosts (Vitasse et al. 2014). Forecasts for our study region (Handler et al. 2014) predict that date of last frost in spring and first frost in fall are shifting at approximately the same rate as canopy tree phenology, suggesting that there is a possibility that faster shifting seedling phenology may increase seedling exposure to frost events and potentially counteract the benefits of increased access to light. Late frost would then disproportionately

affect early-leafing *A. saccharum* seedlings compared to late-leafing *Q. rubra* seedlings, offsetting any potential benefits of early phenology.

CONCLUSION

Taken together, our results indicate that the process underlying these species' seedling carbon assimilation depends on a combination of seasonal access to light, the ability to withstand negative carbon accumulation in summer, and interactions with neighboring canopy trees. Seedlings are predicted to benefit from longer springs and to suffer from hotter, drier summers. Interestingly, our models project that *Q. rubra* seedlings will be unable to maintain positive carbon balances if global carbon emissions are not reduced (Scenario 2), regardless of biotic environment, whereas *A. saccharum* seedlings may be able to survive when located near conspecific canopy trees. Therefore, our results suggest that *A. saccharum* would continue to successfully recruit in areas where it is already established whereas *Q. rubra* would decrease in abundance across the landscape, despite their relatively higher drought tolerance.

Our approach was novel because it combined two potential mechanisms, shifting phenology and seasonal photosynthetic performance, that are projected to affect seedling carbon budgets under the predicted climate scenarios for the region. Integrated assessment provided a more realistic assessment of future trends than those from individual processes (Ibáñez et al. 2017). Furthermore, although limited to two canopy treatments, we were able to assess the effects of the biotic environment on seedling photosynthetic performance. Parameters from our models can help fit future recruitment dynamics and inform vegetation models that seek to predict changes in forest structure and composition. Finally, our results suggest that seedling performance of temperate tree species will suffer with climate change, which in turn could lead

to a change in the structure and composition of these forests. Without a reduction in current carbon emissions, we are likely to see strong changes in eastern North American forests in the coming century.

REFERENCES

Allen, C. D., A. K. Macalady, H Chenchouni, D. Bachelet, N. McDowell, M. Vennetier, T. Kitzberger, A. Rigling, D. D. Breshears, E. H. Hogg, P. Gonzalez, R. Fensham, Z. Zhang, J. Castro, N. Demidova, J.-H. Lim, G. Allard, S. W. Running, and N. Cobb. 2010. A global overview of drought and heat-induced tree mortality reveals emerging climate change risks for forests. Forest Ecology and Management 259: 660-684.

Augspurger, C. K. 2008. Early spring leaf out enhances growth and survival of saplings in a temperate deciduous forest. Oecologia 156: 281-286.

Augspurger, C. K., and E. A. Bartlett. 2003. Differences in leaf phenology between juvenile and adult trees in a temperate deciduous forest. Tree Physiology 23: 517-525.

Baurle, W. L., R. Oren, D. A. Way, S. S. Qian, P. C. Stoy, P. E. Thornton, J. D. Bowden, F. M. Hoffman, and R. F. Reynolds. 2012. Photoperiodic regulation of the seasonal pattern of photosynthetic capacity and the implications for carbon cycling. Proceedings of the National Academy of Sciences 109: 8612-8617.

Caemmerer, S. 2000. Biochemical models of leaf photosynthesis. Techniques in Plant Sciences, 2. CSIRO Publishing, Collingwood, VIC, Australia.

Caemmerer, S., and J. R. Evans. 1991. Determination of the average partial pressure of Co2 in chloroplasts from elaves of several C3 plants. Functional Plant Biology 18: 287-305.

Canham, C. D., K. D. Coates, P. Bartemucci, and S. Quaglia. 1999. Measurement and modeling of spatially explicit variation in light transmission through interior cedar-hemlock forests of British Columbia. Canadian Journal of Forest Research 29: 1775-1783.

Cannell, M. G. R., and J. H. M. Thornley. 2000. Modelling the components of plant respiration: Some guiding principles. Annals of Botany 85: 45-54.

Chen, X., S. An, D. W. Inouye, and M. D. Schwartz. 2015. Temperature and snowfall trigger alpine vegetation green-up on the world's roof. Global Change Biology 21: 3635-3646. https://doi.org/10.1111/gcb.12954

Choat, B., S. Jansen, T. J. Brodribb, H. Cochard, S. Delzon, R. Bhaskar, S. J. Bucci, T. S. Feild, S. M. Gleason, U. G. Hacke, A. L. Jacobsen, F. Lens, H. Maherali, J. Martínez-Vilalta, S. Mayr, M. Mencuccini, P. J. Mitchell, A. Nardini, J. Pittermann, R. B. Pratt, J. S. Sperry, M. Westoby, I. J. Wright, and A. E. Zanne. 2012. Global convergence in the vulnerability of forests to drought. Nature 491: 752-755.

Chuine, I. 2010. Why does phenology drive species distribution? Philosophical Transactions of the Royal Society B: Biological Sciences 365: 3149-3160.

Chuine, I., and E. Beaubien. 2001. Phenology is a major determinant of tree species range. Ecology Letters 4: 500-510.

Classen, A. T., M. K. Sundqvist, J. A. Henning, G. S. Newman, J. A. M. Moore, M. A. Cregger, L. C. Moorhead, and C. M. Patterson. 2015. Direct and indirect effects of climate change on soil microbial and soil microbial-plant interactions: What lies ahead? Ecosphere 6: 1:21.

Collier, D. E., and B. A. Thibodeau. 1995. Changes in respiration and chemical content during autumnal senescence of *Populus tremuloides* and *Quercus rubra* leaves. Tree Physiology 15: 759-764.

Denny, E. G., K. L. Gerst, A. J. Miller-Rushing, G. L. Tierney, T. M. Crimmins, C. A. F. Enquist, P. Guertin, A. H. Rosemartin, M. D. Schwartz, K. A. Thomas, and J. F. Weltzin. 2014. Standardized phenology monitoring methods to track plant and animal activity for science and resource management applications. International Journal of Biometeorology 58: 591-601.

Diez, J. M., I. Ibáñez, J. A. Silander, Jr., R. Primack, H. Higuchi, H. Kobori, A. Sen, and T. Y. James. 2014. Beyond seasonal climate: Statistical estimation of phenological responses to weather. Ecological Applications 24: 1793-1802.

Dobrowski, S. Z., A. K. Swanson, J. T. Abatzoglou, Z. A. Holden, H. D. Safford, M. K. Schwartz, and D. G. Gavin. 2015. Forest structure and species traits mediate projected recruitment declines in western US tree species. Global Ecology and Biogeography 24: 917-927.

Elliott, K. J., C. F. Miniat, N. Pederson, and S. H. Laseter. 2015. Forest tree growth response to hydroclimate variability in the southern Appalachians. Global Change Biology 21:4627-4641.

Fahey, R. T. 2016. Variation in responsiveness of woody plant leaf out phenology to anomalous spring onset. Ecosphere 7: 1-15.

Farquhar, G. D., S. von Caemmerer, and J. A. Berry. 1980. A biochemical model of photosynthetic CO2 assimilation in leaves of C3 species. Planta 149: 78-90.

Farquhar, G. D., and S. C. Wong. 1984. An empirical model of stomatal conductance. Australian Journal of Plant Physiology 11: 191-210.

Finzi, A. C., N. Van Breemen, and C. D. Canham. 1998. Canopy tree-soil interactions within temperate forests: Species effects on soil carbon and nitrogen. Ecological Applications 8: 440-446.

Fridley, J. D. 2012. Extended leaf phenology and the autumn niche in deciduous forest invasions. Nature 485: 359-362.

Fu, Y. S. H., M. Campioli, Y. Vitasse, H. J. De Boeck, J. Van den Berge, H. AbdElgawad, H. Asard, S. Piao, G. Deckmynm and I. A. Janssens. 2014. Variation in leaf flushing date influences autumnal senescence and next year's flushing date in two temperate tree species. Proceedings of the National Academy of Sciences 111: 7355-7360.

Gelman, A. and D. B. Rubin. 1992. Inference from iterative simulation. Statistical Science 7: 457-511.

Gill, D. S., J. S. Amthor, and F. H. Bormann. 1998. Leaf phenology, photosynthesis, and the persistence of saplings and shrubs in a mature northern hardwood forest. Tree Physiology 18: 281-289.

Gill, A. L., A. S. Gallinat, R. Sanders-Demott, A. J. Rigden, D. J. S. Gianotti, J. A. Mantooth, and P. H. Templer. 2015. Changes in autumn senescence in northern hemisphere deciduous trees: a meta-analysis of autumn phenology studies. Annals of Botany 116: 875-888.

Gómez-Aparicio, L., and C. D. Canham. 2008. Neighbourhood analyses of the allelopathic effects of the invasive tree *Ailanthus altissima* in temperate forests. Journal of Ecology 96: 447-458.

Green, P. T., K. E. Harms, and J. H. Connell. 2014. Nonrandom, diversifying processes are disproportionately strong in the smallest size classes of a tropical forest. Proceedings of the National Academy of Sciences 111: 18649-18654.

Gustafson, C. A., and B. R. Sturtevant. 2013. Modeling forest mortality caused by drought stress: Implications for climate change. Ecosystems 16: 60-74.

Handler, S., M. J. Duveneck, L. Iverson, E. Peters, R. M. Scheller, K. R. Wythers, L. Brandt, P. Butler, M. Janowiak, P. D. Shannon, C. Swanston, A. C. Eagle, J. G. Cohen, R. Corner, P. B. Reich, T. Baker, S. Chhin, E. Clark, D. Fehringer, J. Fosgitt, J. Gries, C. Hall, K. R. Hall, R. Heyd, C. L. Hoving, I. Ibáñez, D. Kuhr, S. Matthews, J. Muladore, K. Nadelhoffer, D. Neumann, M. Peters, A. Prasad, M. Sands, R. Swaty, L. Wonch, J. Daley, M. Davenport, M. R. Emery, G. Johnson, L. Johnson, D. Neitzel, A. Rissman, C. Rittenhouse, and R. Ziel. 2014. Michigan forest ecosystem vulnerability assessment and synthesis: A report from the Northwoods Climate Change Response Framework. US Department of Agriculture, Forest Service, Northern Research Station, General Technical Report NRS-129, Newtown Square, PA.

Hartmann, H. 2011. Will a 385 million year-struggle for light become a struggle for water and for carbon? – How trees may cope with more frequent climate change-type drought events. Global Change Biology 17: 642-655.

Hausfather, Z. H. and G. P. Peters. 2020. Emissions – the 'business as usual' story is misleading. *Nature*, 577: 618-620. https://10.1038/d41586-020-00177-3

Heberling, J. M., C. M. MacKenzie, J. D. Fridley, S. Kalisz, and R. B. Primack. 2019. Phenological mismatch with trees reduces wildflower carbon budgets. Ecology Letters 22: 616-623.

Ibáñez, I., R. B. Primack, A. J. Miller-Rushing, E. Ellwood, H. Higuchi, S. D. Lee, H. Kobori, and J. A. Silander. 2010. Forecasting phenology under global warming. Philosophical Transactions of the Royal Society B 365: 3247-3260.

Ibáñez, I., E. S. Gornish, L. Buckley, D. M. Debinski, J. Hellmann, B. Helmuth, J. HilleRisLambers, A. M. Latimer, A. J. Miller-Rushing, and M. Uriarte. 2013. Moving forward in global-change ecology: capitalizing on natural variability. Ecology and Evolution 3: 170-181.

Ibáñez, I., D. S. W. Katz, and B. R. Lee. 2017. The contrasting effects of short-term climate change on the early recruitment of tree species. Oecologia 184: 701-713.

IPCC, 2014: Climate Change 2014: Synthesis Report. Contribution of Working Groups I, II and III to the Fifth Assessment Report of the Intergovernmental Panel on Climate Change [Core Writing Team, R.K. Pachauri and L.A. Meyer (eds.)]. IPCC, Geneva, Switzerland, 151 pp.

Iverson, L. R., A. M. Prasad, S. N. Matthews, and M. Peters. 2008. Estimating potential habitat for 134 eastern US tree species under six climate scenarios. Forest Ecology and Management 254: 390-406.

Jackson, S. T. and J. W. Williams. 2004. Modern analogs in quaternary paleoecology: Here today, gone yesterday, gone tomorrow? *Annual Review of Earth and Planetary Sciences*, 32: 495-537. https://doi.org/10.1146/annurev.earth.32.101802.120435

Keenan, T. F., J. Gray, M. A. Friedl, M. Toomey, G. Bohrer, D. Y. Hollinger, J. W. Munger, J. O'Keefe, H. P. Schmid, I. S. Wing, B. Yang, and A. D. Richardson. 2014. Net carbon uptake has increased through warming-induced changes in temperate forest phenology. Nature Climate Change 4: 598-604.

Kobe, R. K., S. W. Pacala, J. A. Silander Jr., and C. D. Canham. 1995. Juvenile tree survivorship as a component of shade tolerance. Ecological Applications 5: 517-532.

Kwit, M. C., L. S. Rigg, and D. Goldblum. 2010. Sugar maple seedling carbon assimilation at the northern limit of its range: The importance of seasonal light. Canadian Journal of Forest Research 40: 385-393.

Lunn, D., D. Spiegelhalter, A. Thomas, and N. Best. 2009. The BUGS project: Evolution, critique and future directions. Statistics in Medicine 28: 3049-3067.

Marchin, R. M., C. F. Salk, W. A. Hoffman, and R. R. Dunn. 2015. Temperature alone does not explain phenological variation of diverse temperate plants under experimental warming. Global Change Biology 21: 3138-3151.

McCarthy-Neumann, S. and I. Ibáñez. 2012. Tree range expansion may be enhanced by escape from negative plant-soil feedbacks. Ecology 93: 2637-2649.

McCarthy-Neumann, S. and I. Ibáñez. 2013. Plant-soil feedback links negative distance dependence and light gradient partitioning during seedling establishment. Ecology 94: 780-786.

McDowell, N. G., W. T. Pockman, C. D. Allen, D. D. Breshears, N. Cobb, T. Kolb, J. Plaut, J. S. Sperry, A. West, D. G. Williams, and E. A. Yepez. 2008. Mechanisms of plant survival and mortality during drought: Why do some plants survive while others succumb to drought? New Phytologist 178: 719-739.

McDowell, N. G., and S. Sevanto. 2010. The mechanisms of carbon starvation: how, when, or does it even occur at all? New Phytologist 186: 264-266.

Menzel, A., and P. Fabian. 1999. Growing season extended in Europe. Nature 397: 659.

Niinemets, Ü. 2010. Responses of forest trees to single and multiple environmental stresses from seedlings to mature plants: Past stress history, stress interactions, tolerance and acclimation. Forest Ecology and Management 260: 1623-1639.

Niinemets, Ü., A. Diaz-Espejo, J. Flexas, J. Galmes, and C. R. Warren. 2009. Importance of mesophyll diffusion conductance in estimation of plant photosynthesis in the field. Journal of Experimental Botany 60: 2271-2282.

Oren, R., J. S. Sperry, G. G. Katul, D. E. Pataki, B. E. Ewers, N. Phillips, and K. V. R. Schäfer. 1999. Survey and synthesis of intra- and interspecific variation in stomatal sensitivity to vapour pressure deficit. Plant, Cell & Environment 22: 1515-1526.

Patrick, L. D., K. Ogle, and D. T. Tissue. 2009. A hierarchical Bayesian approach for estimation of photosynthetic parameters of C3 plants. Plant, Cell & Environment 32: 1695-1709.

Pellissier, F., and X. C. Souto. 1999. Allelopathy in northern temperate and boreal semi-natural woodland. Critical Reviews in Plant Sciences 18: 637-652.

Peltier, D. M. P., and I. Ibáñez. 2015. Patterns and variability in seedling carbon assimilation: Implications for tree recruitment under climate change. Tree Physiology 35: 71-85.

Phillips, R. P., and T. J. Fahey. 2006. Tree species and mycorrhizal associations influence the magnitude of rhizosphere effects. Ecology 87: 1302-1313.

Piao, S., Q. Liu, A. Chen, I. A. Janssens, Y. Fu, J. Dai, L. Liu, X. Lian, M. Shen, and X. Zhu. 2019. Plant phenology and global climate change: Current progresses and challenges. Global Change Biology 25: 1922-1940.

Pryor, S. C., D. Scavia, C. Downer, M. Gaden, L. Iverson, R. Nordstrom, J. Patz, and G. P. Roberson. 2014. Ch. 18: Midwest. Pages 418-440 in J. M. Melillo, T. Richmond, and G. Yohe, editors. Climate Change Impacts in the United States: The Third National Climate Assessment. U.S. Global Change Research Program.

Reich, P. B., M. B. Walters, D. S. Ellsworth, J. M. Vose, J. C. Volin, C. Gresham, and W. D. Bowman. 1998. Relationships of leaf dark respiration to leaf nitrogen, specific leaf area and leaf life-span: a test across biomes and functional groups. Oecologia 114: 471-482.

Richardson, A. D., A. S. Bailey, E. G. Denny, C. W. Martin, and J. O'Keefe. 2006. Phenology of a northern hardwood forest canopy. Global Change Biology 12: 1174-1188.

Roberts, A. M. I., C. Tansey, R. J. Smithers, and A. B. Phillimore. 2015. Predicting a change in the order of spring phenology in temperate forests. Global Change Biology 21: 2603-2611.

Roman, D. T., K. A. Novick, E. R. Brzostek, D. Dragoni, F. Rahman, and R. P. Phillips. 2015. The role of isohydric and anisohydric species in determining ecosystem-scale response to severe drought. Physiological Ecology 179: 641-654.

Root, T. L., J. T. Price, K. R. Hall, and S. H. Schneider. 2003. Fingerprints of global warming on wild animals and plants. Nature 421: 57-60.

Ruan, X., C. Pan, R. Liu, Z. Li, S. Li, D. Jiang, J. Zhang, G. Wang, Y. Zhao, and Q. Wang. 2016. Effects of climate warming on plant autotoxicity in forest evolution: A case simulation analysis for Picea schrenkiana regeneration. Ecology and Evolution 6: 5854-5866.

Sack, L. 2004. Responses of temperate woody seedlings to shade and drought: Do trade-offs limit potential niche differentiation? Oikos 107: 110-127.

Sack, L., and P. J. Grubb. 2002. The combined impacts of deep shade and drought on the growth and biomass allocation of shade-tolerant woody seedlings. Oecologia 131: 175-185.

Schneider, C. A., W. S. Rasband, and K. W. Eliceiri. 2012. NIH image to ImageJ: 25 years of image analysis. Nature Methods 9: 671-675.

Sendall, K. M., P. B. Reich, C. Zhao, H. Jihua, X. Wei, A. Stefanski, K. Rice, R. L. Rich, and R. A. Montgomery. 2014. Acclimation of photosynthetic temperature optima of temperate and boreal tree species in response to experimental forest warming. Global Change Biology 21: 1342-1357.

Spiegelhalter, D. J., N. G. Best, B. P. Carlin, and A. van der Linde. 2002. Bayesian measures of model complexity and fit. Journal of the Royal Statistical Society B 64: 583-639.

Tang, J., B. Sun, R. Cheng, Z. Shi, D. Luo, S. Liu, and M. Centritto. 2019. Effects of soil nitrogen (N) deficiency on photosynthetic N-use efficiency in N-fixing and non-N-fixing tree seedlings in subtropical China. Nature Scientific Reports 9.

Umaña, M. N., J. Forero-Montaña, R. Muscarella, C. J. Nytch, J. Thompson, M. Uriarte, J. Zimmermann, and N. G. Swenson. 2016. Interspecific functional convergence and divergence and intraspecific negative density dependence underlie the seed-to-seedling transition in tropical trees. The American Naturalist 187: 99-109.

Visser, M. E., A. J. van Noordwijk, J. M. Tinbergen, and C. M. Lessells. 1998. Warmer springs lead to mistimed reproduction in great tits (Parus major). Proceedings of the Royal Society B 265: 1867-1870.

Visser, M. E., and L. J. M. Holleman. 2001. Warmer springs disrupt the synchrony of oak and winter moth phenology. Proceedings of the Royal Society B 268: 289-294.

Vitasse, Y., A. Lenz, G. Hoch, and C. Körner. 2014. Earlier leaf-out rather than difference in freezing resistance puts juvenile trees at greater risk of damage than adult trees. Journal of Ecology 102: 981-988.

Way, D. A., and R. A. Montgomery. 2015. Photoperiod constraints on tree phenology, performance and migration in a warming world. Plant, Cell & Environment 38: 1725-1736.

Wilczek, A. M., L. T. Burghardt, A. R. Cobb, M. D. Cooper, S. M. Welch, and J. Schmitt. 2010. Genetic and physiological bases for phenological responses to current and predicted climates. Philosophical Transactions of the Royal Society B 365: 3129-3147. https://doi.org/10.1098/rstb.2010.0128

Williams, A. P., C. D. Allen, A. K. Macalady, D. Griffin, C. A. Woodhouse, D. M. Meko, T. W. Swetnam, S. A. Rauscher, R. Seager, H. D. Grissino-Mayer, J. S. Dean, E. R. Cook, C. Gangodagamage, M. Cai, and N. G. McDowell. 2012. Temperature as a potent driver of regional forest drought stress and tree mortality. Nature Climate Change 3: 292-297.

Wilson, K. B., D. D. Baldocchi, and P. J. Hanson. 2000. Quantifying stomatal and non-stomatal limitations to carbon assimilation resulting from leaf aging and drought in mature deciduous tree species. Tree Physiology 20: 787-797.

Wolkovitch, E. M., B. I. Cook, J. M. Allen, T. M. Crimmins, J. L. Betancourt, S. E. Travers, S. Pau, J. Regetz, T. J. Davies, N. J. B. Kraft, T. R. Ault, K. Bolmgren, S. J. Mazer, G. J. McCabe, B. J. McGill, C. Parmesan, N. Salamin, M. D. Schwartz, and E. E. Cleland. 2012. Warming experiments underpredict plant phenological responses to climate change. Nature 485: 494-497.

Zangerl, A. R., A. M. Arntz, and M. R. Berenbaum. 1997. Physiological price of an induced chemical defense: Photosynthesis, respiration, biosynthesis, and growth. Oecologia 109: 433-441.

Zhao, M., and S. W. Running. 2010. Drought-induced reduction in global terrestrial net primary production from 2000 through 2009. Science 329: 940-943.

Figure 2.1 - Conceptual diagram of phenological shifts and consequent changes to net carbon assimilation

(a) As spring temperatures in temperate forests increase with climate change, leaf expansion phenology of canopy trees (green triangles) is expected to shift earlier. However, it is unclear if leaf expansion of tree seedlings (blue circles) will shift at a rate that is (i) slower than, (ii) equal to, or (iii) faster than the rate of canopy phenology shifts. This has strong implications for the ability of seedlings to access light (height of black bars). (b) Net carbon accumulation (black) is calculated as the sum of gross carbon assimilation (solid grey) and gross respiration costs (hatched grey). Under current climate conditions, tree seedlings are able to maintain slightly positive net carbon accumulation due to assimilation being greater than respiration. However, carbon accumulation in future climate conditions will depend on whether seedlings experience decreased (i), maintained (ii), or increased (iii) access to spring light and an associated increase in gross carbon assimilation.

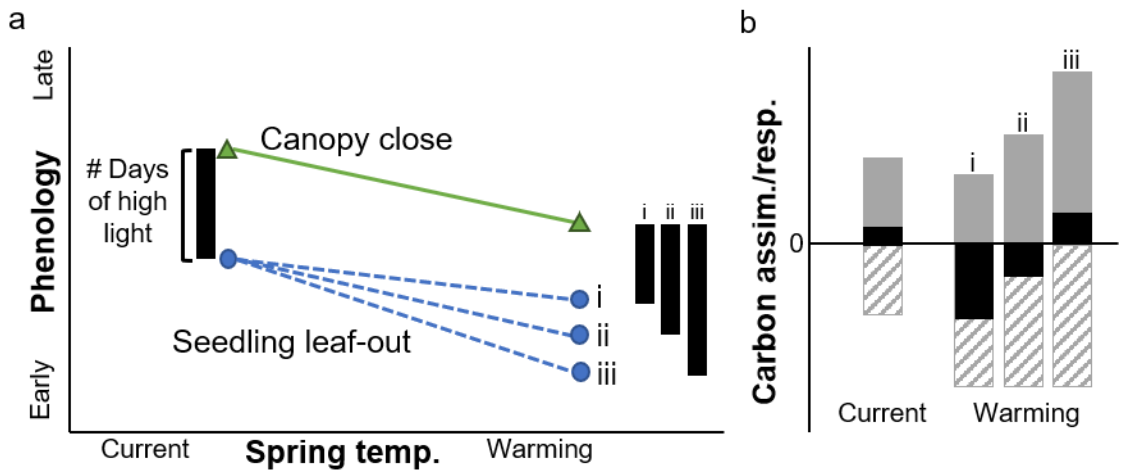

Figure 2.2 - Phenological shifts in response to temperature

(a and d): Observed (symbols, jittered slightly so they are distinguishable from on another) day of year of (a) canopy closure and seedling leaf out phenology as a function of average March-April (listed here as 'spring') and February temperatures, and (d) canopy reopening and seedling senescence phenology as a function of average August temperatures. Lines represent posterior predicted means (bold lines) and 95% predictive intervals (light lines). (b and e): Posterior estimated mean values (and 95% confidence intervals) of phenology model β parameters for (b) spring and (e) fall phenology. Posterior estimates are considered significant if the confidence interval does not overlap 0. (c and f): Predicted phenology dates (means and 95% predictive intervals) for (c) seedling leaf out and canopy closure and (f) seedling senescence and canopy reopening under current average climate conditions (C), a moderate climate change scenario (S1), and a business as usual climate change scenario (S2).

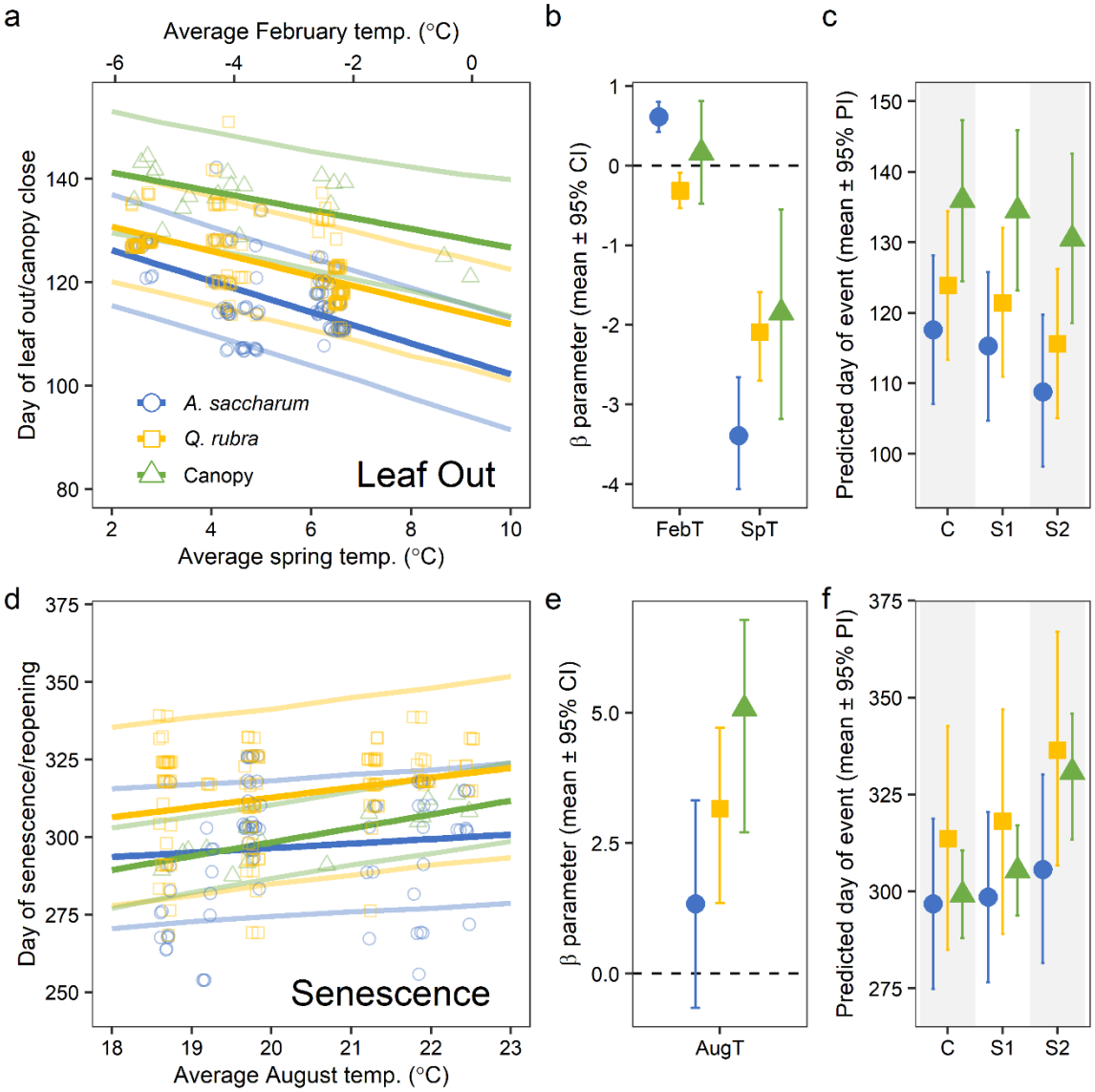

Figure 2.3 - Seasonal carbon assimilation: A. saccharum seedlings

Posterior estimates of mean daily net assimilation rates (a and b) and simulated net carbon accumulation (c and d) of *A. saccharum* seedlings planted beneath *A. saccharum* (left two panels) and *Q. rubra* (right panels) canopy trees. Line type and color represent predictions under current climate conditions (solid, black), climate in 2100 under Scenario 1 (dashed, blue), and under Scenario 2 (dotted, red). *Values fall outside the range of the figure; the full extent of this panel is included in Appendix S1: Figure S7.

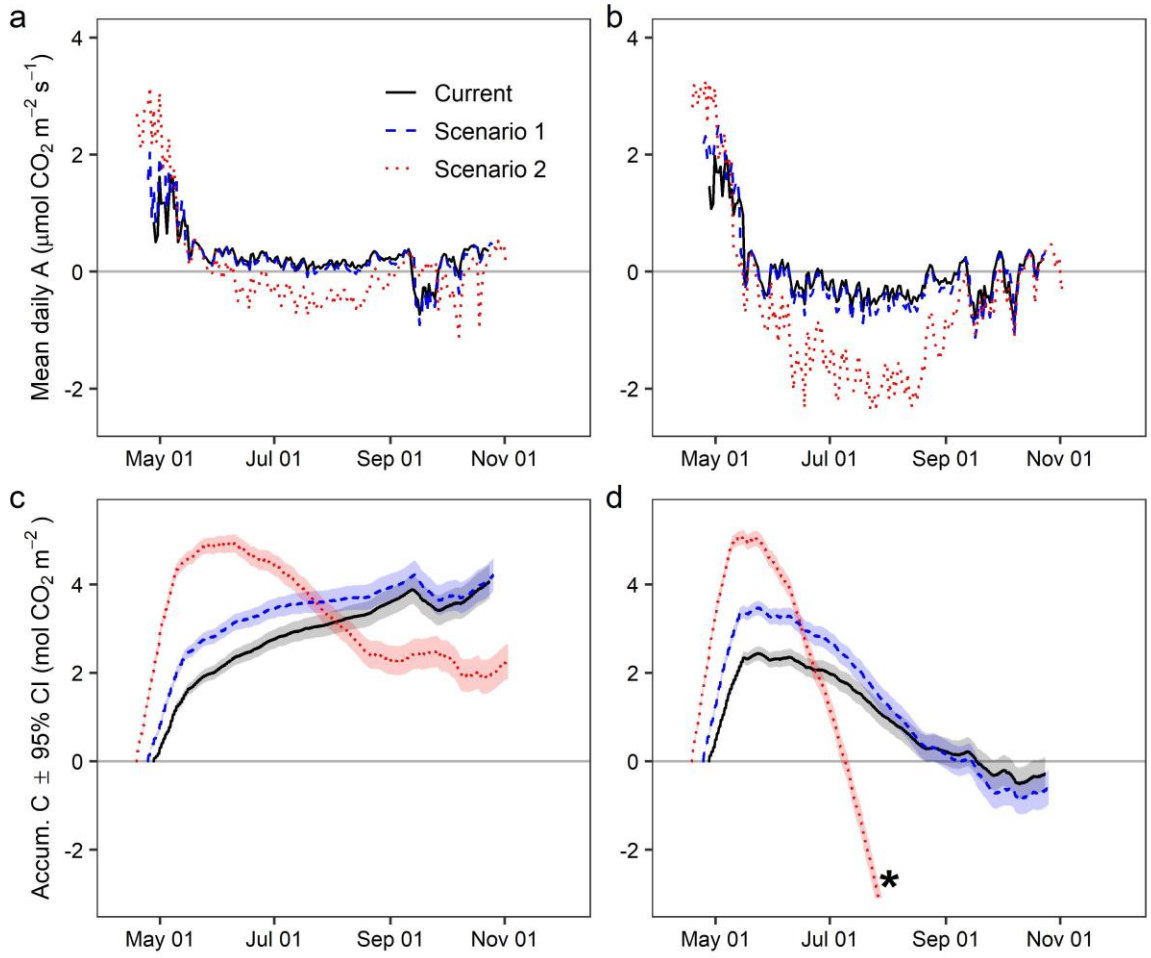

Figure 2.4 - Seasonal carbon assimilation: Q. rubra seedlings

Posterior estimates of mean daily net assimilation rates (a and b) and simulated net carbon accumulation (c and d) of *Q. rubra* seedlings planted beneath *A. saccharum* (left two panels) and *Q. rubra* (right panels) canopy trees. Line type and color represent predictions under current climate conditions (solid, black), climate in 2100 under Scenario 1 (dashed, blue), and under Scenario 2 (dotted, red).

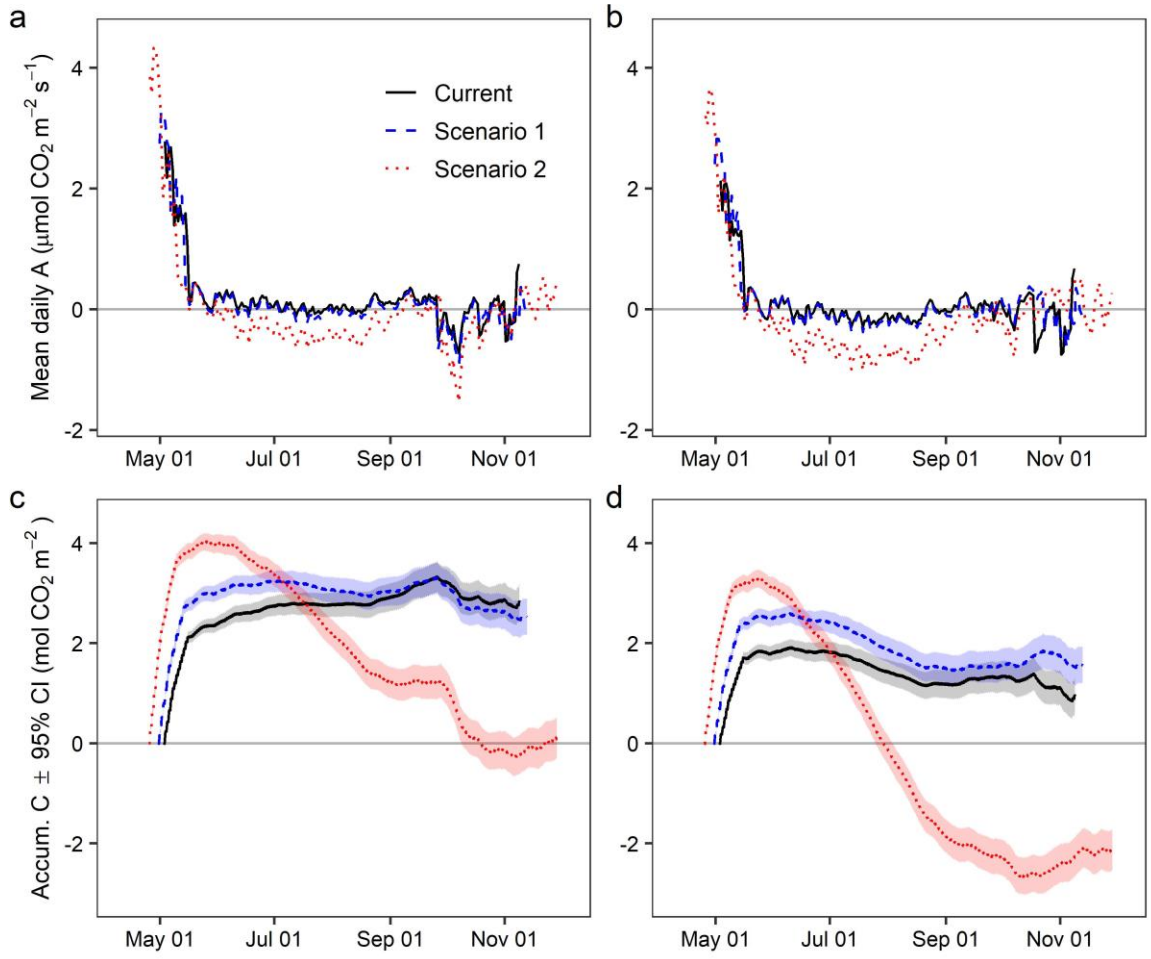

Figure 2.5 - Projected annual carbon assimilation

Predicted annual carbon gain, carbon loss, and carbon accumulated over one growing season for *A. saccharum* (blue) and *Q. rubra* (yellow) seedlings planted under (a) *A. saccharum* and (b) *Q. rubra* canopy trees in current climate conditions and two climate change scenarios. Lighter-colored bars represent gross carbon assimilation and hatched bars represent gross respiration.

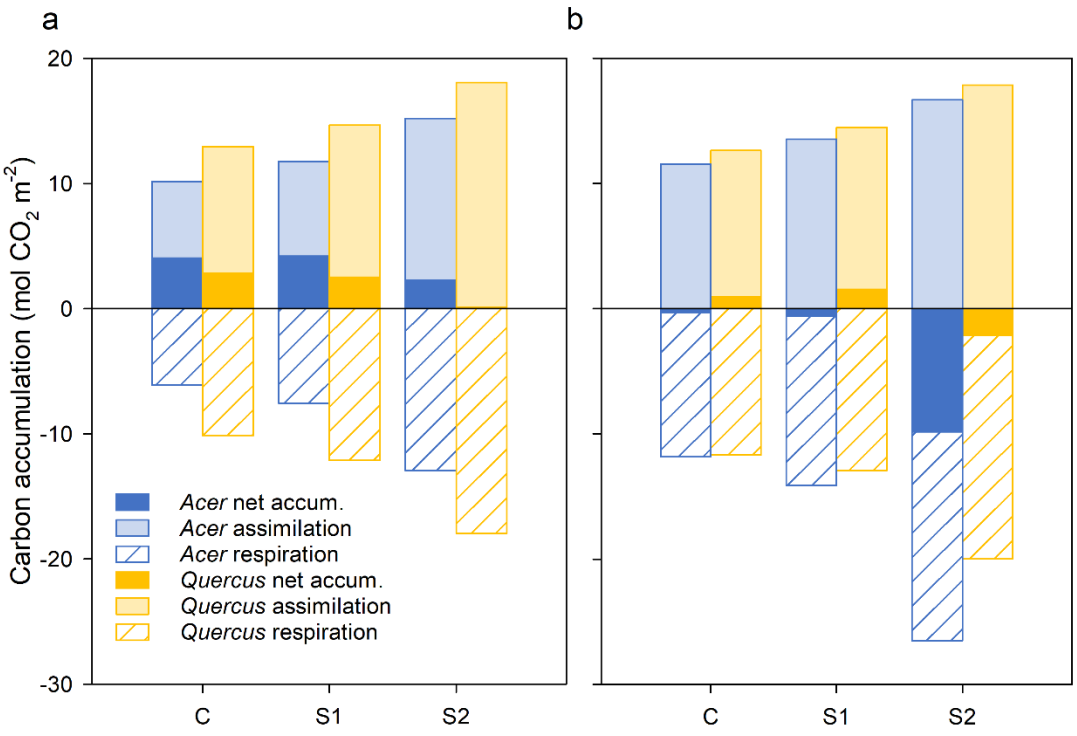

Supporting Information 2.1 - Supplementary Tables and Figures

Table SI 2.1 - Seed sources

Seed source and planting information for each cohort of both species. *A. saccharum* was not planted in 2015 due to poor seed quality and insufficient germination. Seedlings were planted at all three sites in 2014, but due to insufficient germination in 2015 and 2016, we only planted at a subset of the sites. Site abbreviations: Radrick Forest (RF), George Reserve (GR), and Saginaw Forest (SF). *Seeds obtained from Sheffield's Seed Company, coordinates unspecified.

Year	Species	North/ South		Source Coordinates	Number of Seedlings	Sites Planted
2014	*Acer saccharum*	North		46.8005, -89.6304	75	All sites
				46.6004, -85.2085	10	RF, GR
		South		42.659685, -84.440532	85	All sites
	Quercus rubra	North		44.9232, -84.6967	25	GR
				45.8769, -87.0477	60	RF, SF
		South		Illinois*	85	All sites
2015	*Quercus rubra*	South		42.436982, -84.559407	30	RF
2016	*Acer saccharum*	South		Kentucky* (Northern Zone 6)	120	RF, GR
	Quercus rubra	South		42.437869, -84.560008	120	RF, GR

Table SI 2.2 - Climate projections for study region

Predicted changes in temperature and soil moisture for scenarios S1 and S2.

Season	**Predicted [CO_2] (ppm)**		**Predicted Change in Temperature (°C)**		**Predicted Change in Soil Moisture (%)**	
	S1	*S2*	*S1*	*S2*	*S1*	*S2*
Winter (Dec-Feb)	550	970	1.4	4.1	20.0	14.5
Spring (Mar-May)			0.9	3.3	11.0	35.6
Summer (June-Aug)			1.2	6.2	10.2	-38.8
Fall (Sep-Nov)			1.5	4.6	-3.3	15.2

Table SI 2.3 - Seasonal carbon assimilation

Integrated gross carbon assimilation (μmol CO_2 m^{-2}; means and 95% predictive intervals) binned seasonally for each of the three climate simulations. These values were calculated by setting respiration rate to 0 μmol CO_2 m^{-2} s^{-1} and therefore represent only carbon gained from photosynthesis

		Acer canopy			*Quercus* canopy		
	Season	**Current**	**Scen. 1**	**Scen. 2**	**Current**	**Scen. 1**	**Scen. 2**
Acer seedlings	Spring	1.87 (1.80, 1.95)	2.74 (2.66, 2.82)	5.00 (4.91, 5.10)	2.56 (2.48, 2.65)	3.62 (3.56, 3.68)	5.37 (5.31, 5.43)
	Summer	5.99 (5.93, 6.04)	6.58 (6.53, 6.63)	7.99 (7.96, 8.01)	6.44 (6.42, 6.46)	7.23 (7.21, 7.25)	8.78 (8.76, 8.79)
	Fall1	1.07 (1.05, 1.08)	1.31 (1.30, 1.32)	1.81 (1.75, 1.87)	1.18 (1.18, 1.19)	1.43 (1.42, 1.44)	2.11 (2.06, 2.16)
	Fall2	1.22 (1.17, 1.26)	1.15 (1.10, 1.19)	0.40 (0.39, 0.41)	1.37 (1.36, 1.38)	1.25 (1.24, 1.26)	0.42 (0.42, 0.43)
	Total	**10.14 (10.05, 10.14)**	**11.77 (11.67, 11.87)**	**15.20 (15.09, 15.32)**	**11.55 (11.46, 11.64)**	**13.53 (13.46, 13.60)**	**16.68 (16.60, 16.76)**
Quercus seedlings	Spring	2.67 (2.59, 2.75)	3.45 (3.37, 3.53)	4.66 (4.58, 4.75)	2.33 (2.25, 2.41)	3.18 (3.10, 3.26)	4.22 (4.14, 4.29)
	Summer	7.69 (7.68, 7.71)	8.30 (8.28, 8.31)	9.24 (9.22, 9.25)	7.73 (7.71, 7.74)	8.34 (8.32, 8.35)	9.34 (9.32, 9.36)
	Fall1	1.30 (1.29, 1.30)	1.66 (1.65, 1.67)	3.02 (3.01, 3.03)	1.28 (1.25, 1.30)	1.72 (1.70, 1.73)	3.17 (3.15, 3.18)
	Fall2	1.30 (1.28, 1.32)	1.26 (1.25, 1.27)	1.15 (1.14, 1.16)	1.31 (1.29, 1.33)	1.25 (1.24, 1.26)	1.13 (1.12, 1.14)
	Total	**12.96 (12.88, 13.04)**	**14.66 (14.58, 14.75)**	**18.07 (17.98, 18.15)**	**12.64 (12.55, 12.72)**	**14.49 (14.41, 14.57)**	**17.86 (17.78, 17.94)**

Table SI 2.4 - Seasonal respiration

Integrated gross carbon loss due to respiration (μmol CO_2 m^{-2}; means and 95% predictive intervals) binned seasonally for each of the three climate simulations.

		Acer canopy			*Quercus* canopy		
	Season	**Current**	**Scen. 1**	**Scen. 2**	**Current**	**Scen. 1**	**Scen. 2**
Acer seedlings	Spring	0.24 (0.23, 0.25)	0.35 (0.34, 0.37)	0.66 (0.64, 0.69)	0.22 (0.23, 0.21)	0.29 (0.28, 0.30)	0.43 (0.41, 0.44)
	Summer	3.74 (3.70, 3.79)	4.75 (4.69, 4.80)	9.83 (9.73, 9.94)	8.57 (8.45, 8.67)	10.51 (10.37, 10.64)	23.31 (23.02, 23.59)
	Fall1	1.43 (1.38, 1.47)	1.79 (1.73, 1.84)	2.23 (2.18, 2.28)	1.60 (1.54, 1.66)	2.15 (2.08, 2.22)	2.38 (2.32, 2.45)
	Fall2	0.66 (0.65, 0.68)	0.67 (0.65, 0.69)	0.21 (0.20, 0.22)	1.45 (1.40, 1.49)	1.16 (1.13, 1.20)	0.39 (0.37, 0.41)
	Total	**6.08 (6.01, 6.15)**	**7.56 (7.47, 7.64)**	**12.94 (12.82, 13.06)**	**11.84 (11.70, 11.97)**	**14.11 (13.95, 14.26)**	**26.51 (26.22, 26.80)**
Quercus seedlings	Spring	0.55 (0.53, 0.58)	0.73 (0.69, 0.76)	1.02 (0.98, 1.06)	0.63 (0.60, 0.66)	0.83 (0.79, 0.86)	1.16 (1.11, 1.20)
	Summer	6.48 (6.42, 6.55)	7.71 (7.63, 7.79)	11.62 (11.50, 11.74)	8.09 (8.00, 8.18)	9.15 (9.05, 9.25)	14.65 (14.49, 14.80)
	Fall1	1.69 (1.64, 1.74)	2.31 (2.25, 2.37)	4.38 (4.30, 4.47)	1.23 (1.19, 1.26)	1.40 (1.37, 1.44)	3.02 (2.96, 3.08)
	Fall2	1.40 (1.36, 1.44)	1.39 (1.35, 1.43)	0.92 (0.89, 0.95)	1.74 (1.69, 1.79)	1.54 (1.50, 1.58)	1.16 (1.13, 1.20)
	Total	**10.13 (10.04, 10.23)**	**12.13 (12.02, 12.25)**	**17.95 (17.79, 18.11)**	**11.68 (11.57, 11.79)**	**12.93 (12.81, 13.04)**	**19.99 (19.81, 20.16)**

Figure SI 2.6 - Example light data

Examples of how canopy closure (a, from 2015) and reopening (b, from 2018) were calculated from site-level light data. Colors represent different sites, horizontal lines represent the thresholds described in the text (100 and 20 μmol m^2 s^{-1} in spring and fall, respectively), and vertical lines represent the calculated day of event for each site.

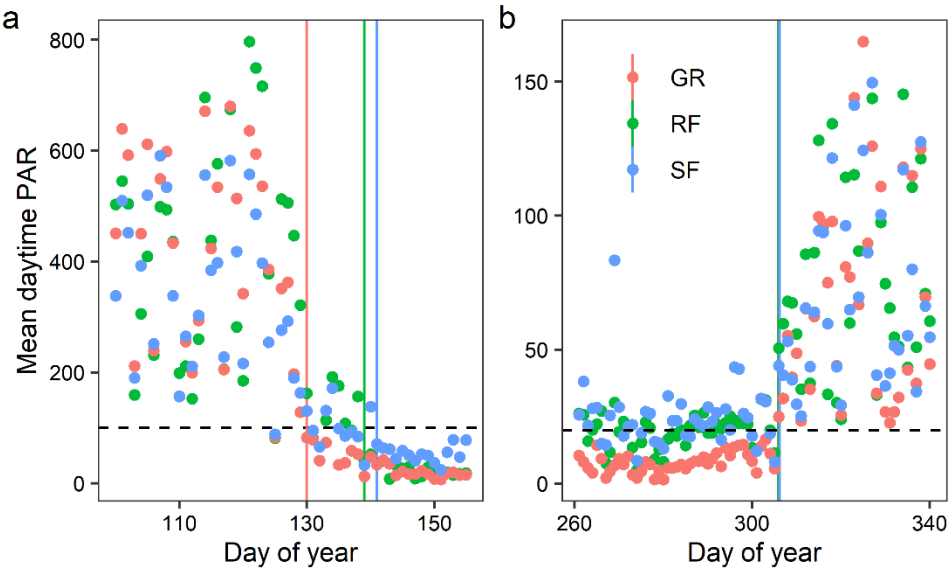

Figure SI 2.7 - General modeling framework

General modeling framework used for this study. Tab icons represent model input data, rectangles represent model parameter outputs and simulations, and the oval represents the final simulated estimation of net carbon assimilation. Model flow is described for our seedling photosynthetic models (i), seedling and canopy phenology models (ii), environmental simulation data generation (iii), and model integration (iv). Colors indicate data and parameters associated with gas exchange and photosynthesis (blue), phenology (green), climate/environment (yellow), and model integration and final calculations (orange).

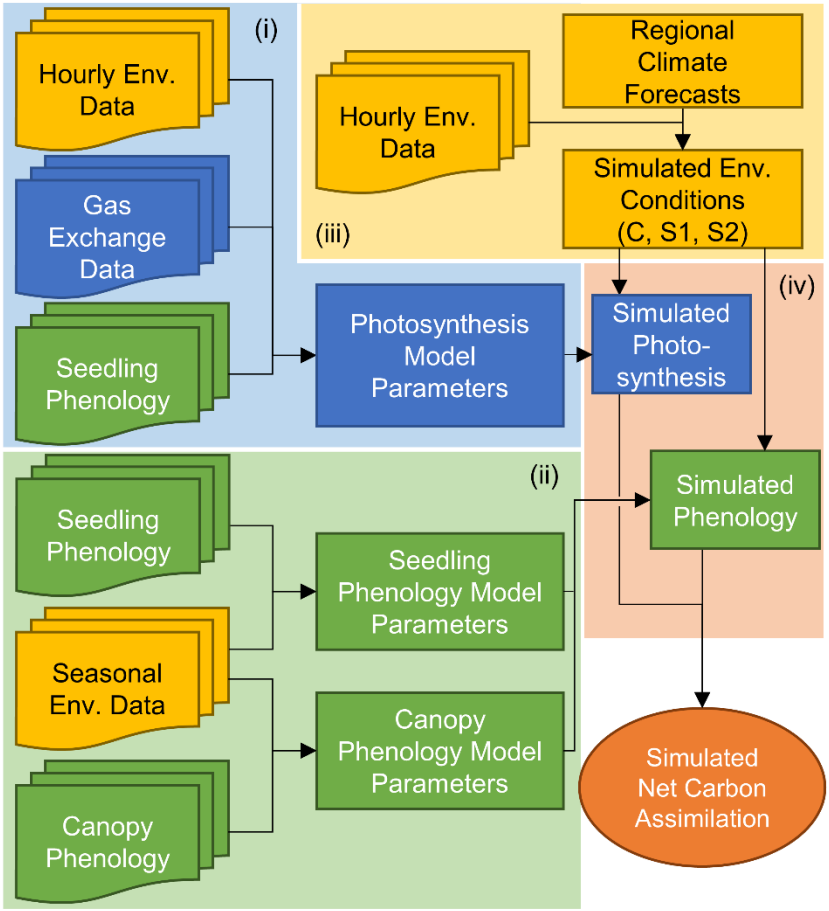

Figure SI 2.8 - Initial leaf coloring phenology

(a) Observed (symbols) day of canopy reopening and seedling initial leaf color change as a function of average August temperatures. Lines represent posterior predicted means (bold lines) and 95% predictive intervals (light lines). (b) Posterior estimated mean values (and 95% confidence intervals) of phenology model β parameters. Posterior estimates are considered significant if the confidence interval does not overlap 0. (c) Predicted phenology dates (means and 95% predictive intervals) for initial leaf color change and canopy reopening under current average climate conditions (C), a moderate climate change scenario (S1), and a business as usual climate change scenario (S2).

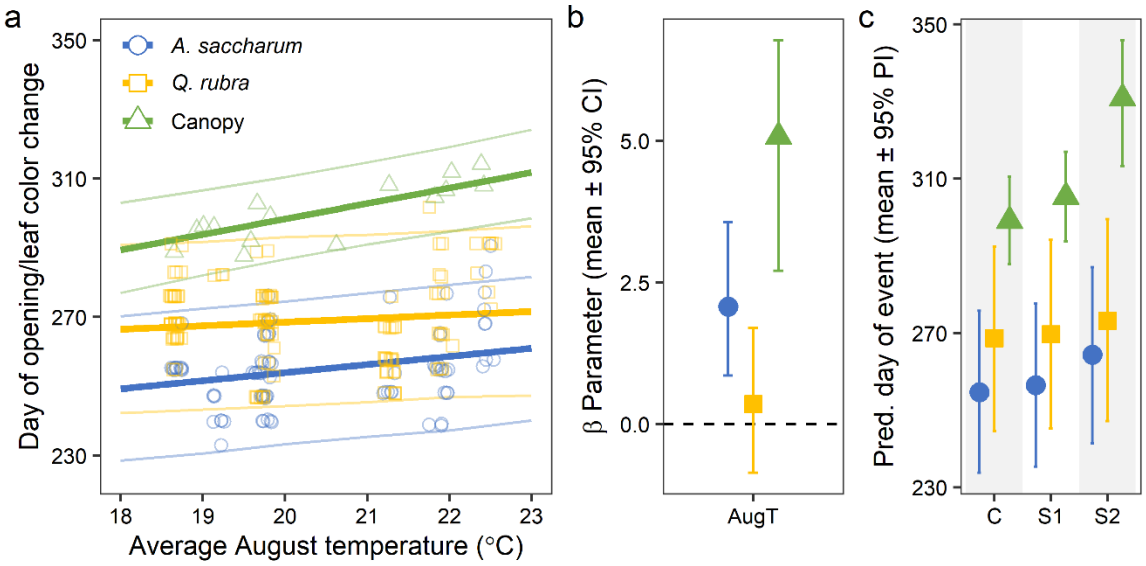

Figure SI 2.9 - 50% leaf coloring phenology

(a) Observed (symbols) day of canopy reopening and seedling 50% leaf color change as a function of average August temperatures. Lines represent posterior predicted means (bold lines) and 95% predictive intervals (light lines). (b) Posterior estimated mean values (and 95% confidence intervals) of phenology model β parameters. Posterior estimates are considered significant if the confidence interval does not overlap 0. (c) Predicted phenology dates (means and 95% predictive intervals) for 50% leaf color change and canopy reopening under current average climate conditions (C), a moderate climate change scenario (S1), and a business as usual climate change scenario (S2).

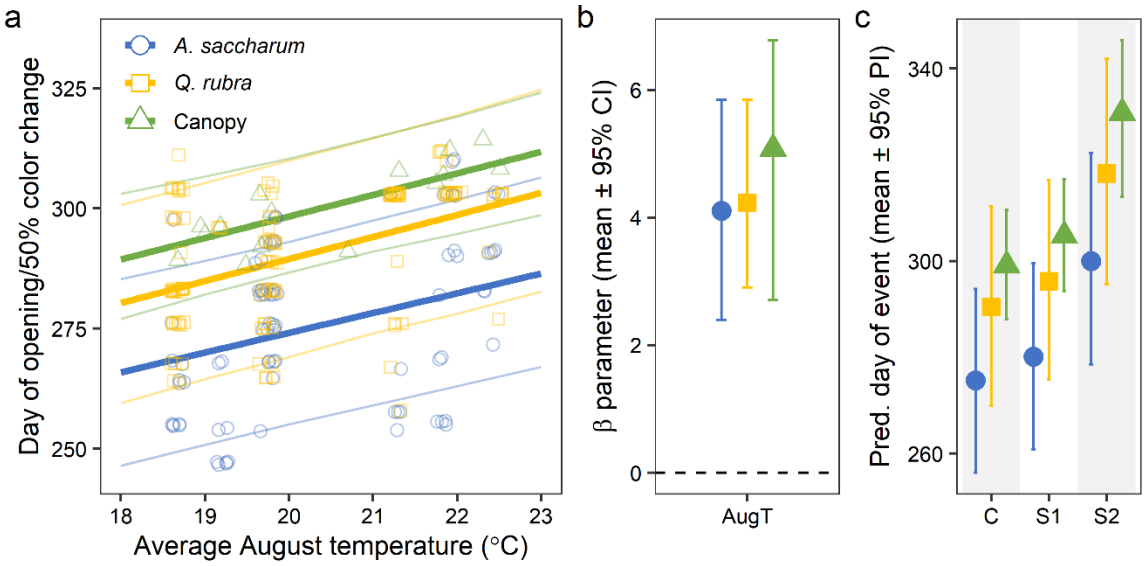

Figure SI 2.10 - Posterior estimates of photosynthetic parameters

Posterior estimates of temperature-corrected photosynthetic parameters (means ± 95% confidence intervals for *A. saccharum* (blue) and *Q. rubra* (yellow) seedlings planted under *A. saccharum* (circles) and *Q. rubra* (triangles) canopy trees.

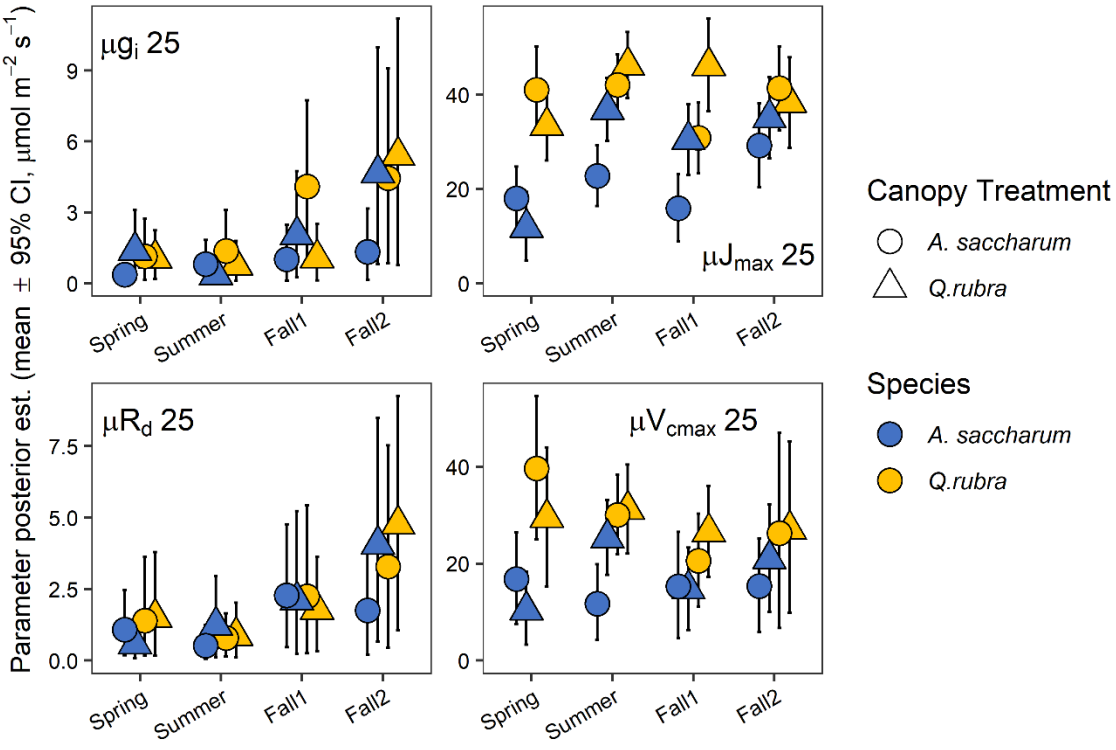

Figure SI 2.11 - Posterior estimates of SM and VPD effects

Posterior estimates (means and 95% confidence intervals) for the direct effects of soil moisture (SM) and VPD on Rubisco carboxylation-limited (V_{cmax}, a-b) and RuBP regeneration-limited (J_{max}, c-d) carbon assimilation rates. Colors indicate posterior estimates for *A. saccharum* seedlings (blue) and *Q. rubra* seedlings (yellow). Effects are considered significant if 95% confidence intervals do not overlap 0.

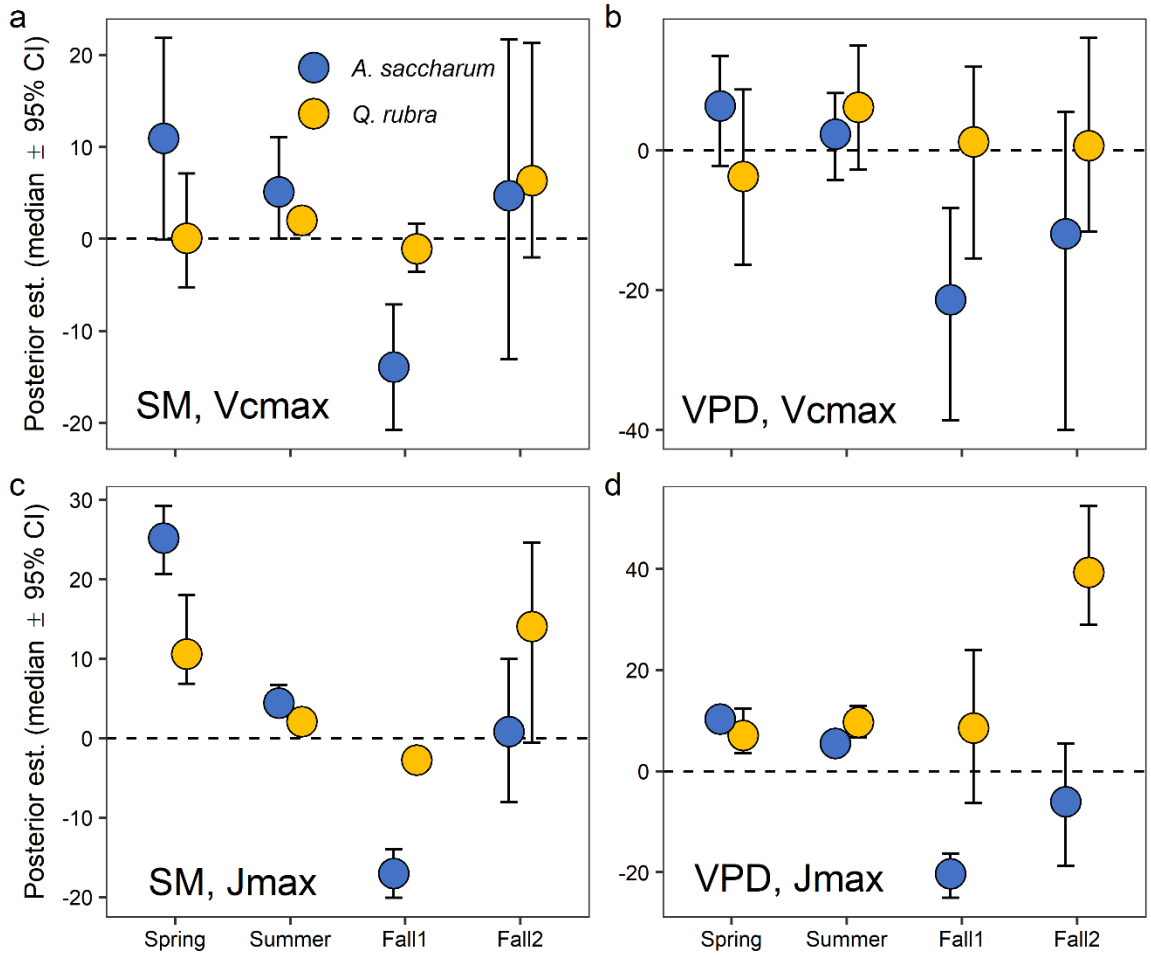

Figure SI 2.12 - Full version of Fig. 2.3d

Entire extent of net carbon accumulation of *A. saccharum* seedlings planted under *Q. rubra* canopy trees. See Figure 2.3 for a full description of the graph.

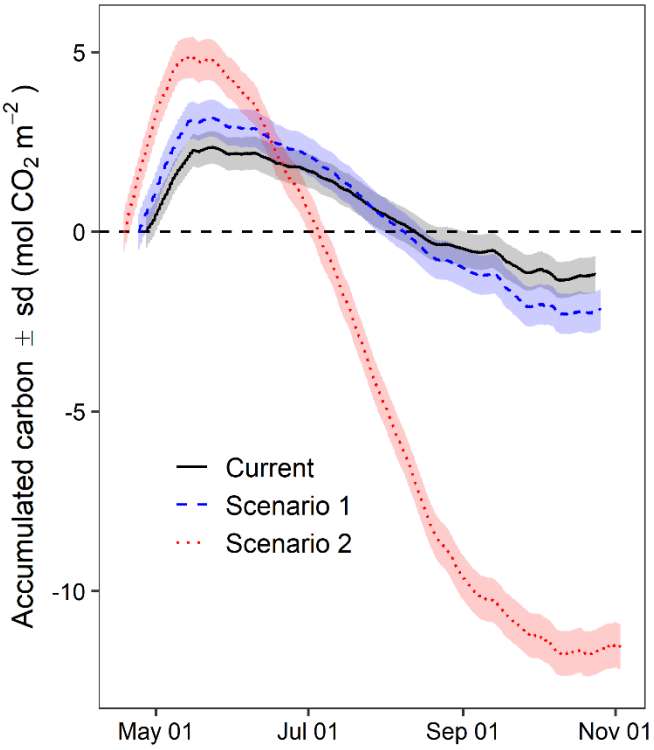

Supporting Information 2.2 - Full description of photosynthesis model

The photosynthetic model we use in this analysis is minimally modified from the model previously published by Peltier and Ibáñez (2015).

Model Description

Following Peltier and Ibáñez (2015), the observed assimilation rate, A_{obs}, for observation i at light level Q and at intercellular CO_2 concentration Ci, was modeled with a Normal likelihood function with mean μA and variance σ^2:

$$A_{obs_i} \sim Normal(\mu A, \sigma^2) \tag{1}$$

where the value of μA depends on the transitional concentration of CO_2 (C_{crit}). When a plant is Rubisco carboxylation-limited (i.e. when $Ci < C_{crit}$), $\mu A = A_V$, and when a plant is RuBP-regeneration-limited (i.e. when $Ci > C_{crit}$), $\mu A = A_J$. For each observation i in curve c, the assimilation rate is thus equal either to:

$$A_{V_i} = \frac{-b1_i + \sqrt{{b1_i}^2 - 4 \times a1_i \times c1_i}}{2 \times a1_i} \tag{2}$$

where

$$a1_i = -\frac{1}{g_{m_c}} \tag{2a}$$

$$b1_i = \frac{V_{cmax_c} - R_{d_c}}{g_{m_c}} + Ci_i + K_{c_c}\left(\frac{1 + O_i}{K_{o_c}}\right) \tag{2b}$$

$$c1_i = R_{d_c}\left(Ci_i + K_{c_c}\left(\frac{1 + O_i}{K_{o_c}}\right)\right) - V_{cmax_c}(Ci_i - {\Gamma^*}_c) \tag{2c}$$

or to:

$$A_{J_i} = \frac{-b2_i + \sqrt{{b2_i}^2 - 4 \times a2_i \times c2_i}}{2 \times a2_i} \tag{3}$$

where

$$a2_i = -\frac{1}{g_{m_c}} \tag{3a}$$

$$b2_i = \frac{\left(J_i/4\right) - R_{d_c}}{g_{m_c}} + Ci_i + \Gamma^*{}_c \tag{3b}$$

$$c2_i = R_{d_c}(Ci_i + 2\Gamma^*{}_c) - \frac{J_i}{4}(Ci_i - \Gamma^*{}_c) \tag{3c}$$

Electron transport rate (J_i) incorporates light dependency:

$$J_i = \frac{Q2_i + J_{max_c} - \sqrt{\left(Q2_i + J_{max_c}\right)^2 - 4 \times \theta_{season(c),plant(c)} \times Q2_i \times J_{max_c}}}{2 \times \theta_{season(c),plant(c)}} \tag{4}$$

$$Q2_i = \frac{Q_i \times \alpha(1-f)}{2} \tag{5}$$

The seedlings used in this study did not encounter conditions in which their photosynthetic rate was limited by triose phosphate utilization (TPU; Lombardozzi et al. 2018), and so it was not included in our model fit.

Parameters were estimated at the curve level to account for substantial variation among individuals. Seasonal bins were assigned to each measurement based on light availability or leaf-level foliar phenology. For a detailed list of parameters, their definitions, and the prior distributions we used to estimate their values, see Table SI 2.5. Measurements taken at the beginning of the growing season before canopy closure (assessed *post hoc*, as described in the text) were placed in the Spring bin. Following canopy closure, measurements fell into the Summer bin until the leaf being measured had begun to change color. Measurements taken between initial color change and when the leaf had achieved >50% color change were binned into Fall1 and any measurements taken between then and leaf senescence were binned into Fall2.

As with Peltier and Ibáñez (2015), we allowed the θ parameter, an empirical curvature factor for the light dependency equation (Eq. 4) to vary across season (fixed effects) and plants (random effects):

$$\theta_{season(c),plant(c)} \sim Normal\left(\mu\theta_{season(c)}, \theta\sigma^2{}_{season(c)}\right) \quad (6)$$

Because this parameter is calculated only using data from the A-Q curves and not from the A-Ci curves, we presume that parameter value in each A-Ci curve is equal to that of the A-Q curve measured immediately before it.

The model uses linear Arrhenius functions standardized to 25 °C to account for temperature dependence in Rubisco carboxylation and oxygenation rates (Bjorkman et al. 1980, Patrick et al. 2009). Maximum Rubisco carboxylation rate, maximum electron transport rate, mesophyll conductance, dark respiration, Michaelis-Menten constants for oxygenation and carboxylation, and CO_2 photocompensation points (V_{cmax}, J_{max}, g_m, R_d, K_c, K_o, and Γ^*, respectively) are all temperature-corrected for each curve, c, at temperature T_i. Following Peltier and Ibáñez (2015), the same function was used for all seven parameters (p), where $p25_c$ is the value of the parameter at 25 °C for curve c and E_p is its associated activation energy:

$$p_c = p25_c \times \mathrm{Exp}\left(E_p(T_i - 298)/(298 \times R \times T_i)\right) \quad (7)$$

We also found relationships between light- and CO_2-saturated assimilation rates and soil moisture by season. In contrast to Peltier and Ibáñez (2015), we found no difference in VPD across planting treatments, but instead found differences in VPD by season in our preliminary data analysis. We therefore incorporated similar linear terms for seasonal variation in soil moisture (as volumetric water content) and VPD for V_{cmax} and J_{max} using mean-centered data (see *Soil Moisture Sub-model* and *VPD Sub-model* below) in a semi-mechanistic model:

$$p_c = p25_c \times \exp\left(E_p(T_i - 298)/(298 \times R \times T_i)\right) + \beta 1_{season(c)} soil\ m_c + \beta 2_{season(c)} VPD_c \quad (8)$$

Importantly, the addition of soil moisture and VPD here means that estimates for V_{cmax} and J_{max} in our model are not equal to the 'true' values of these parameters in the absence of stomatal limitation, but rather they represent 'effective' V_{cmax} and J_{max} under the mean environmental

conditions observed in a given species and planting treatment for that species (Peltier and Ibáñez 2015).

The version of this model used by Peltier and Ibáñez (2015) included habitat differences in their calculations of temperature-corrected $V_{cmax}25$ and $J_{max}25$ because of potential differences in acclimation to light levels between their gap and understory planting treatments. Seedlings in our experiment did not experience different access to light across planting treatments throughout most of the growing season (data not shown), however in our preliminary data analysis we found that including planting treatment (i.e., canopy tree under which they were planted) significantly improved model performance. Additionally, results from our preliminary analysis showed that mesophyll conductance and daytime dark respiration also varied with planting treatment, so we decided to account for all four parameters in the same way, taking into account seedling-level variation at the same time:

$$p25_c = \alpha p25_{season(c),treatment(c),plant(c)} \tag{9}$$

$$\alpha p25_{season(c),treatment(c),plant(c)} \sim Normal\left(\mu p25_{season,treatment},\ p\sigma^2{}_{season,treatment}\right) \tag{10}$$

We fit the model and obtained posterior densities of each parameter using OpenBUGS 3.2.3 software (Lunn et al. 2009). We ran models separately for each species using two chains for a burn-in of 50,000 iterations, after which samples were monitored to assess convergence of the chains using the Brooks-Gelman-Rubin statistic (Gelman and Rubin 1992). Chains were run after convergence to obtain at least 3000 independent samples for all parameters after thinning to remove within-chain autocorrelation. Model fit was evaluated using the R^2 between predicted and observed values. Parameter posterior estimates (mean, standard deviation, and 95% credible intervals) are reported in Table SI 2.6.

Soil Moisture Sub-model

We collected two soil moisture measurements concurrently with each photosynthetic sample (one sample included one *A*-*Q* and one *A*-*Ci* curve) and then estimated the hourly soil moisture environment of each seedling by fitting individual regressions as described in Peltier and Ibáñez (2015). Seedling soil moisture measurements (response variable) were predicted using site-level average hourly HOBO microstation soil moisture data (explanatory variable, see Supporting Information 2.3 for how hourly averages were calculated). The subsequent fit was used to predict soil moisture for individual seedlings at specific times *t*:

$$Soil\ moisture_t \sim Normal(\mu_t, \sigma^2)$$

$$1/\sigma^2 \sim Gamma(0.01, 0.01)$$

Process:

$$\mu_t = \alpha_{seedling(t)} + \beta_{seedling(t)} * HOBO_t$$

Priors:

$$\alpha_{seedling(t)}, \beta_{seedling(t)} \sim Normal(0, 1000)$$

Curve-level and hourly soil moisture were then standardized around the mean soil moisture from the hourly data for use in fitting the photosynthetic model and for calculating assimilation in our climate projections, respectively:

$$tSoilM_{curve/hour} = \frac{SoilM_{curve/hour} - meanSoilM}{2 * sdSoilM}$$

Model code and data are available (see Data Availability).

VPD Sub-model

Rather than include a specific sub-model for VPD (Peltier and Ibáñez 2015), we decided to account for changes in VPD associated with climate change by combining individual seedling-

level VPD data collected by the LI-6400 during photosynthetic measurements and hourly VPD calculated from hourly temperature (*T*, °C) and relative humidity (*RH*, %) HOBO microstation data (see Supporting Information 2.3 for how hourly averages were calculated). Hourly VPD was then calculated using the Arrhenius equation:

$$es = 0.6108 * e^{17.27*(T/T+237.3)}$$

$$ea = \frac{RH}{100} * es$$

$$VPD = ea - es$$

As with soil moisture, curve-level and hourly VPD (*tVPD*; for use in the photosynthetic model and climate change projection models, respectively) were converted to a standardized value (*tVPDS*) following Peltier and Ibáñez (2015) using mean and standard deviation calculated from the average hourly VPD calculations:

$$tVPDS_{curve/hour} = \frac{\left(tVPD_{curve/hour} - meanVPD\right)}{2 * sdVPD}$$

Table SI 2.5 - Photosynthesis model terms

Definitions of model parameters and hyperparameters used in photosynthetic model. Subscripts indicate the level at which the parameter is estimated: individual observation (*i*), curve (*c*), season (*s*), planting treatment (*t*), or plant (*p*). Parameters without subscripts are estimated at the species level. Prior distributions can be found in the model description above and in Peltier and Ibáñez (2015, Table 1).

Abbreviation	**Definition (units)**
σ	Model standard deviation
Av_i, Aj_i	Rubisco carboxylation- and RUBP regeneration-limited rates of CO_2 assimilation (μmol m^{-2} s^{-1})
α	PSII activity in bundle sheath (0.85, unitless)
($C_{crit(c)}$) Ci	(Transitional) Intercellular CO_2 concentration (Pa)
E_p	Activation energy for temperature responses of V_{cmax}, J_{max}, g_m, R_d, K_c, K_o, or Γ* (kJ mol^{-1})
f	Spectral light quality factor (0.15, unitless)
g_{m_c}	Mesophyll conductance (μmol m^{-2} s^{-1})
Γ^*_c	CO_2 compensation point without dark respiration (μmol m^{-2} s^{-1})
J_{max_c}	Maximum electron transport rate (μmol m^{-2} s^{-1})
K_{c_c}, K_{o_c}	Michaelis-Menten constants for Rubisco for CO_2 and O_2 (Pa, kPa)
O_i	Intercellular O_2 partial pressure (Pa)
P_i	Pressure (Pa)
Q_i ($Q2_i$)	Photosynthetically active radiation (μmol m^{-2} s^{-1}) (absorbed by PSII)
R	Universal gas constant (0.008314 J K^{-1} mol^{-1})
R_{d_c}	Daytime rate of mitochondrial respiration (μmol m^{-2} s^{-1})
T_i	Leaf temperature (K)
V_{cmax_c}	Maximum Rubisco carboxylation rate (μmol m^{-2} s^{-1})
$\theta_{s,p}$, $\mu\theta_s$	Empirical curvature factor
$\theta\sigma^2_s$	Variance associated with $\mu\theta_s$
$p25_c$	Temperature adjusted V_{cmax}, J_{max}, g_m, R_d, Γ*; K_c; or K_o to 25 °C (μmol m^{-2} s^{-1}, Pa, kPa)
$\alpha p25_{s,t,p}$	Hyperparameter value for V_{cmax}, J_{max}, g_m, or R_d (μmol m^{-2} s^{-1})
$\mu p25_{s,t}$	Mean value for V_{cmax}, J_{max}, g_m, or R_d (μmol m^{-2} s^{-1})
$p\sigma^2{}_{s,t}$	Variance associated with $\alpha p25_{s,t,p}$ hyperparameters
$\beta 1_s$, $\beta 2_s$	Soil moisture ($\beta 1_s$) and VPD ($\beta 2_s$) coefficients for $V_{cmax}25$ and $J_{max}25$

Table SI 2.6 - Photosynthesis model posterior parameter estimates

Final model parameter estimates and 95% credible intervals. 95% credible intervals that do not overlap indicate significance. Different symbols indicate highly significant differences between species (*), seasons (a, b, c, d), or planting treatments (†).

		Acer saccharum	*Quercus rubra*
Parameter		Mean ± s.d. (95% CI)	Mean ± s.d. (95% CI)
Model	Variance	0.8489±0.0193* (0.8083, 0.8851)	0.3744±0.01348* (0.3355, 0.3954)
θm	Spring	0.224±0.0674 (0.1053, 0.3696)	0.5112±0.08364 (0.3355, 0.6761)
	Summer	0.3676±0.1015 (0.1842, 0.5904)	0.3839±0.07891 (0.2297, 0.5349)
	Fall1	0.3823±0.08754 (0.2083, 0.547)	0.3414±0.1095 (0.1013, 0.5459)
	Fall2	0.5018±0.1198 (0.2721, 0.7418)	0.5415±0.09515 (0.3634, 0.7326)
$\theta\tau$ ($1/\theta\sigma^2$)	Spring	164.5±189.2 (25.34, 710.1)	29.05±20.38 (10.88, 77.57)
	Summer	78.81±252.0 (12.18, 289.9)	38.15±32.57 (12.05, 119.4)
	Fall1	47.46±60.53 (12.84, 186.5)	136.9±573.8 (14.48, 748.4)
	Fall2	54.55±87.52 (13.31, 216.1)	41.08±34.9 (12.55, 141.0)
Temperature	E_{gm}	31.73±6.214 (20.07, 44.54)	23.28±5.46 (12.68, 33.4)
	E_{Rd}	108.9±11.48 (82.91, 125.4)	73.25±11.55 (45.92, 91.68)
	E_{Vcmax}	62.79±8.772 (46.47, 80.07)	76.28±8.404 (59.9, 92.4)
	E_{Jmax}	34.01±9.404 (15.62, 52.4)	27.09±9.543 (8.322, 45.84)
	E_{Kc}	57.56±8.582 (40.2, 74.13)	45.06±8.391 (28.72, 61.63)

	E_{Ko}	-10.64±4.579 (-19.35, -0.8589)	-21.6±3.909 (-29.16, -14.25)
	$E_{\Gamma*}$	155.0±18.3 (100.3, 175.6)	137.8±26.67 (43.32, 162.5)
Michaelis-Menten Constants	*Kc25*	27.82±3.019 (22.08, 34.15)	29.48±3.664 (22.55, 36.96)
	Ko25	16580±32.06 (16520, 16650)	16580±32.35 (16520, 16650)
Soil moisture linear effects on *Vcmax* (SM1)	Spring	10.8±5.602[a] (-0.09325, 21.83)	0.4084±3.636 (-5.23, 7.119)
	Summer	5.215±2.793[a] (0.0254, 11.08)	1.987±0.7396 (0.4592, 3.363)
	Fall1	-13.96±3.471*[b] (-20.77, -7.119)	-1.057±1.338* (-3.852, 1.691)
	Fall2	4.453±8.832[ab] (-13.09, 21.69)	7.06±5.771 (-1.993, 21.27)
Soil moisture linear effects on *Jmax* (SM2)	Spring	25.08±2.237*[a] (20.68, 29.23)	10.98±2.888*[a] (6.832, 17.99)
	Summer	4.512±0.9711*[b] (2.809, 6.686)	2.114±0.3167*[b] (1.528, 2.759)
	Fall1	-17.06±1.553*[c] (-20.09, -13.99)	-2.756±0.5673*[c] (-3.884, -1.684)
	Fall2	0.8902±4.623[b] (-8.024, 9.961)	13.11±6.852[ab] (-0.5896, 24.56)
VPD linear effects on *Vcmax* (VM1)	Spring	6.179±4.087[a] (-2.237, 13.44)	-3.719±6.621 (-16.39, 8.651)
	Summer	2.221±3.212[a] (-4.324, 8.16)	6.133±4.477 (-2.799, 14.96)
	Fall1	-21.84±7.651[b] (-38.67, -8.293)	0.3819±6.712 (-15.46, 11.91)
	Fall2	-13.16±11.73[ab] (-40.03, 5.513)	0.9717±6.873 (-11.7, 16.02)
VPD linear effects on *Jmax* (VM2)	Spring	10.27±1.134[a] (7.767, 12.39)	7.202±2.075[a] (3.546, 12.31)

	Summer	5.491±0.8425[b] (3.886, 7.136)	9.652±1.633[a] (6.619, 12.84)
	Fall1	-20.38±2.141*[c] (-25.04, -16.29)	8.668±7.81*[a] (-6.272, 23.99)
	Fall2	-6.234±6.085*[bc] (-18.68, 5.435)	39.94±5.982*[b] (29.01, 52.46)
µgm25 (*Acer saccharum* canopy)	Spring	0.3642±0.08927 (0.2303, 0.5907)	1.076±0.3505 (0.4828, 1.86)
	Summer	0.7742±0.355 (0.2712, 1.638)	1.319±0.4567 (0.5942, 2.354)
	Fall1	0.9614±0.3614 (0.3681, 1.814)	4.099±1.578 (0.6994, 6.728)
	Fall2	1.277±0.6224 (0.4226, 2.874)	4.379±1.55 (1.335, 7.094)
µgm25 (*Quercus rubra* canopy)	Spring	1.315±0.6386[ab] (0.3344, 2.846)	1.029±0.347 (0.421, 1.818)
	Summer	0.3386±0.1023[a] (0.1894, 0.5847)	0.7292±0.1912 (0.4071, 1.153)
	Fall1	1.952±0.7851[b] (0.5917, 3.683)	1.015±0.2965 (0.5915, 1.726)
	Fall2	4.557±1.388[b] (1.354, 6.938)	5.313±2.553 (0.7998, 10.75)
gm25 τ ($1/\sigma^2$) (*Acer saccharum* canopy)	Spring	37.59±28.76 (6.721, 110.2)	2.927±3.467 (0.5056, 12.91)
	Summer	10.02±15.12 (0.708, 55.39)	2.918±3.388 (0.4202, 12.52)
	Fall1	4.121±4.566 (0.6198, 18.01)	0.8738±3.425 (0.1017, 8.375)
	Fall2	3.226±4.456 (0.2453, 15.47)	0.4394±0.7987 (0.1022, 2.933)
gm25 τ ($1/\sigma^2$) (*Quercus rubra* canopy)	Spring	3.371±7.101[ab] (0.2013, 23.67)	6.598±8.875 (0.8123, 31.55)
	Summer	24.82±21.11[a] (4.302, 81.27)	6.936±5.023 (1.726, 20.84)

	Fall1	1.101±1.917[ab] (0.1316, 6.65)	3.486±2.272 (0.7266, 9.06)
	Fall2	0.2583±0.4711[b] (0.1011, 1.585)	0.6274±1.745 (0.1021, 4.981)
μRd25 (*Acer saccharum* canopy)	Spring	1.038±0.2004[ab] (0.6894, 1.461)	1.314±0.3478[ab] (0.685, 2.088)
	Summer	0.4883±0.1287[a] (0.2883, 0.7896)	0.7777±0.153[a] (0.5182, 1.121)
	Fall1	2.249±0.5737[b] (1.017, 3.386)	2.144±0.7544[ab] (1.087, 4.018)
	Fall2	1.697±0.9028[ab] (0.4844, 3.813)	3.2±1.12[b] (1.247, 5.511)
μRd25 (*Quercus rubra* canopy)	Spring	0.5498±0.143[a] (0.3218, 0.8761)	1.42±0.4784[ab] (0.7118, 2.563)
	Summer	1.132±0.2386[ab] (0.724, 1.66)	0.8321±0.1788[a] (0.5358, 1.234)
	Fall1	1.957±0.5888[b] (1.091, 3.38)	1.773±0.631[ab] (0.6715, 3.119)
	Fall2	3.998±1.488[b] (1.54, 7.041)	4.718±1.504[b] (1.266, 7.618)
Rd25 τ ($1/\sigma^2$) (*Acer saccharum* canopy)	Spring	3.683±4.619 (1.177, 7.985)	1.571±1.671[ab] (0.4042, 5.126)
	Summer	13.08±8.13 (3.329, 34.4)	9.603±5.888[a] (2.496, 24.67)
	Fall1	1.181±1.779 (0.2561, 4.163)	0.8312±0.6785[ab] (0.1315, 2.637)
	Fall2	5.175±10.97 (0.1988, 30.75)	0.4705±0.6351[b] (0.105, 2.084)
Rd25 τ ($1/\sigma^2$) (*Quercus rubra* canopy)	Spring	12.22±9.331[a] (2.791, 36.28)	1.611±1.471 (0.2622, 5.486)
	Summer	1.833±0.8658[ab] (0.6553, 3.859)	4.701±2.606 (1.432, 11.28)
	Fall1	0.7657±0.5356[b] (0.169, 2.012)	2.902±6.034 (0.2385, 17.46)

	Fall2	0.5611±0.8671[ab] (0.1039, 2.949)	0.4236±1.056 (0.1029, 2.995)
μVcmax25 (*Acer saccharum* canopy)	Spring	16.83±3.574* (9.751, 23.78)	39.57±6.799* (23.86, 50.85)
	Summer	11.67±2.559*† (7.371, 17.07)	30.04±2.697* (24.16, 35.59)
	Fall1	15.39±5.117 (7.791, 25.73)	20.6±3.823 (13.87, 28.41)
	Fall2	15.29±4.149 (7.853, 24.87)	26.29±9.712 (15.77, 50.33)
μVcmax25 (*Quercus rubra* canopy)	Spring	10.39±2.87*[a] (5.633, 15.96)	29.52±6.532* (16.0, 40.6)
	Summer	25.33±2.505†[b] (20.65, 30.23)	31.17±3.626 (21.44, 36.85)
	Fall1	14.71±3.121*[a] (8.454, 20.14)	26.52±3.705* (20.22, 33.51)
	Fall2	21.07±4.762[ab] (13.31, 32.69)	26.95±8.471 (12.56, 46.1)
Vcmax25 τ ($1/\sigma^2$) (*Acer saccharum* canopy)	Spring	0.1488±0.0897 (0.1007, 0.3822)	0.1834±0.1518 (0.1011, 0.5851)
	Summer	0.1697±0.1538 (0.101, 0.4851)	0.164±0.1155 (0.1009, 0.4544)
	Fall1	0.2296±0.3661 (0.1014, 0.8437)	0.1834±0.1626 (0.1011, 0.5685)
	Fall2	0.2126±0.2006 (0.1015, 0.7184)	0.1881±0.1833 (0.1012, 0.5725)
Vcmax25 τ ($1/\sigma^2$) (*Quercus rubra* canopy)	Spring	0.2023±0.2676 (0.1014, 0.593)	0.1766±0.1443 (0.1012, 0.5357)
	Summer	0.1863±0.1792 (0.1013, 0.5353)	0.205±0.2278 (0.1012, 0.725)
	Fall1	0.1468±0.07101 (0.1008, 0.3371)	0.1937±0.1616 (0.1014, 0.5766)
	Fall2	0.1952±0.2114 (0.1012, 0.6587)	0.2059±0.2354 (0.1013, 0.7024)

μJmax25 (*Acer saccharum* canopy)	Spring	18.0±1.667*†[ab] (14.99, 21.48)	41.02±3.55*[ab] (31.77, 47.28)
	Summer	22.81±1.167*†[bc] (20.53, 25.07)	42.01±1.35*[b] (39.37, 44.66)
	Fall1	15.96±1.804*†[a] (12.58, 19.65)	30.84±2.347*†[a] (26.22, 35.47)
	Fall2	29.18±3.67[c] (22.79, 37.8)	41.38±3.421[ab] (33.44, 47.02)
μJmax25 (*Quercus rubra* canopy)	Spring	11.81±1.447*†[a] (9.034, 14.72)	33.48±2.211*[a] (29.25, 37.78)
	Summer	36.9±1.548*†[b] (33.73, 39.74)	46.24±1.849*[b] (42.5, 49.87)
	Fall1	30.44±2.292*†[b] (26.35, 35.37)	46.19±4.084*†[ab] (36.8, 54.19)
	Fall2	35.15±2.998[b] (29.41, 41.36)	38.28±3.74[ab] (30.8, 46.09)
Jmax25 τ ($1/\sigma^2$) (*Acer saccharum* canopy)	Spring	0.1096±0.01223 (0.1002, 0.1427)	0.1085±0.02027 (0.1001, 0.1416)
	Summer	0.1118±0.01538 (0.1002, 0.1491)	0.1054±0.006564 (0.1001, 0.1222)
	Fall1	0.1349±0.05913 (0.1006, 0.2636)	0.1133±0.01525 (0.1003, 0.1541)
	Fall2	0.2022±0.3715 (0.1011, 0.63)	0.1107±0.01373 (0.1002, 0.1469)
Jmax25 τ ($1/\sigma^2$) (*Quercus rubra* canopy)	Spring	0.1206±0.06702 (0.1004, 0.1886)	0.1098±0.01421 (0.1002, 0.1415)
	Summer	0.1107±0.01513 (0.1002, 0.1435)	0.1113±0.01383 (0.1002, 0.148)
	Fall1	0.1106±0.01312 (0.1002, 0.1445)	0.1773±0.2531 (0.101, 0.5192)
	Fall2	0.1645±0.1331 (0.1009, 0.427)	0.1249±0.04007 (0.1005, 0.22)

Literature Cited for Supporting Information 2-2:

Björkman, O., M. R. Badger, and P. A. Armond. 1980. Response and adaptation of photosynthesis to high temperatrues. In: Turner, N. C., and P. J. Kramer, editors. Adaptation of plants to water and high temperature stress. Wiley, New York, pp. 233-249.

Dubois, J. J. B., E. L. Fiscus, F. L. Booker, M. D. Flowers, and C. D. Reid. 2007. Optimizing the statistical estimation of the parameters of the Farquhar-von Caemmerer-Berry model of photosynthesis. New Phytologist 176: 402-414.

Evans, J. R. 1989. Photosynthesis and nitrogen relationships in leaves of C3 plants. Oecologia 78: 9-19.

Gelman, A. and D. B. Rubin. 1992. Inference from iterative simulation. Statistical Science 7: 457-511.

Lunn, D., D. Spiegelhalter, A. Thomas, and N. Best. 2009. The BUGS project: Evolution, critique and future directions. Statistics in Medicine 28: 3049-3067.

Niinemets, Ü., A. Diaz-Espejo, J. Flexas, J. Galmes, and C. R. Warren. 2009. Importance of mesophyll diffusion conductance in estimation of plant photosynthesis in the field. Journal of Experimental Botany 60: 2271-2282.

Peltier, D. M. P., and I. Ibáñez. 2015. Patterns and variability in seedling carbon assimilation: Implications for tree recruitment under climate change. Tree Physiology 35: 71-85.

Supporting Information 2.3 - Climate data simulation and model projections

In order to predict the effects of climate change on seedling photosynthetic rates, we first needed to determine what an 'average year' of current climate conditions was. The variability of climate conditions in the four years included in this study was reasonably wide, so we decided to simply average the hourly climatic data (for relative humidity, temperature, and soil moisture) across all four years and all three sites, excluding data missing due to sensor damage (Fig. SI 2.13). VPD was calculated from relative humidity and temperature and then both VPD and soil moisture data were centered around the annual mean (see Supporting Information 2.2).

Climate conditions in the two climate scenarios were then estimated using the predicted seasonal changes in temperature and precipitation for Michigan in 2100 (Handler et al. 2014; Table SI 2.2). Projected increases in temperature were added to hourly temperature data, but because our measurements differed from the projection units for water availability (soil moisture vs. precipitation), we instead used percent change in precipitation to estimate percent change in soil moisture for the climate change scenarios. Changes in relative humidity in this region are difficult to predict (Handler et al. 2014), so VPD in the two climate change scenarios are based solely on predicted changes in temperature.

Light availability (photosynthetic active radiation, PAR) was more complicated to average and project due to differences in light availability and seasonality between sites. Averaging hourly PAR across the three sites worked well for approximating light availability in spring and fall (when the canopy was open). After averaging the data, canopy close and reopening under the current climate scenario were calculated the same was as described in the text using the site-level annual PAR data. Spring and fall light data were then shifted earlier or later based on predicted canopy phenology from the phenology models (Fig. 2.2).

PAR values in summer were consistently low, however, presumably due to variation in sunflecks and cloudiness between sites at any given hour. Therefore, hourly summer PAR was estimated by averaging hourly PAR from all three sites across 14 days in the summer of 2018 when weather was consistently sunny across all three sites. Hourly PAR was then assumed to be the same each day starting the day following canopy close and ending the day before canopy re-opening. It is important to note that this approach means that our projected climate data still does not account for potential peaks in light availability due to sunflecks, and so the estimation of summer light in this study should be seen as a conservative estimate.

Lastly, although CO_2 concentrations in the second scenario are elevated such that seedling photosynthesis may experience triose phosphate utilization (TPU) limitation instead of Rubisco carboxylation or RuBP regeneration limitation, we did not include TPU limitations in our projections (Fig. 2.3-2.4). A recent review (Lombardozzi et al. 2018) noted that it is particularly important to include TPU limitation in models where the temperature response of V_{cmax} is not accounted for, in part because there is evidence that plant physiological processes may acclimate to increased CO_2 (Ainsworth and Rogers 2007), which may therefore change photosynthetic limitations in the future. Still, in the interest of transparency, we included carbon assimilation estimates that include TPU-limitations at $TPU = 0.167*V_{cmax}$ (Fig. SI 2.14), according to Lombardozzi et al. (2018). Although spring carbon assimilation was somewhat diminished by the addition of the TPU limitation, the overall trends were the same (i.e., all species-treatment combinations that had positive carbon balances without the TPU limitation maintained positive carbon balances when it was included).

Figure SI 2.13 - Hourly climate data

Environmental data used in estimation of ‘Current’ climate scenario. Each point represents an hourly average of temperature (A), relative humidity (B), or soil moisture (C).

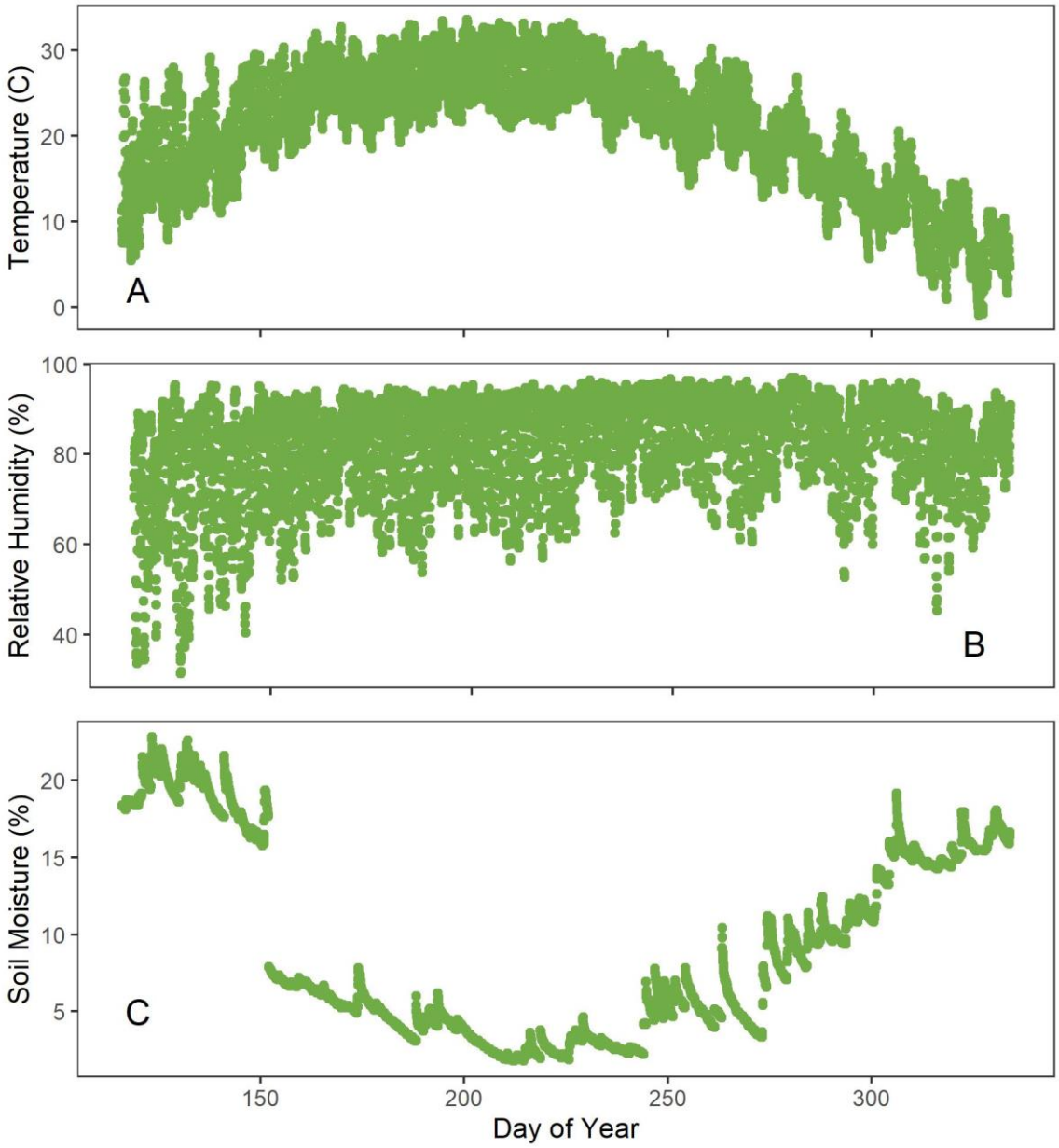

Figure SI 2.14 - Net carbon assimilation with TPU limitation

Net carbon accumulation using a model that includes TPU limitation of carbon assimilation of *A. saccharum* (A and B) and *Q. rubra* seedlings (C and D) planted under *A. saccharum* (A and C) and *Q. rubra* (B and D) canopy trees. Different lines and associated shading color represent predicted accumulation (and standard deviation of predicted values) under current climate conditions (solid, red), climate in 2100 assuming a reduction in global carbon emissions (dotted, green), and climate in 2100 assuming no reduction in global carbon emissions (dashed, blue). Negative accumulation is shown but is potentially unrealistic given that seedlings are likely to die shortly after reaching negative accumulation due to a limited capacity to store carbon from previous years. Carbon accumulation was extremely negative for *A. saccharum* seedlings planted under *Q. rubra* canopy trees (* in panel B) and was not included in this graph.

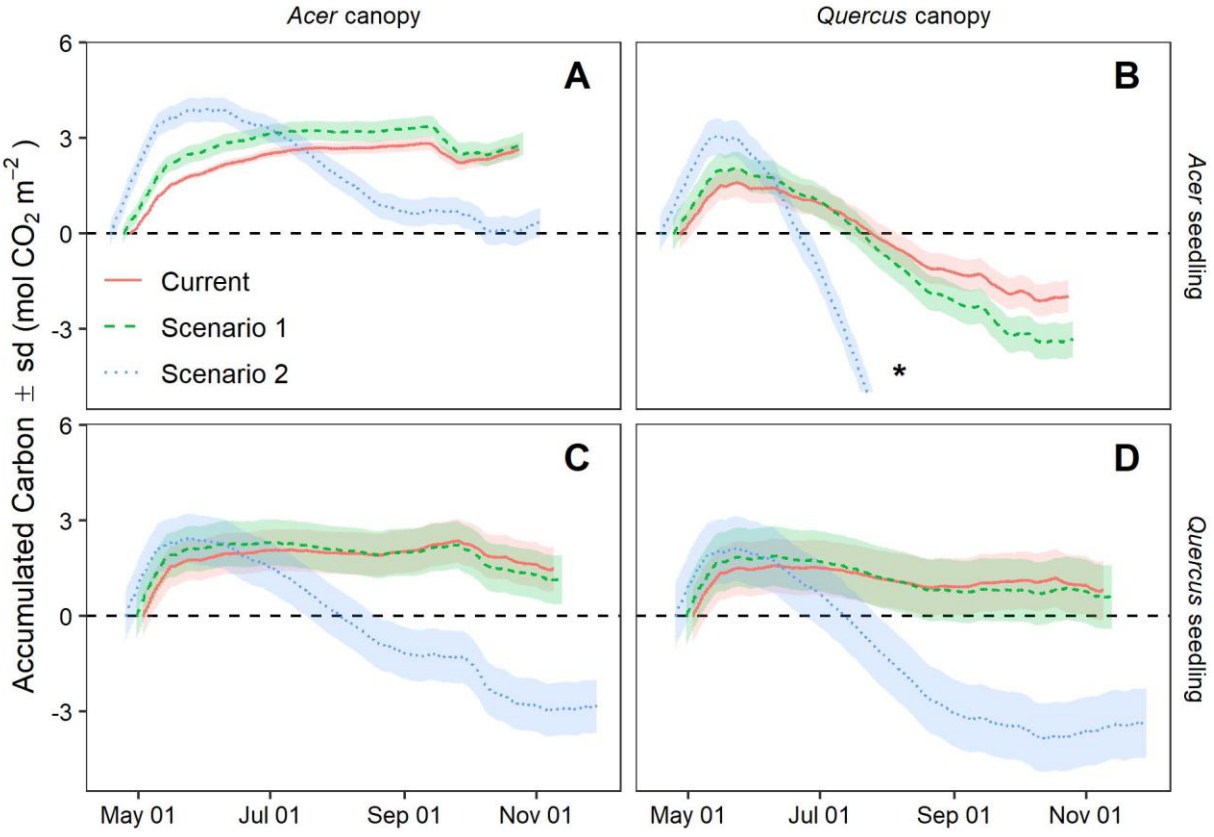

References for Supporting Information 2.3

Ainsworth, E. A., and A. Rogers. 2007. The response of photosynthesis and stomatal conductance to rising (CO2): Mechanisms and environmental interactions. Plant, Cell & Environment 30: 258-270.

Handler, S., M. J. Duveneck, L. Iverson, E. Peters, R. M. Scheller, K. R. Wythers, L. Brandt, P. Butler, M. Janowiak, P. D. Shannon, C. Swanston, A. C. Eagle, J. G. Cohen, R. Corner, P. B. Reich, T. Baker, S. Chhin, E. Clark, D. Fehringer, J. Fosgitt, J. Gries, C. Hall, K. R. Hall, R. Heyd, C. L. Hoving, I. Ibáñez, D. Kuhr, S. Matthews, J. Muladore, K. Nadelhoffer, D. Neumann, M. Peters, A. Prasad, M. Sands, R. Swaty, L. Wonch, J. Daley, M. Davenport, M. R. Emery, G. Johnson, L. Johnson, D. Neitzel, A. Rissman, C. Rittenhouse, and R. Ziel. 2014. Michigan forest ecosystem vulnerability assessment and synthesis: A report from the Northwoods Climate Change Response Framework. US Department of Agriculture, Forest Service, Northern Research Station, General Technical Report NRS-129, Newtown Square, PA.

Lombardozzi, D. L., N. G. Smith, S. J. Cheng, J. S. Dukes, T. D. Sharkey, A. Rogers, R. Fisher, and G. B. Bonan. 2018. Triose phosphate limitation in photosynthesis models reduces leaf photosynthesis and global terrestrial carbon storage. Environmental Research Letters 13: 074025.

Chapter 3 Carbon Assimilation and Tree Seedling Performance

ABSTRACT

In temperate forests climate change is expected to result in net reductions to tree seedling annual carbon budgets as a result of increased costs in respiration associated with hotter and drier summers. This suggests that temperate tree recruitment will suffer from reduced seedling demographic performance. However, the beginning of the growing season (i.e., leaf expansion) is also advancing in response to warming. Many understory species, including seedlings of deciduous tree species, have been shown to rely on early spring light availability, prior to canopy closure, to assimilate the majority of their annual carbon budgets. If seedlings and canopy shift phenology at different paces this period of high light will also change and will consequentially affect seedlings carbon budgets. Despite its relevance to tree recruitment, this relationship between earlier springs and drier summers has not been quantified in combination.

In this study, we used estimated annual carbon budgets for individual tree seedlings of two temperate tree species commonly found across eastern North America (*Acer saccharum* and *Quercus rubra*), modeled the relationship between carbon accumulation and demographic performance (i.e., survival and growth), and then used output from these models to forecast tree seedling performance under two climate change scenarios. Annual carbon accumulation was found to be significantly and positively associated with survival of seedlings of both species and with the growth of *A. saccharum* seedlings, suggesting that seedlings of these two species rely heavily on current growing season carbon accumulation as opposed to stored carbon sources from previous years. Moderate climate change was projected to have virtually no effect on

seedling performance (growth or survival), but extreme climate change was projected to result in dramatic reductions in performance, particularly for *A. saccharum*. Both species are projected to maintain their rates of seedling survival and growth, largely due to increases in spring carbon accumulation associated with earlier spring leaf-out relative to canopy closure. Our results suggest that phenology shifts, and the seasonal light harvesting they provide, could play a significant role in determining future forest recruitment and should be accounted for in vegetation models.

INTRODUCTION

Forest understory plants often struggle to maintain positive carbon budgets due to insufficient access to light (e.g., Augspurger et al., 2005). Deciduous tree seedlings often overcome this light deficiency by expanding their leaves several days or weeks before the canopy closes in order to make use of direct sunlight (Augspurger & Bartlett, 2003; Augspurger, 2008), a strategy referred to as phenological escape (Jacques et al., 2015). This process has been demonstrated to allow plants to assimilate 25-100%, of their annual carbon budget in the first few weeks of the growing season (Kwit et al., 2010; Heberling, Cassidy, et al. 2019; Chapter 2). The duration of this period is thus critically important for seedling performance. Recently it has been shown that climate change is causing understory plant leaf out phenology shift earlier in spring at rates that are either faster (Chapter 2) or slower (Heberling, McDonough MacKenzie, et al., 2019) than the shift rates of co-occurring canopy trees, leading to projected changes in understory light availability in spring, and consequently in the amount of carbon plants are able to assimilate. Previous studies have demonstrated that changing access to spring light affects understory plant performance (Routhier & Lapointe, 2002; Seiwa 2003; Augspurger, 2008);

however, to our knowledge, the quantitative change in carbon assimilation by seedlings during this period prior to canopy leaf-out has not previously been measured.

Determining how carbon assimilation, i.e., photosynthetic performance, of tree seedlings affects demographic performance is of critical importance to understand what future forests will look like. Tree seedling recruitment is a strong bottleneck that filters which individuals eventually recruit into the canopy (Harper, 1977; Grubb, 1977), and it is also the stage at which trees are most likely to experience nonrandom, directional mortality (Green et al., 2014, Umaña et al. 2016). Most previous studies that have investigated the effects of climate change on tree seedling recruitment rely on correlations between demographic performance and environmental conditions (e.g., Gamache & Payette, 2005; Batllori et al., 2009), but this has been shown to be problematic if these relationships are nonlinear (Wolkovich et al., 2012; Ibáñez et al, 2017) or if plants experience novel climates (Jackson & Williams, 2004). Therefore, there is a need for a more mechanistic approach to assess future performance.

Connecting demographic and physiological performance can bring us closer to that mechanism-based forecasting. Plant carbon status, often referred to as a "carbon budget" or "carbon balance", is a particularly important physiological metric because it reflects if plants have enough carbon to perform basic metabolic functions needed to survive and grow. Carbon status has been experimentally linked to various metrics of plant performance including growth (Korol et al., 1991; Hlásny et al., 2011), survival (Lusk & Del Pozo, 2002; Piper et al., 2009), and fruit production (Hoch et al., 2013). If carbon sinks (e.g., costs associated with maintenance respiration and growth) are larger than carbon sources (i.e., photosynthetic assimilation and labile carbon located in storage tissue), plants will die from carbon starvation (Canham et al., 1999; McDowell et al., 2008; Maguire & Kobe, 2015). Carbon starvation can also occur with

positive carbon budgets, potentially as a result of being unable to successfully move labile carbon to where it is needed in the plant (Sala et al., 2010). Plants may also experience reduced growth due to prioritized allocation of limited carbon to survival-related processes (Imaji & Seiwa, 2010).

Results from previous studies suggest that carbon status may affect growth and survival of temperate tree seedlings differently, and that the effects are species specific. Kaelke et al. (2001), found that shade-tolerant *Acer saccharum* and moderately-shade-tolerant *Quercus rubra* tree seedlings experienced modest increases in growth associated with greater canopy openness and higher photosynthetic capacity, but that growth plateaued after reaching ~15% maximum light availability. In contrast, they found that shade-intolerant *Populus tremuloides* seedlings experienced a near-linear increase in growth for light levels greater than 5%, which suggests that differences exist in how much carbon species allocate to growth under non-limiting conditions. They monitored seedling survival for one year and they did not find substantial differences among the three species. However, they noted that an informal census the following year revealed no surviving *Populus* seedlings in low-light conditions compared to relatively high survival of the *Quercus* and *Acer* seedlings (Kaelke et al., 2001), suggesting that the relationship between demographic performance and carbon status is strongly dependent on shade-tolerance, a result which is supported by results from other studies of temperate tree seedlings (Lusk & Del Pozo, 2002; Imaji & Seiwa, 2010). If seedling demographic performance is indeed linked to carbon assimilation and if seedling carbon budgets decrease due to high respiration rates in summer, then increases in spring assimilation associated with earlier leaf-out relative to the canopy may be particularly important for recruitment of temperate tree species.

In this study, our goal was to evaluate the extent to which seasonal carbon accumulation is associated with the performance of seedlings of two temperate tree species. Importantly, this study is distinguished from Chapter 2 in that we estimate carbon assimilation at the individual level (rather than at the species and treatment levels) and use those data to model seedling demographic performance directly. Specifically, we addressed the following questions: 1) Does carbon accumulation directly affect the demographic performance (survival and growth) of temperate tree seedlings? If so, 2) what does this link between physiological and demographic performance tell us about seedling recruitment under scenarios of future environmental change? 3) Could shifts in the timing of leaf out phenology predicted in Chapter 2 play a significant role in determining future seedling demography? Answering these questions may provide a mechanistic link between climate change and tree seedling recruitment that could be used to improve our predictions of tree population dynamics under climate change conditions.

METHODS

Experimental Design

Study locations

This study took place at three sites in southeastern Michigan, USA: Saginaw Forest (42.270977 N, 83.806022 W), Radrick Forest (42.287083 N, 83.658056 W), and the E. S. George Reserve (42.457104 N, 84.020226 W). Forests in all three locations were established in the early 1900's following forest clearing and are currently dominated by mid- and late-successional canopy species, such as *Acer*, *Carya*, *Prunus*, and *Quercus*. Radrick Forest and the E. S. George Reserve have relatively diverse canopies while plots in Saginaw Forest were established in former monocultures of *Acer saccharum* and *Quercus rubra*. Climate across all

sites is similar, with average June-August temperatures of 22 °C, average December-February temperatures of -6 °C, and average annual precipitation of 925 mm distributed evenly throughout the year.

Study species

We planted seedlings of two species native to and commonly co-occurring across eastern North America: late-successional *Acer saccharum* (Marsh.) and mid-successional *Quercus rubra* (L.). These two species were chosen because they differ in their shade tolerance (Crow, 1988; Lei & Lechowicz, 1990; Walters & Reich, 1996), capacity for phenological escape (Augspurger & Bartlett, 2003), and photosynthetic capacity (Kaelke et al., 2001; Peltier & Ibáñez, 2015). *Acer saccharum* seedlings are highly shade tolerant and are typically one of the first species in these forests to leaf out in spring whereas *Q. rubra* seedlings are only moderately shade tolerant and leaf out later in spring, sometimes at the same time as canopy closure. *Quercus rubra* seedlings typically have higher maximum photosynthetic rates than *A. saccharum* seedlings and are also considered to be more drought tolerant. Adults of these species have also been demonstrated to differ in drought tolerance (Bahari et al., 1985; Abrams, 1990; Loewenstein & Pallardy, 1998), stomatal regulation (Loewenstein & Pallardy, 1998; Cavender-Bares & Bazzaz, 2000), and wood anatomy (diffuse- vs. ring-porous xylem, respectively; Roman et al., 2015), although most of these traits have not been directly measured in seedlings and may not be consistent across ontogeny (Cavender-Bares & Bazzaz, 2000).

Field experimental set-up

For three consecutive years, 2014-2016, seeds from each species sourced from several populations (Table SI 2.1) were cold-stratified and sown in a greenhouse in large tubs of potting soil (Sun Gro Horticulture; Agawam, MA, USA). Following germination and development of their first true leaves, seedlings were bare root transplanted to the field. At each site and in each year, 5-10 seedlings were planted under the canopy of three mature adult *A. saccharum* individuals and three mature *Q. rubra* individuals (each canopy tree is considered one plot). In total we planted 290 *A. saccharum* seedlings and 320 *Q. rubra* seedlings. Detailed information on the plantings is described in Chapter 2.

Data Collection

Foliar phenology

We observed individual dates of seedling leaf expansion in spring and dates of initial leaf color change, 50% leaf color change, and leaf senescence in fall beginning the year after planting and going through the end of the 2018 growing season. Phenology was observed weekly in spring and fall, ending in spring when all seedlings had expanded their leaves or been declared dead and ending in fall when all seedlings had fully senesced their leaves.

Seedling growth and survival

Individual mortality was recorded during the phenology and damage censuses when mortality was obvious (e.g., for fully uprooted plants) or during spring of the following year if the individual did not produce new leaves. Seedling height (distance from soil to apical meristem) was recorded prior to planting to approximate maternal effects (which have been

shown to correlate with seedling phenology; Seiwa & Kikuzawa, 1991) and annually thereafter at the end of each growing season.

Damage

Leaf damage can affect seedling demographic performance directly (Gerhardt, 1998; Seiwa, 2003) and indirectly through reductions in photosynthetic capacity, so we observed leaf damage for all seedlings coinciding with the weekly phenology observations in spring and fall and then approximately monthly over the rest of the summer. Leaf damage was assessed by approximating the total percent area per leaf removed by herbivory or infected by a foliar pathogen to the nearest 5%. Herbivory damage was classified as either mammal (white-tailed deer, *Odocoileus virginianus*) or invertebrate herbivory based on visual analysis. Deer herbivory was identified when herbivory also damaged surrounding stem tissue, whereas invertebrate herbivory was usually incremental and typically did not damage stem tissue. Plant infection was identified as discoloration of leaf tissue not attributable to resorption of nutrients (i.e., leaves becoming grey, brown, or black midseason). Although these two types of damage were most common, other sources of damage were noted when they occurred, including whole plant uprooting (likely by squirrels or chipmunks), stem damage (e.g. stem snapping from a large branch falling on top of it), and leaf desiccation (when leaves remained green but became dry and brittle). We calculated a percent damage for each seedling which reflected the proportion of leaf area lost to herbivory or infection on an annual basis.

Environmental data

Environmental data stations were set up at each site to collect data in closed-canopy environments. Each station was equipped to measure hourly temperature (°C) and relative humidity (%) using HOBO U23 Pro v2 data loggers (Onset Computer Corp., Bourne, MA, USA) and hourly soil moisture (%) and photosynthetically active radiation (PAR; μmol photons m^{-2} s^{-1}) using HOBO Smart Sensors in combination with HOBO Micro Stations (Onset Computer Corp.). Additionally, plot-level variation in soil moisture was measured using a Fieldscout TDR300 soil moisture meter (Spectrum Technologies; Aurora, IL, USA) at multiple times throughout the growing season. Plot-level variation in midseason light availability was measured by taking hemispherical canopy photos at a height of 1 m above seedling level with a Sigma SD14 camera equipped with a Sigma 4.5 mm circular fisheye lens (Sigma Corporation, Japan) each year after the canopy at each plot had completely closed. For each photo we calculated the Global Site Factor (GSF) using Hemiview software (Delta-T Devices, Cambridge, UK), which is a continuous value that represents proportion of canopy openness ranging from zero (fully closed) to one (fully open).

Carbon assimilation

In previous work (Chapter 2) we collected seedling photosynthetic measurements using a LI-6400 Portable Photosynthesis System equipped with a CO_2 mixer assembly, LI-02B LED red/blue light source, and LI-06 PAR sensor (Li-COR Biosciences, Lincoln, NE, USA). Measurements were taken for a subset of planted seedlings every two weeks in spring and fall and approximately monthly over the summer between 2015 and 2017. For a detailed description of photosynthetic methods see Supporting Information 3.2. These data were used to estimate hourly carbon assimilation and respiration rates for each seedling using a hierarchical Bayesian

adaptation of the Farquhar et al. (1980) model of C3 photosynthesis (Patrick et al., 2009; Peltier & Ibáñez, 2015). A full description of the model used in this analysis (including seasonal parameter estimates, model code, and gas exchange measurements used to fit the model) is included in Chapter 2 (Supporting Information 2.2).

We were thus able to estimate carbon assimilation rates for at the leaf and seedling levels over the entire growing season by inputting hourly climate data (temperature, vapor pressure deficit [VPD], soil moisture, and PAR) collected from our site-level environmental stations and simulated at the plot level (see Supporting Information 3.2). Using season-specific parameters (Supporting Information 2.2), hourly carbon accumulation was then calculated by multiplying the assimilation rate (μmol m^{-2} s^{-1}) by the estimated leaf area (m^2) of each seedling. Seasonal and annual carbon accumulation was then calculated as the sum of hourly accumulation for each seedling (Fig. 3.1). A full description of this process is included in Supporting Information 3.2. Importantly, the light estimates used in this study were calculated differently than described in Chapter 2 (Supporting Information 2.3); here, light availability was adjusted according to mid-season canopy openness. The estimates in this chapter tended to be greater than the light estimates in Chapter 2.

Analyses

Survival

We analyzed seedling survival using a hierarchical Bayesian Bernoulli model where the probability of survival (p) for each seedling (i) in year (t), dead $Survival_{i,t} = 0$ or alive $Survival_{i,t} = 1$, is estimated with likelihood: $Survival_{i,t} \sim Bernoulli(p_{i,t})$, and process model: $logit(p_{i,t}) = log\left(\frac{p_{i,t}}{1-p_{i,t}}\right) = \bar{\beta} X_{i,t}$. We systematically evaluated models for best fit using

different combinations of eight covariates and seven categorical variables (Table 3.1), the latter included as random effects. Models started with an intercept (β_0) and a carbon accumulation term (β_C):

$$logit(p_{i,t}) = \beta_0 + \beta_C * C_{Annual_{i,t}}$$

Where C_{Annual} is each seedling's annual carbon accumulation for a given year. Values of all continuous covariates, including C_{Annual}, were standardized around their respective means, separately for each species (standardized value = [observed – mean]/[2*standard deviation]). Covariates and random effects (Table 3.1) were then added one at a time with models being iteratively chosen based on best fit according to the area under the receiving operator characteristic curve (AUROC; Metz, 1978; Murtaugh, 1996). Importantly, one of the covariates tested in the model was leaf-out date (*LOD*). Because individual leaf-out phenology, and thus effects related to light availability, is already included in our estimations of C_{Annual}, this term represented other potential effects related to the timing of leaf-out such as increased risk of frost damage (Vitasse et al., 2014). A description of the AUROC criterion is available in Supporting Information 3.3, and posterior estimates of intercepts, covariates, and random effects are available in Table SI 3.2. Each species was analyzed independently.

Growth

Only seedlings with non-negative growth values were included in this analysis. Negative growth values were generally associated with stem die-back or deer herbivory and did not represent the realized growth of each seedling. Growth measurements were standardized around the mean and variance for each species, as described above. Seedling growth for each seedling *i* and year *t* was analyzed with a normal likelihood: $Growth_{i,t} \sim N(\rho_{i,t}, \sigma^2)$, limited to positive

values, and process model: $\rho_{i,t} = \beta_0 + \bar{\beta} X_{i,t}$. We evaluated models for best fit using combinations of C_{Annual} and the same covariates described in the survival analysis, with the addition of a seedling random effect. Model selection for growth models was done based on comparisons of the Deviance Information Criterion (DIC; Spiegelhalter et al., 2002) and on goodness of fit (R^2, predicted vs. observed), fully described in Supporting Information 3.3. Posterior estimates of all growth model parameters are available in Table SI 3.2. Species were analyzed individually.

In both analyses, covariate parameters were estimated from non-informative normal distributions $\beta_* \sim N(0, 1000)$. Random effect parameters associated with the qualitative variables were estimated from hierarchical normal distributions $\alpha_* \sim N(0, {\sigma^2}_{\alpha*})$. Precision parameters (1/variance) were estimated from non-informative gamma prior distributions ${1/\sigma^2}_{\alpha*} \sim Gamma(0.001, 0.001)$.

All models were run using OpenBUGS software v3.2.3 (Lunn et al., 2009). We tracked 40,000 iterations for two Monte Carlo chains following a 30,000-iteration burn-in period. Convergence of parameters was assessed visually and by using the Brooks-Gelman-Rubin statistic (Gelman & Rubin, 1992), and models were iterated until convergence was reached. Parameter values (means, variances, and covariances) were estimated from their posterior distributions.

Climate change projections

In order to project changes in seedling performance in response to climate change we combined our growth and survival models (i.e., estimated parameter means, variances, and covariances) with predicted changes in seasonal carbon accumulation for these two species under

simulated current climate conditions and under two climate change scenarios predicted for the region (Handler et al., 2014; Fig. 3.1). Current carbon accumulation was estimated as the mean accumulation values using all seedlings of each species. Scenario 1 represents the projected climate in 2100 assuming reductions in global carbon emissions ($[CO_2]$ = 550 ppm) and Scenario 2 is a more extreme climate scenario that assumes no reduction in global emissions ($[CO_2]$ = 970 ppm) by 2100 projected by the USDA climate change vulnerability assessment for the study region (Handler et al., 2014). This reflects increases in average summer temperatures of 1.2 and 6.2 °C and changes in average summer soil moisture of 10.2% and -38.8% for Scenarios 1 and 2, respectively. A table containing the seasonal predicted changes in climate can be found in Table SI 2.2. We then applied those changes to the Current climate average values and estimated carbon accumulation (Fig. 3.1). Climate projections assumed that continuous covariates besides C_{Annual} were average and binary covariates were zero and projected changes in carbon accumulation were averaged across both canopy tree treatments.

RESULTS

Out of 170 *A. saccharum* seedlings planted in the 2014 cohort, 34 survived transplant stress and the first growing season and only 4 survived through the end of 2018. From the 120 seedlings planted in the 2016 cohort 36 survived to reach the second growing season and 23 survived through the end of 2018. Out of the 170 *Q. rubra* seedlings planted in 2014, 20 survived the first growing season and 4 survived through the end of 2018. Six of the 30 *Q. rubra* seedlings planted in 2015 survived the first growing season with only 1 surviving to the end of the study. Survival was proportionally highest for the 2016 *Q. rubra* cohort, with 89 of the 120 seedlings surviving the first growing season and 42 seedlings surviving to the end of the study. *Quercus*

rubra seedlings (146.2 ± 34.9 mm) were taller on average than *A. saccharum* seedlings (76.7 ± 14.4 mm) at the time of planting but had slightly lower annual growth rates thereafter (19.7 ± 14.9 mm y^{-1} and 23.7 ± 16.1 mm y^{-1}, respectively).

Carbon accumulation

Annual carbon accumulation calculated at the individual level ranged from -0.014 to 0.364 mol and 0.001 to 0.453 mol for *A. saccharum* and *Q. rubra* seedlings, respectively. For *A. saccharum* seedlings, an average of 84.3% of annual carbon was assimilated in spring, 15.9% was assimilated in summer and -0.2% was assimilated in fall (i.e., respiration in fall was greater than photosynthetic assimilation for this species; Fig. 3.1). In contrast, an average of 52.5% of *Q. rubra* seedling annual carbon was assimilated in spring, 43.5% was assimilated in summer, and 4.0% was assimilated in fall (Fig. 3.1). These ratios changed in the two climate change scenarios, with relatively more assimilation in spring and less assimilation in summer (Fig. 3.1), particularly in Scenario 2. For both species, the modeled total annual carbon accumulation increased slightly in climate Scenario 1 due to increased spring carbon accumulation but decreased dramatically in Scenario 2 due to high respiration costs in summer (Fig. 3.1).

Seedling survival

The models resulted in AUROC values of 0.913 and 0.890 for *A. saccharum* and *Q. rubra*, respectively, meaning that the models were able to correctly predict seedling survival about 90% of the time. In addition to C_{Annual}, the best fit survival models for both species included covariates for presence of foliar desiccation and percent foliar damage, with the *A. saccharum* survival model also including a term for signs of deer herbivory. The effect of annual

carbon was positive and significant for both species while the effects of desiccation and percent leaf damage were negative and significant (Fig. 3.2). Deer herbivory had a negative but non-significant effect on *A. saccharum* survival (Fig. 3.2a). The best fit *A. saccharum* model included site random effects whereas the best fit *Q. rubra* model included plot random effects. All parameter values can be found in Table SI 3.2.

Seedling growth

The best fit *A. saccharum* growth model had a goodness of fit $R^2 = 0.497$; goodness of fit for *Q. rubra* was 0.467. The best fit growth models each included C_{Annual} and only one other covariate. *Acer saccharum* growth was best predicted by a model that included GSF (i.e., light) whereas *Q. rubra* growth was best predicted by a model that included signs of deer herbivory. All covariates were positively associated with growth for both species, but the only significant relationship was between C_{Annual} and *A. saccharum* growth (Fig. 3.3). Models for both species included plot, site, and seedling random effects, with the *A. saccharum* model also including a random effect for year and the *Q. rubra* model including additional random effects for seedling age and planting cohort. All parameter values can be found in Table SI 3.3.

Performance under climate change projections

Survival

Seedlings accumulating the estimated average values of annual carbon were predicted to survive (i.e., probability of survival ≥ 0.5) in all three climate simulations across both species (Fig. 3.4; assuming no desiccation, no leaf damage, and no deer herbivory). Survival estimates were consistently higher for *A. saccharum* seedlings compared to *Q. rubra* seedlings across all

three simulations, although the difference in survival probability between the two species decreased in the more severe climate change scenario. Survival under the moderate climate change scenario (Scenario 1; filled symbols in Fig. 3.4) was predicted to be very similar to survival in current conditions for both species, but survival under more extreme climate change (Scenario 2; open symbols in Fig. 3.4) decreased by 17.6% and 6.5% compared to current condition survival for *A. saccharum* and *Q. rubra*, respectively.

Growth

Growth projections were qualitatively similar to the survival projections, with *A. saccharum* seedlings expected to have higher growth than *Q. rubra* seedlings across all three climate simulations (Fig. 3.5). The difference in growth between the two species decreased from 3.56 mm yr^{-1} under current climate conditions to 0.38 mm yr^{-1} in Scenario 2. Scenario 1 predictions did not differ greatly from the current climate predictions, with growth in Scenario 2 projected to decrease by 4.01 mm yr^{-1} (17.7%) and 0.83 mm yr^{-1} (4.3%) compared to growth in current conditions for *A. saccharum* and *Q. rubra* seedlings, respectively.

DISCUSSION

For many temperate plant species current trends in climate change will bring earlier springs and drier summers (Piao et al., 2019), but only recently have ecologists focused on the effect that these changes will have on plant carbon status (Routhier & Lapointe, 2002; Seiwa 2003; Augspurger, 2008). In particular, the mismatch between the ground layers, where seedlings recruit, and the canopy is critical for the annual carbon budget of the seedlings (Chapter 2). Previous studies have directly linked plant carbon status to demographic

performance (e.g., Korol et al., 1991; Kaelke et al., 2001; Piper et al., 2009), but little work has been done linking changes in demographic performance through changes in plant carbon status associated with shifting phenologies. Here, we quantified how demographic performance of seedlings of two temperate tree species commonly found across eastern North America is directly affected by plant carbon status. Furthermore, we used this relationship to assess future demographic performance on the basis of predicted carbon accumulation under forecasted climate scenarios, i.e., carbon budgets that account for shifting phenology. As expected, our analyses show that plant demographic performance (i.e., survival and growth) depend on carbon accumulation. Our results also show that phenological escape in spring will allow *A. saccharum*, a drought-intolerant species, to maintain positive recruitment under climate change. However, under a more extreme climate change scenario, carbon accumulation will substantially decrease in both species resulting in lower demographic performance.

Carbon accumulation and demography

Plants rely on photosynthetic carbon assimilation to survive, grow, reproduce, and defend themselves (Mooney, 1972). Our results reflect that dependency. Survival of both species was significantly associated with carbon accumulation (Fig. 3.2), but the relationship between carbon and growth was only significant for *A. saccharum* seedlings (Fig. 3.3a).This likely reflects intrinsic differences in shade tolerance between the two species since all seedlings in this study were planted in closed-canopy locations. We speculate that shade-tolerant *A. saccharum* seedlings were able to efficiently allocate carbon to survival with enough excess carbon left over to allocate to aboveground growth. Moderately-shade-tolerant *Q. rubra* seedlings assimilated enough carbon to facilitate survival but either did not have enough to allocate to aboveground

growth or they allocated their excess carbon to other functions such as defense, belowground growth, or storage (e.g., Canham et al., 1999). This speculation is consistent with a previous study that found that 2-year-old *Q. rubra* seedlings allocated more carbon to storage than *A. saccharum*, *A. rubrum*, and *Prunus serotina* seedlings on a mass basis (Canham et al., 1999). It is also consistent with work showing that the cost of allocating carbon to storage decreases under low-light conditions (Kobe, 1997), suggesting that understory plants will prioritize storage ahead of growth. In addition to labile carbon allocation, tree seedlings have also been demonstrated to adjust biomass allocation in response to shade (Curt et al. 2005) and drought (Schall et al. 2012). The lack of strong relationships between growth and carbon in our study could thus be partially explained by increased biomass allocation to belowground growth (a variable we did not measure).

Survival models for both species also showed significantly negative associations with desiccation and foliar damage due to pathogens and herbivory. We already accounted for the negative effects that decreased water availability can have on photosynthetic performance (Supporting Information 3.2), so this additional effect of desiccation suggests that temperate tree seedlings are also vulnerable to dying from hydraulic failure (McDowell et al., 2008). Hydraulic failure, whereby plants die from catastrophic embolisms resulting from extremely negative water potentials, is particularly common in arid ecosystems such as the U.S. southwest (McDowell et al., 2008), but it commonly occurs in mesic systems as well (Hoffmann et al., 2011; Choat et al., 2012). This dynamic may be accentuated for tree seedlings because of their relative inability to access deeper sources of water (Cavender-Bares & Bazzaz, 2000). Similarly, leaf damage, after accounting for photosynthetic area in our carbon accumulation calculations (Supporting Information 3.2), also reduced survival. We can only speculate about the mechanism behind this

effect, but one possible explanation is that foliar damage is correlated with systemic damage such as whole-plant infection that could be a contributing factor in mortality (Jain et al., 2019).

The impact of deer herbivory was found to be important for *A. saccharum* survival and *Q. rubra* growth but with opposite effects. Although the association between *A. saccharum* survival and deer herbivory was negative, signs of deer herbivory had a positive association with *Q. rubra* growth, suggesting that seedlings of this species grew more in response to deer herbivory events. This result, although initially counterintuitive, is consistent with previously documented compensatory growth dynamics (McNaughton, 1983), and could reflect a potential trade-off between growth and foliar defense (Coley, 1988). Therefore, our results speculatively suggest that *Q. rubra* seedlings are allocating assimilated carbon to storage in the form of non-structural carbohydrates that they can then mobilize for regrowth following herbivory.

Seedling performance under scenarios of climate change

Climate change vegetation forecasts for temperate forests often predict an increase in drought-tolerant anisohydric tree species (e.g., Gustafson & Sturtevant, 2013), largely due to decreased water availability. However, our results suggest that, at least with respect to tree seedling recruitment, drought-intolerant species like *A. saccharum* could maintain their recruitment performance if they are able to shift their spring phenology faster than canopy trees shift theirs; *A. saccharum* seedlings maintained higher performance than the moderately drought-tolerant *Q. rubra* seedlings across all three climate simulations assessed in this study (Fig. 3.4 and 3.5). Although *Q. rubra* seedlings accumulate more carbon per individual, they are bigger seedlings with likely higher maintenance respiration costs (Amthor, 1984) and allocate a greater proportion of their carbon to root growth and carbon storage (Canham et al., 1999). In our

experiment, still ongoing, we did not harvest the seedlings and are therefore unable to estimate carbon accumulation on the basis of seedling full biomass (Canham et al., 1999). Thus, even if *A. saccharum* seedlings lose more carbon in absolute terms under Scenario 2 (Fig. 3.1), this loss would affect survival and growth to a lesser extent than in *Q. rubra* seedlings.

Furthermore, our climate change predictions account for concurrent increases in respiration costs associated with warmer summers, so this difference suggests that seedlings are allocating assimilated carbon differently, with *Q. rubra* seedlings allocating proportionately more carbon to belowground growth, storage tissue, construction of new leaf tissue, or secondary metabolite production. This agrees with previous research which found that *Q. rubra* seedlings maintain non-structural carbohydrate pools in moderately stressful conditions whereas *A. rubrum* seedlings, a similar species to *A. saccharum* with respect to shade- and drought-tolerance (Houle, 1994; Hirons et al., 2015), do not (Maguire & Kobe, 2015). It is also consistent with research published by Frost and Hunter (2008), who found that defoliation of *Q. rubra* seedlings led to increased allocation of carbon to storage and to growth of replacement leaf tissue. We solely measured aboveground vertical growth, so we are only able to speculate about allocation to belowground growth or carbon storage in the form of non-structural carbohydrates, the latter of which has been shown to correlate with *Q. rubra* survival (Canham et al., 1999). This suggests that *A. saccharum* may not necessarily outperform *Q. rubra* in the future. Growth and survival for both species did not change under moderate climate change (Scenario 1), whereas more extreme climate change (Scenario 2) resulted in sharp decreases in performance, particularly for *A. saccharum* seedlings. The interspecific differences were cause by 1) a greater total decrease in predicted annual carbon accumulation, and 2) steeper slopes for the prediction trends for *A. saccharum* compared to *Q. rubra*.

Role of spring phenology in determining seedling demography

Still, the increase in projected spring carbon assimilation by *A. saccharum* seedings (Fig. 3.1) will play a large role in its future demographic performance, particularly under extreme climate change conditions. The shift to earlier spring phenology predicted for this species in Chapter 2 accounts for a 0.028 mol increase in spring carbon accumulation from the current climate scenario, making up more than half of the net annual carbon accumulation for this species under Scenario 2. Without this additional carbon assimilation, expected survival would drop from 64% to 53%. In contrast, *Q. rubra* seedlings are projected to gain 0.014 mol of carbon accumulation in spring due to earlier leaf out, without which expected survival would only fall from 59% to 55%. Therefore, earlier springs will be proportionally more important for *A. saccharum* seedlings than for *Q. rubra* seedlings under future climate change.

CONCLUSION

The results from this study suggest that successful temperate tree recruitment under climate change scenarios will depend strongly on the capacity of seedlings to access spring light via phenological escape mechanisms, particularly for species that rely heavily on spring photosynthetic activity for the majority of their annual carbon assimilation. The simulated responses to climate change scenarios in our study suggest that climate change will result in sharp decreases in performance if global carbon emissions are not reduced, but that the magnitude of these reductions could be somewhat attenuated by increasing access to spring light.

REFERENCES

Abrams, M. D. (1990). Adaptations and responses to drought in *Quercus* species of North America. *Tree Physiology, 7,* 227-238. https://doi.org/10.1093/treephys/7.1-2-3-4.227

Amthor, J. S. (1984). The role of maintenance respiration in plant growth. *Plant, Cell & Environment, 7,* 561-569. https://doi.org/10.1111/1365-3040.ep11591833

Augspurger, C. K. (2008). Early spring leaf out enhances growth and survival of saplings in a temperate deciduous forest. *Oecologia, 156,* 281-286. http://doi.org/10.1007/s00442-008-1000-7

Augspurger, C. K., & Bartlett, E. A. (2003). Differences in leaf phenology between juvenile and adult trees in a temperate deciduous forest. *Tree Physiology, 23,* 517-525. https://doi.org/10.1093/treephys/23.8.517

Augspurger, C. K., Cheeseman, J. M., & Salk, C. F. (2005). Light gains and physiological capacity of understorey woody plants during phenological avoidance of canopy shade. *Functional Ecology, 19,* 537-546. https://doi.org/10.1111/j.1365-2435.2005.01027.x

Bahari, Z. A., Pallardy, S. G., & Parker, W. C. (1985). Photosynthesis, water relations, and drought adaptation in six woody species of oak-hickory forests in central Missouri. *Forest Science, 31,* 557-569. https://doi.org/10.1093/forestscience/31.3.557

Batllori, E.; Camarero, J. J., Ninot, J. M., & Gutiérrez, E. (2009). Seedling recruitment, survival and facilitation in alpine *Pinus uncinate* tree line ecotones. Implications and potential response to climate warming. *Global Ecology and Biogeography, 18,* 460-472. https://doi.org/10.1111/j.1466-8238.2009.00464.x

Canham, C. D., Kobe, R. K., Latty, E. F., & Chazdon, R. L. (1999). Interspecific and intraspecific variation in tree seedling survival: effects of allocation to roots versus carbohydrate reserves. *Oecologia, 121,* 1-11. https://doi.org/10.1007/s004420050900

Cavender-Bares, J., & Bazzaz, F. A. (2000). Changes in drought response strategies with ontogeny in *Quercus rubra*: Implications for scaling from seedlings to mature trees. *Oecologia, 124,* 8-18. https://doi.org/10.1007/PL00008865

Choat, B., Jansen, S., Brodribb, T. J., Cochard, H., Delzon, S., Bhaskar, R., Bucci, S. J., Feild, T. S., Gleason, S. M., Hacke, U. G., Jacobsen, A. L., Lens, F., Maherali, H., Martínez-Vilalta, J., Mayr, S., Mencuccini, M., Mitchell, P. J., Nardini, A., Pittermann, J., Pratt, R. B., Sperry, J. S., Westoby, M., Wright, I. J., & Zanne, A. E. (2012). Global convergence in the vulnerability of forests to drought. *Nature, 491,* 752-755. https://doi.org/10.1038/nature11688

Coley, P. D. (1988). Effects of plant growth rate and leaf lifetime on the amount and type of anti-herbivore defense. *Oecologia, 74,* 531-536. https://doi.org/10.1007.BF00380050

Crow, T. R. (1988). Reproductive mode and mechanisms for self-replacement of Northern Red Oak (*Quercus rubra*) – A review. *Forest Science, 34,* 19-40. https://doi.org/10.1093/forestscience/34.1.19

Curt, T., Coll, L., Prévosto, B., Balandier, P, & Kunstler, G. (2005). Plasticity in growth, biomass allocation and root morphology in beech seedlings as induced by irradiance and herbaceous competition. *Annals of Forest Science, 62,* 51-60. http://doi.org/10.1051/forest:2004092

Farquhar, G. D., von Caemmerer, S., & Barry, J. A. (1980). A biochemical model of photosynthetic CO2 assimilation in leaves of C3 species. *Planta, 149,* 78-90. https://doi.org/10.1007/BF00386231

Frost, C. J., & Hunter, M. D. (2008). Herbivore-induced shifts in carbon and nitrogen allocation in red oak seedlings. *New Phytologist, 178,* 835-845. https://doi.org/10.1111/j.1469-8137.2008.02420.x

Gamache, I., & Payette, S. (2005). Latitudinal response of subarctic tree lines to recent climate change in eastern Canada. *Journal of Biogeography, 32,* 849-862. https://doi.org/10.1111/j.1365-2699.2004.01182.x

Gelman, A., & Rubin, D. B. (1992). Inference from iterative simulation. *Statistical Science, 7,* 457-472. https://doi.org/10.1214/ss/1177011136

Gerhardt, K. (1998). Leaf defoliation of tropical dry forest tree seedlings – implications for survival and growth. *Trees, 13,* 88-95. https://doi.org/10.1007/PL00009741

Green, P. T., Harms, K. E., & Connell, J. H. (2014). Nonrandom, diversifying processes are disproportionately strong in the smallest size classes of a tropical forest. *Proceedings of the National Academy of Sciences, 111,* 18649-18654. https://doi.org/10.1073/pnas.1321892112

Grubb, P. J. (1977). The maintenance of species-richness in plant communities: The importance of the regeneration niche. *Biological Reviews, 52,* 107-145. https://doi.org/10.1111/j.1469-185X.1977.tb01347.x

Handler, S., Duveneck, M. J., Iverson, L., Peters, E., Scheller, R. M., Wythers, K. R., Brandt, L., Butler, P., Janowiak, M., Shannon, P. D., Swanston, C., Eagle, A. C., Cohen, J. G., Corner, R., Reich, P. B., Baker, T., Chhin, S., Clark, E., Fehringer, D., Fosgitt, J., Gries, J., Hall, C., Hall, K. R., Heyd, R., Hoving, C. L., Ibáñez, I., Kuhr, D., Matthews, S., Muladore, J., Nadelhoffer, K., Neumann, D., Peters, M., Prasad, A., Sands, M., Swaty, R., Wonch, L., Daley, J., Davenport, M., Emery, M. R., Johnson, G., Johnson, L., Neitzel, D., Rissman, A., Rittenhouse, C., & Ziel, R. (2014). Michigan forest ecosystem vulnerability assessment and synthesis: a report from the Northwoods Climate Change Response Framework project. In *General Technical Report NRS-129*. https://doi.org/10.2737/NRS-GTR-129

Harper, J. L. (1977). *Population Biology of Plants*. Academic Press. London, UK. ISBN 13: 9780123258502

Heberling, J. M., Cassidy, S. T., Fridley, J. D., & Kalisz, S. (2019). Carbon gain phenologies of spring-flowering perennials in a deciduous forest indicate a novel niche for a widespread invader. *New Phytologist, 221,* 778-788. https://doi.org/10.1111/nph.15404

Heberling, J. M., McDonough MacKenzie, C., Fridley, J. D., Kalisz, S., & Primack, R. B. (2019). Phenological mismatch with trees reduces wildflower carbon budgets. *Ecology Letters, 22,* 616-623. https://doi.org/10.1111/ele.13224

Hlásny, T., Barcza, Z., Fabrika, M., Balázs, B., Churkina, G., Pajtík, J., Sedmák, R., & Turˇáni, M. (2011). Climate change impacts on growth and carbon balance of forests in Central Europe. *Climate Research, 47,* 219-236. https://doi.org/10.3354/cr01024

Hoch, G., Siegwold, R. T. W., Keel, S. G., Körner, C., & Han, Q. (2013). Fruit production in three masting tree species does not rely on stored carbon reserves. *Oecologia, 171,* 653-662. https://doi.org/10.1007/s00442-012-2579-2

Hoffmann, W. A., Marchin, R. M., Abit, P., & Lau, O. L. (2011). Hydraulic failure and tree dieback are associated with high wood density in a temperate forest under extreme drought. *Global Change Biology, 17,* 2731-2742. https://doi.org/10.1111/j.1365-2486.2011.02401.x

Houle, G. (1994). Spatiotemporal patterns in the components of regeneration of four sympatric tree species – *Acer rubrum, A. saccharum, Betula alleghaniensis* and *Fagus grandifolia*. *Journal of Ecology, 82,* 39-53. https://doi.org/10.2307/2261384

Ibáñez, I., Katz, D. S. W., & Lee, B. R. (2017). The contrasting effects of short-term climate change on the early recruitment of tree species. *Oecologia, 184,* 701-713. https://doi.org/10.1007/s00442-017-3889-1

Imaji, A., & Seiwa, K. (2010). Carbon allocation to defense, storage, and growth in seedlings of two temperate broad-leaved tree species. *Oecologia, 162,* 273-281. https://doi.org/10.1007/s00442-009-1453-3

Jackson, S. T., & Williams, J. W. (2004). Modern analogs in quaternary paleoecology: Here today, gone yesterday, gone tomorrow? *Annual Review of Earth and Planetary Sciences, 32,* 495-537. https://doi.org/10.1146/annurev.earth.32.101802.120435

Jacques, M. -H., Lapointe, L., Rice, K., Montgomery, R. A., Stefanski, A., & Reich, P. B. (2015). Responses of two understory herbs, *Maianthemum canadense* and *Eurybia macrophylla*, to experimental forest warming: Early emergence is the key to enhanced reproductive output. *American Journal of Botany, 102,* 1610-1624. https://doi.org/10.3732/ajb.1500046

Jain, A., Sarsaiya, S., Wu, Q., Lu, Y., & Shi, J. (2019). A review of plant leaf fungal diseases and its environment speciation. *Bioengineered, 10,* 409-424. https://doi.org/10.1080/21655979.2019.1649520

Kaelke, C. M., Kruger, E. L., & Reich, P. B. (2001). Trade-offs in seedling survival, growth, and physiology among hardwoord species of contrasting successional status along a light-availability gradient. *Canadian Journal of Forest Research, 31,* 1602-1616. http://doi.org/10.1139/cjfr-31-9-1602.

Kobe, R. K. (1997). Carbohydrate allocation to storage as a basis of interspecific variation in sapling survivorship and growth. *Oioks, 80,* 226-233. https://doi.org/10.2307/3546590

Korol, R. L., Running, S. W., Milner, K. S., & Hunt, Jr., E. R. (1991). Testing a mechanistic carbon balance model against observed tree growth. *Canadian Journal of Forest Research, 21,* 1098-1105. https://doi.org/10.1139/x91-151

Kwit, M. C., Rigg, L. S., & Goldblum, D. (2010). Sugar maple seedling carbon assimilation at the northern limit of its range: The importance of seasonal light. *Canadian Journal of Forest Research, 40,* 385-393. https://doi.org/10.1139/X09-196

Lei, T. T., & Lechowicz, M. J. (1990). Shade adaptation and shade tolerance in saplings of three *Acer* species from eastern North America. *Oecologia, 84,* 224-228. https://doi.org/10.1007/BF00318275

Loewenstein, N. J., & Pallardy, S. G. (1998). Drought tolerance, xylen sap abscisic acid and stomatal conductance during soil drying: a comparison of canopy trees of three temperate deciduous angiosperms. *Tree Physiology, 18,* 431-439. https://doi.org/10.1093/treephys/18.7.431

Lunn, D., Spiegelhalter, D., Thomas, A., & Best, N. (2009). The BUGS project: Evolution, critique and future directions. *Statistics in Medicine, 28,* 3049-3067. https://doi.org/10.1002/sim.3680

Lusk, C. H., & Del Pozo, A. (2008). Survival and growth of seedlings of 12 Chilean rainforest trees in two light environments: Gas exchange and biomass distribution correlates. *Austral Ecology, 27,* 173-182. https://doi.org/10.1046/j.1442-9993.2002.01168.x

Maguire, A. J., & Kobe, R. K. (2015). Drought and shade deplete nonstructural carbohydrate reserves in seedlings of five temperate tree species. *Ecology and Evolution, 5,* 5711-5721. https://doi.org/10.1002/ece3.1819

McDowell, N., Pockman, W. T., Allen, C. D., Breshears, D. D., Cobb, N., Kolb, T., Plaut, J., Sperry, J., West, A., Williams, D. G., & Yepez, E. A. (2008). Mechanisms of plant survival and mortality during drought: Why do some plants survive while others succumb to drought? *New Phytologist, 178,* 719-739. https://doi.org/10.1111/j.1469-8137.2008.02436.x

McNaughton, S. J. (1983). Compensatory plant growth as a response to herbivory. *Oikos, 40,* 329-336. https://doi.org/10.2307/3544305

Metz, C. E. (1978). Basic principles of ROC analysis. *Seminars in Nuclear Medicine, 8,* 283-298. https://doi.org/10.1016/s0001-2998(78)80014-2

Mooney, H. A. (1972). The carbon balance of plants. *Annual Review of Ecology and Systematics, 3,* 315-346. https://doi.org/10.1146/annurev.es.03.110172.001531

Murtaugh, P. A. (1996). The statistical evaluation of ecological indicators. *Ecological Applications, 6,* 132-139. https://doi.oorg/10.2307/2269559

Neufeld, H. S., & Young, D. R. (2014). Ecophysiology of the Herbaceous Layer in Temperate Deciduous Forests. In F. S. Gilliam (Ed.), *The Herbaceous Layer in Forests of Eastern North America* (2nd ed., pp. 35–95). Oxford University Press.

Patrick, L. D., Ogle, K., & Tissue, D. T. (2009). A hierarchical Bayesian approach for estimation of photosynthetic parameters of C3 plants. *Plant, Cell & Environment, 32,* 1695-1709. https://doi.org/10.1111/j.1365-3040.2009.02029.x

Peltier, D. M. P., & Ibáñez, I. (2015). Patterns and variability in seedling carbon assimilation: Implications for tree recruitment under climate change. *Tree Physiology, 35,* 71-85. https://doi.org/10.1093/treephys/tpu103

Piao, S., Liu, Q., Chen, A., Janssens, I. A., Fu, Y., Dai, J., Liu, L., Lian, X., Shen, M., & Zhu, X. (2019). Plant phenology and global climate change: Current progresses and challenges. *Global Change Biology, 25,* 1922-1940. https://doi.org/10.1111/gcb/14619

Piper, F. I., Reyes-Díaz, M., Corcuera, L. J., & Lusk, C. H. (2009). Carbohydrate storage, survival, and growth of two evergreen *Nothofagus* species in two contrasting light environments. *Ecological Research, 24,* 1233-1241. https://doi.org/10.1007/s11284-009-0606-5

Roman, D. T., Novick, K. A., Brzostek, E. R., Dragoni, D., Rahman, F., & Phillips, R. P. (2015). The role of isohydric and anisohydric species in determining ecosystem-scale response to severe drought. *Oecologia, 179,* 641-654. https://doi.org/10.1007/s00442-015-3380-9

Routhier, M. -C., Lapointe, L. (2002). Impact of tree leaf phenology on growth rates and reproduction in the spring flowering species *Trillium erectum* (Liliaceae). *American Journal of Botany, 89,* 500-505. https://doi.org/10.3732/ajb.89.3.500

Sala, A., Piper, F. I., & Hoch, G. (2010). Physiological mechanisms of drought-induced tree mortality are far from being resolved. *New Phytologist, 186,* 274-281. https://doi.org/10.1111/j.1469-8137.2009.03167.x

Schall, P., Lödige, C., Beck, M., & Ammer, C. (2012). Biomass allocation to roots and shoots is more sensitive to shade and drought in European beech than in Norway spruce seedlings. *Forest Ecology and Management, 266,* 246-253. https://doi.org/10.1016/j.foreco.2011.11.017

Seiwa, K. (2003). Advantages of early germination for growth and survival of seedlings of *Acer mono* under different overstorey phenologies in deciduous broad-leaved forests. *Journal of Ecology, 86,* 219-228. https://doi.org/10.1046/j.1365-2745.1998.00245.x

Seiwa, K., & Kikuzawa, K. (1991). Phenology of tree seedlings in relation to seed size. *Canadian Journal of Botany, 69,* 532-538. https://doi.org/10.1139/b91-072

Sjöman, H., Hirons, A. D., & Bassuk, N. L. (2015). Urban forest resilience through tree selection – Variation in drought tolerance in *Acer. Urban Forestry & Urban Greening, 14,* 858-865. https://doi.org/10.1016/j.ufug.2015.08.004

Spiegelhalter, D. J., Best, N. G., Carlin, B. P., & Van Der Linde, A. (2002). Bayesian measures of model complexity and fit. *Journal of the Royal Statistical Society: B, 64,* 583-639. https://doi.org/10.1111/1467-9868.00353

Umaña, M. N., Forero-Montaña, J., Muscarella, R., Nytch, C. J., Thompson, J., Uriarte, M., Zimmermann, J., & Swenson, N. G. (2016). Interspecific functional convergence and divergence and intraspecific negative density dependence underlie the seed-to-seedling transition in tropical trees. *The American Naturalist, 187,* 99-109. https://doi.org/10.1086/684174

Vitasse, Y., Lenz, A., Hoch, G., & Körner, C. 2014. Earlier leaf-out rather than difference in freezing resistance puts juvenile trees at greater risk of damage than adult trees. *Journal of Ecology, 102,* 981-988. https://doi.org/10.1111/1365-2745.12251

Walters, M. B., & Reich, P. B. (1996). Are shade tolerance, survival, and growth linked? Low light and nitrogen effects on hardwood seedlings. *Ecology, 77,* 841-853. https://doi.org/10.2307/2265505

Wolkovich, E. M., Cook, B. I., Allen, J. M., Crimmins, T. M., Betancourt, J. L., Travers, S. E., Pau, S., Regetz, J., Davies, T. J., Kraft, N. J. B., Ault, T. R., Bolmgren, K., Mazer, S. J., McCabe, G. J., McGill, B. J., Parmesan, C., Salamin, N., Schwartz, M. D., & Cleland, E. E. (2012). Warming experiments underpredict plant phenological responses to climate change. *Nature, 485,* 494-497. https://doi.org/10.1038/nature11014

Table 3.1 - Covariates and random effects in survival and growth models

A list of the covariates and random effects evaluated during model selection along with descriptions and information for the number of levels included in each random effect.

Variable	Type of variable	Description
Carbon	Covariate	Annual seedling-level carbon accumulation
PrevC	Covariate	Carbon accumulation from previous year*
%Damage	Covariate	Percent of total leaf area lost to herbivores and pathogens
LOD	Covariate	Leaf-out day in spring
GSF	Covariate	Plot-level canopy openness (light available)
Height	Covariate	Seedling height at planting
Desiccation	Binary	Signs of leaf desiccation
Deer	Binary	Signs of deer herbivory
Seed Source	Random effect	Population of origin (north or south)
Canopy	Random effect	Species of tree under which seedlings were planted (2 species)
Site	Random effect	Site planted (3 sites)
Plot	Random effect	Plot planted (18 plots)
Cohort	Random effect	Year planted (2-3 planting years)
Age	Random effect	Seedling age (1-4 ages)
Year	Random effect	Year observed (4 years of data collection)

*****Phenology, leaf damage, and other data needed to calculated carbon accumulation were not recorded in the year following transplant. Estimation of first year PrevC is described in SI 3.2.

Figure 3.1 - Seasonal seedling carbon accumulation

Seasonal carbon accumulation (averaged across all seedlings) for (a) *A. saccharum* and (b) *Q. rubra* seedlings in current climate conditions (C), under moderate climate change (S1) and under more extreme climate change (S2). Dashed lines and associated numbers indicate the net annual carbon accumulation for each scenario.

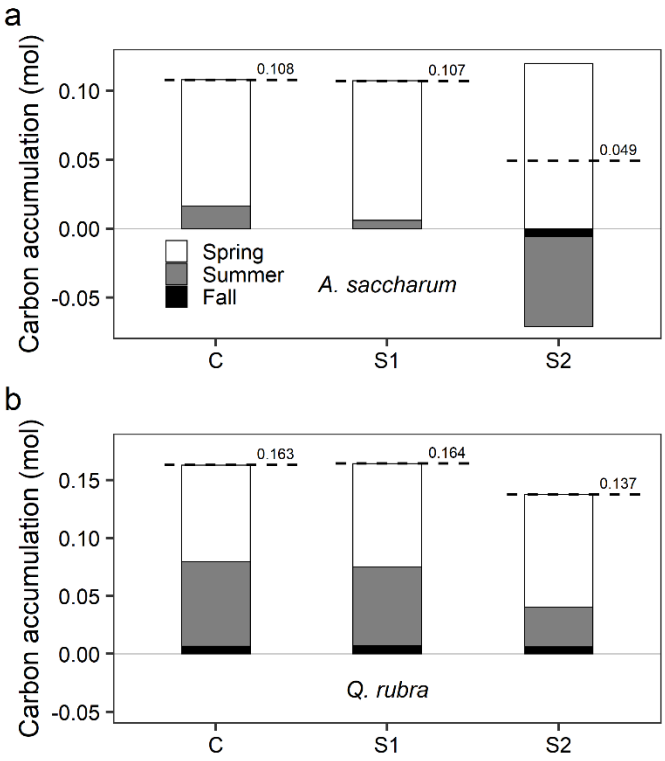

Figure 3.2 - Survival model parameter estimates

Posterior estimated means and 95% credible intervals (CI) for survival model parameters for (a) *A. saccharum* and (b) *Q. rubra*. Asterisks indicate parameter estimates that are significantly different from zero.

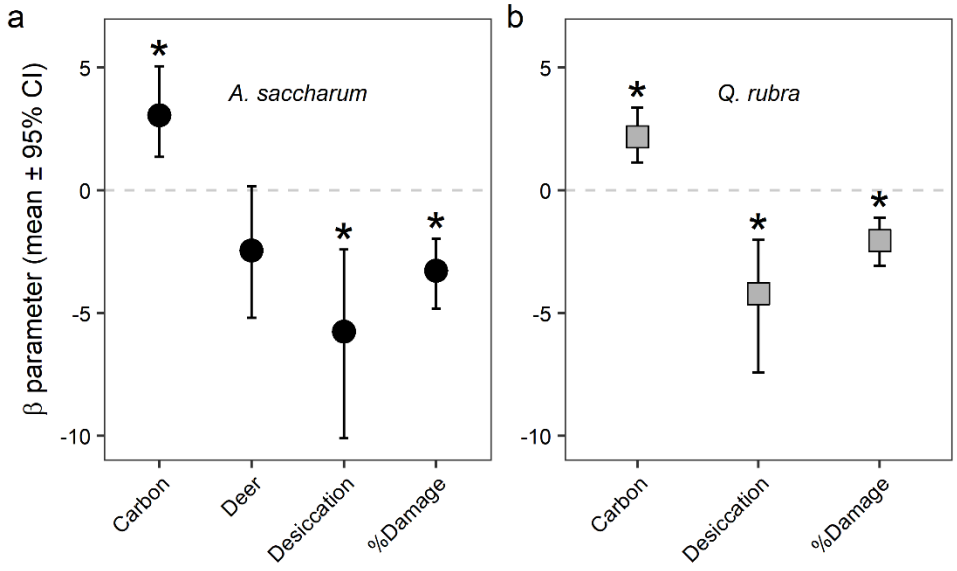

Figure 3.3 - Growth model parameter estimates

Posterior estimated means and 95% credible intervals (CI) for growth model parameters for (a) *A. saccharum* and (b) *Q. rubra*. Asterisks indicate parameter estimates that are significantly different from zero.

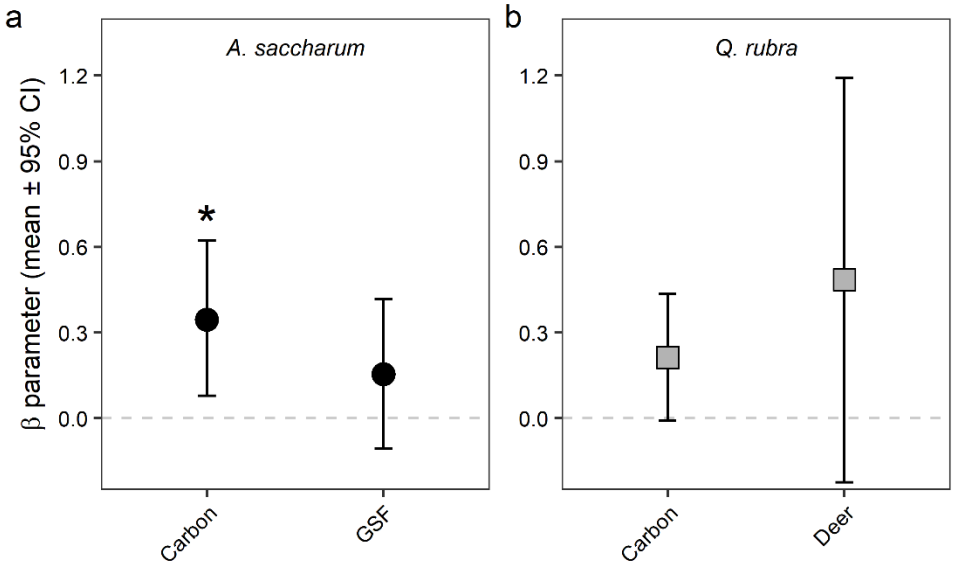

Figure 3.4 - Climate change survival predictions

Predicted probability of survival (lines; mean ± 95% predictive intervals) as a function of annual carbon accumulation for *A. saccharum* (black) and *Q. rubra* seedlings (grey). Vertical lines represent annual carbon accumulation under current climate conditions and symbols represent predicted survival under moderate climate change (Scen. 1; filled symbols) and more extreme climate change (Scen. 2; empty symbols).

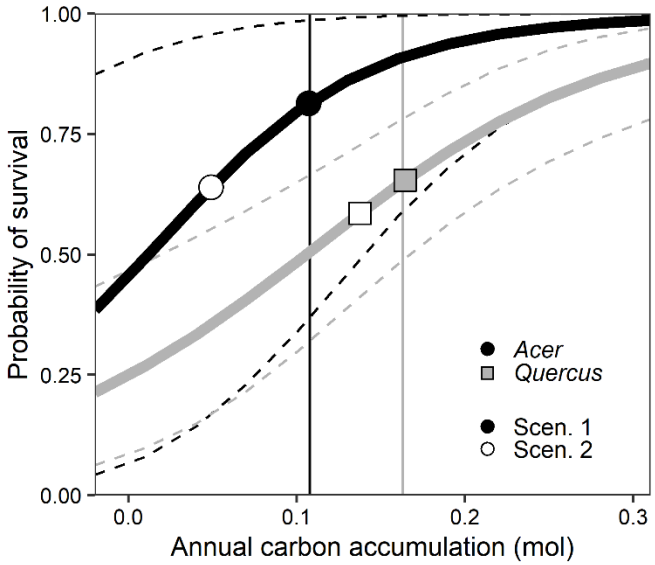

Figure 3.5 - Climate change growth predictions

Predicted growth (lines; mean ± 95% predictive intervals) as a function of annual carbon accumulation for *A. saccharum* (black) and *Q. rubra* seedlings (grey). Vertical lines represent annual carbon accumulation under current climate conditions and symbols represent predicted growth under moderate climate change (Scen. 1; filled symbols) and more extreme climate change (Scen. 2; empty symbols).

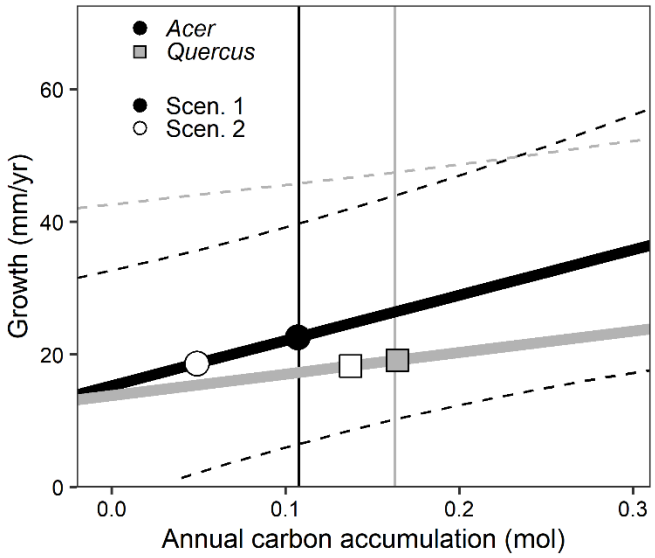

Supporting Information 3.1 - Supplemental Tables and Figures

Table SI 3.2 - Survival parameter posterior estimates

Posterior estimate means (and 95% confidence intervals) of covariate parameters and intercepts and the mean and 95% C.I.s for variance terms associated with random effects for survival models. Bold values indicate covariate estimates that are significantly different from 0 and NA indicates that a covariate or random effect was not present in the best fit model for that species.

		Acer saccharum	*Quercus rubra*
Intercept		1.802 (-0.531, 4.286)	0.638 (-0.045, 1.277)
Covariate	Carbon	**3.061 (1.362, 5.06)**	**2.185 (1.135, 3.371)**
	Deer	-2.451 (-5.197, 0.166)	NA
	Desiccation	**-5.756 (-10.1, -2.413)**	**-4.195 (-7.421, -2.025)**
	%Damage	**-3.279 (-4.814, -1.961)**	**-2.046 (-3.062, -1.111)**
Random effect variance	Site	3.386 (0.029, 11.01)	NA
	Plot	NA	38.64 (0.328, 387.1)
Model AUROC		0.913	0.890

Table SI 3.3 - Growth parameter posterior estimates

Posterior estimate means (and 95% confidence intervals) of covariate parameters and intercepts and the mean and 95% C.I.s for variance terms associated with random effects for growth models. Bold values indicate covariate estimates that are significantly different from 0 and NA indicates that a covariate or random effect was not present in the best-fit model for that species.

		Acer saccharum	*Quercus rubra*
Model variance		6.038 (3.882, 9.135)	5.53 (3.722, 8.0)
Intercept		-0.033 (-0.531, 0.497)	-0.021 (-0.823, 0.933)
Covariate	Carbon	**0.345 (0.079, 0.622)**	0.213 (-0.008, 0.436)
	Deer	NA	0.486 (-0.224, 1.192)
	GSF	0.155 (-0.105, 0.417)	NA
Random effect variance	Seedling	260.8 (11.06, 1530)	298.1 (13.82, 1598)
	Plot	337 (17.57, 1735)	270.7 (13.93, 1526)
	Site	116.6 (1.152, 830.8)	143.7 (1.126, 1002)
	Age	NA	80.65 (1.992, 501.3)
	Year	74.19 (1.583, 507.1)	NA
	Cohort	NA	112.5 (0.323, 982.7)
Model DIC		92.92	116.8
Goodness of fit R^2		0.4974	0.4671

Figure SI 3.6 - LRI x GSF submodel

The relationship between mid-summer Global Site Factor (GSF; i.e., canopy openness) and the Light Reduction Index (LRI) described in Appendix S3. Blue line and grey shading show mean and standard deviation of the regression and black points represent data.

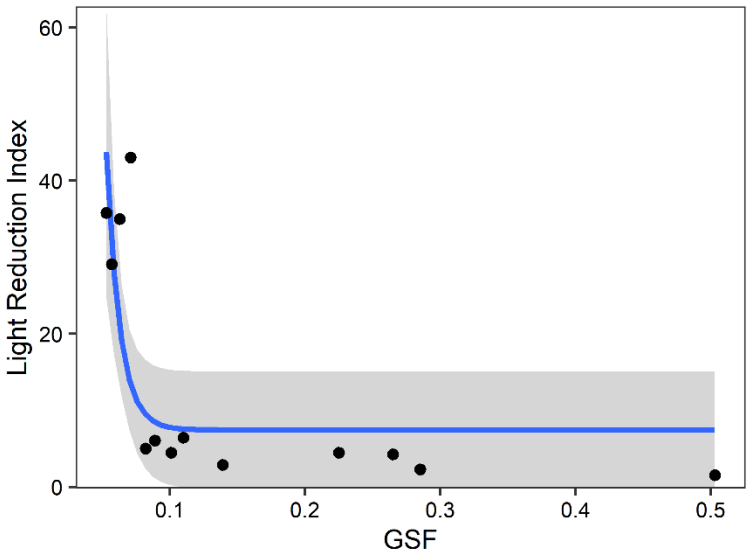

Supporting Information 3.2 - Supplemental Methods

Photosynthetic methods

Seedlings were randomly chosen for use in the gas exchange measurements while allowing for approximately equal representation across species, seed source, and canopy treatments at each site (when possible). A maximum of 10 total seedlings were chosen at each site at each day of observation and the same leaves on the same seedlings were used for all consequent measurements. If a sampled seedling died or lost too much leaf tissue to be measured, it was replaced with another of the same species and treatment where available.

Each gas exchange measurement consisted of a five-minute acclimation period with the chamber attached to the leaf followed by the construction of an A-Q curve (at 1500, 1000, 750, 500, 250, 125, 60, 30, 20, 10, and 0, μmol photon m^{-2} s^{-1}) and an *A-Ci* curve (at 400, 300, 200, 100, 50, 400, 400, 600, 800, 1000, 1250, and 1500 ppm CO_2). Leaves that did not cover the area of the cuvette (6 cm^2) were traced in the field and leaf area was subsequently measured using ImageJ software (Schneider et al., 2012). Soil moisture was measured at the time of each photosynthetic measurement using the Fieldscout soil moisture meter. The time of day was recorded for each measurement to account for possible diurnal variation in photosynthetic behavior and all measurements were taken between 0900-1600 hours. During fall, phenophase of the measured leaf was also recorded (initial leaf coloring, > 50% leaf coloring).

Plot-level environmental simulations

Understory environmental factors that affect photosynthesis and phenology (temperature, relative humidity, soil moisture, and PAR) were collected hourly at each site at locations with closed canopies representative of the variation within the site. Each replicate plot was located within approximately 100 meters of the environmental station at each site, so plot-level

temperature and relative humidity were assumed to be equal to the site-level data. Plot-level VPD was therefore equal to site-level VPD, calculated using the relative humidity and temperature data according to methodology described in Chapter 2. Water and light availability, however, differed among plots and therefore needed to be simulated at the plot level.

Light simulations

In order to simulate plot-level light, we first established the relationship between light availability and Global Site Factor (GSF), a measure of canopy openness calculated from canopy photos for each environmental station. We extracted hourly daytime light values between 0900-1800 hours for 15 days surrounding the day when the canopy photo was taken for each station in each year (day of, seven days before, and seven days after measurement), and averaged these values to determine midsummer light availability for each station (PAR_{summer}). We calculated a similar value in spring using daytime PAR values from day-of-year 100-114 (PAR_{spring}), reflecting light availability prior to canopy closure, which occurred after DOY 114 across all sites and years.

We used these values to calculate a light reduction index ($LRI = PAR_{spring}/PAR_{summer}$), where high LRI values reflect conditions where summer light availability is much lower than spring light availability (i.e., plots with dense canopies and little understory light availability) and low LRI reflects open canopies where spring and summer light availability is more similar. Because of occasionally missing PAR data (e.g., due to sensor damage) and because of relatively low variation in GSF across closed-canopy environmental stations, we supplemented these data with LRI calculated for nearby open-canopy environmental stations located at each site. We then modeled the relationship between GSF and LRI using a negative exponential model:

$$LRI \sim a + b * Exp(-GSF)$$

The model (Fig. SI 3.6) was fit in *R* (version 3.5.3) using the *lm* function in the *stats* package.

In order to simulate hourly plot-level light, we combined the intercept (*a*) and slope (*b*) parameters from the LRI model with plot-level GSF measured yearly at the plot level. This required us to substitute PAR_{spring} in the LRI calculation with hourly PAR data measured at the most open environmental station, where canopy closure was minimal (LRI = 1.55). We used this approach to simulate hourly light for daytime hours during closed canopy conditions for all plots. Nighttime and open-canopy light availability was assumed to be equal to the average PAR across the three closed-canopy environmental sensors. Day of canopy closure in spring and reopening in fall were determined according to the methodology described in Chapter 2.

Soil moisture simulations

In order to estimate plot-level soil moisture we first modeled the relationship between hourly site-level soil moisture and plot-level soil moisture data collected intermittently over the duration of the study period using the Fieldscout soil moisture meter (approximately 5-7 times per year, spread evenly throughout the growing season). We fit simple linear regressions for each plot using the *lm* function in the *stats* package in *R*:

$$SM_{site} \sim a + b * SM_{plot}$$

Where SM_{site} is the site-level soil moisture value recorded at the closed-canopy environmental station at each site at the hour closest to when the plot-level measurement (SM_{plot}) was taken. We then simulated hourly plot-level soil moisture using the intercept and slope parameters estimated from the model and the hourly soil moisture data recorded at the site where the plot was located.

Carbon accumulation detailed methods

We made several assumptions when calculating hourly carbon accumulation regarding phenology, leaf area, leaf damage, and environmental conditions experienced by the plant. With respect to phenology, we assumed that hourly phenophase (used to determine which set of photosynthetic parameter values to use) was the same as the phenophase in the most recent phenology census. This means that plants were assumed to have leaves beginning the first day they were observed to do so and were assumed to maintain them until the day before full senescence was observed. This assumption was made for individual leaves on each plant, which were tracked separately.

We did not measure leaf area for every leaf or every plant, so the leaf area used to calculate carbon accumulation from the simulated carbon assimilation rates was estimated using the average measured area of traced leaves (see Photosynthetic Methods above) and categorical leaf-size data observed at the leaf level. Leaves were traced when they did not fill the entirety of the 2 cm x 3 cm IRGA cuvette, but this was not always due to the measured leaf being too small. For example, leaves were also traced if they had insect herbivory damage to tissue toward the center of the leaf that could not be avoided during the measurement. We also recorded the relative size of each leaf on each plant (including seedlings not used in the gas exchange measurements) as either normal, small (~50% of normal), or very small (~10% of normal). We thus calculated the species-specific average leaf area for all normal-sized leaves that had been traced (42.36 and 21.56 cm^2 for *A. saccharum* and *Q. rubra* leaves, respectively), adjusting to account for the percent damage to each leaf. Small leaves were assumed to have an area of 50% of normal leaf area and very small leaves were assumed to have an area of 10% of normal.

Leaf area values used to calculate carbon accumulation were then further modified by accounting for reductions in leaf area caused by damage from herbivores and pathogens. We used the percent area of leaf damage for each leaf (see Chapter 3 Methods) and the average leaf area values described above to estimate the realized leaf area for the hourly assimilation calculations. As with phenology, leaf damage was assumed to be equal to the leaf damage recorded in the most recent damage census.

The last assumption we made with respect to carbon accumulation was that the environmental conditions each plant experienced were equal to the environmental conditions measured at the site level (temperature, VPD) or estimated at the plot level (soil moisture, PAR).

Carbon accumulation in transplant year (PrevC)

No data other than survival and growth were recorded for seedlings in the year they were transplanted because of the likelihood that transplantation would affect their performance and health. Therefore, in order to calculate the previous year's carbon accumulation (PrevC) in the transplant year for the seedling survival and growth models, we made several assumptions. We assumed that leaf area of each seedling was equal to the average leaf area (not including foliar damage) across all other years where that seedling was observed and that seedlings received the average percent leaf damage over the transplant growing season. Seedlings were transplanted following canopy closure, so light in the first growing season was assumed to be equal to open-canopy light values until the day of transplant, with leaf-out assumed to be two weeks prior to transplant. Seedling phenology in fall was estimated using parameter values from the phenology models estimated in Chapter 2. Because of the uncertainty surrounding these assumptions, the effects of PrevC were also estimated for each model excluding the estimated transplant-year

values. PrevC was not found to have a significant association with the growth or survival of either species, regardless of if the transplant-year estimations were included.

References for Supporting Information 3.2

Schneider, C. A., Rasband, W. S., & Eliceiri, K. W. 2012. NIH image to ImageJ: 25 years of image analysis. *Nature Methods, 9*, 671-675.

Supporting Information 3.3 - Model Selection Criteria

Survival models: AUROC

Model selection of survival models was evaluated by comparing the area under the receiver operating characteristic curve (AUROC; Metz, 1978; Murtaugh, 1996) using the 'pROC' package in *R*. The ROC curve plots the relationship between model sensitivity (i.e., the proportion of true positive observations that are correctly classified by the model) and model specificity (i.e., the proportion of true negative observations that are correctly classified). AUROC values range from 0 to 1 where values of 1 indicate that the model correctly distinguishes between survival and mortality 100% of the time and values of 0 indicate the model correctly distinguishes between classes 0% of the time (i.e., the model is predicting the reciprocal). AUROC of 0.5 indicates that a model is incapable of distinguishing between positive and negative classes. For model selection in this analysis, a model was considered to have a better fit from a previous model if its AUROC value was an improvement of more than 0.01. When AUROC values were equivalent, the simplest model was selected.

Growth models: DIC

Selection of the best fit growth models was done by calculating the Deviance Information Criterion (DIC; Spiegelhalter et al., 2002), which is a useful tool for evaluating the explanatory power of a model while accounting for (and penalizing) overparameterization. For this study, a model was considered to have a better fit than a previous version if its DIC was less than the previous model's DIC by more than 2. In the case of equivalent DIC values (i.e., model DIC values differ by < 2), we selected the model with the highest goodness of fit (R^2 value when comparing predicted vs. observed values). If goodness of fit did not differ by > 0.01, the simpler model (the one with fewer parameters) was selected.

References for Supporting Information 3.3

Metz, C. E. (1978). Basic principles of ROC analysis. *Seminars in Nuclear Medicine, 8,* 283-298. https://doi.org/10.1016/s0001-2998(78)80014-2

Murtaugh, P. A. (1996). The statistical evaluation of ecological indicators. *Ecological Applications, 6,* 132-139. https://doi.oorg/10.2307/2269559

Spiegelhalter, D. J., Best, N. G., Carlin, B. P., & Van Der Linde, A. (2002). Bayesian measures of model complexity and fit. *Journal of the Royal Statistical Society: B, 64,* 583-639. https://doi.org/10.1111/1467-9868.00353

Chapter 4 Vulnerability to Drought-Related Mortality

ABSTRACT

Climate change is expected to cause higher frequencies of drought events across the world and as a result there is a substantial body of work focused on investigating drought effects on forest species, but these studies tend to focus primarily on drought responses of adult trees. Hydraulic strategies employed by seedlings are understudied even though there is evidence that seedling drought response can differ from that of adults. Furthermore, there is also evidence that demographic performance in the seedling age class will have disproportionately strong effects on the assembly dynamics of future forests. Since most tree seedlings recruit under the forest canopy, these shaded conditions could also affect their response to drought; either by exacerbating the impact via carbon starvation (due to closure of stomata in response to drought), or by ameliorating heat stress (due to lower temperature under the canopy). In this study, we measured four indices of hydraulic response to drought (leaf water potential, photosynthetic capacity, non-structural carbohydrate concentration [NSC], and hydraulic conductivity), as well as interaction effects with reduced light treatments, in seedlings of two temperate tree species that differ in their adult drought response: isohydric *Acer saccharum* and anisohydric *Quercus rubra*. We found a strong isohydric response in *A. saccharum* seedlings that included conservation of leaf water potentials (> -1.8 MPa) and reductions in [NSC] consistent with reduction of stomatal conductance. *Quercus rubra* seedlings were able to survive to more negative water potentials, but only rarely, and they showed a similar reduction in photosynthetic capacity as was found for *A. saccharum*. Our results suggest that, although *Q. rubra* seedlings

display some anisohydric responses to drought, they are more isohydric than adults. Both species seem to be relatively similar in their vulnerability to drought, and we did not find any significant differences suggesting drought will affect them differently.

INTRODUCTION

Climate change is projected to increase temperatures and affect global patterns of precipitation, with many areas expected to become drier and hotter (Meehl and Tebaldi 2004). These environmental changes have the potential to strongly affect forest ecosystems (Bartlett et al. 2016). As a result, many studies have addressed the effects that water availability has on the performance of tree species, but primarily with respect to adults (Bréda et al. 2006, Allen et al. 2015, Anderegg et al. 2016). However, in areas where projected climate may not significantly affect adult trees, relatively few studies address the effect that drought has on saplings and seedlings (but see Maguire and Kobe 2015, Kannenberg and Phillips 2020). Relatively small changes in water availability are likely to have profound effects on survival of younger life stages and consequentially affect forest community assembly (Lebrija-Trejos et al. 2010, Green et al. 2014, Bartlett et al. 2016). This represents an important knowledge gap as past research has demonstrated that drought response can significantly differ across ontogeny (Cavender-Bares & Bazzaz 2000), suggesting that tree seedlings are likely to be affected by drought differently than their adult counterparts. Scientists must reconcile these differences in order to better predict the effects of climate change on forest demography.

Drought tolerance is a broad term that encompasses many plant traits including stomatal regulation behavior (i.e., iso/anisohydry), root morphology, xylem anatomy, and leaf abscission behavior (McDowell et al. 2008, Sevanto et al. 2013, Markesteijn and Poorter 2009, Ellmore et

al. 2006, Múnne-Bosch and Alegre 2004). Iso/ansiohydry, referring to whether plants close their stomata during drought to limit water loss (McDowell et al. 2008), is an overarching concept that has been used to categorize a broad range of other drought-related traits. Plants are typically sorted along a gradient ranging from isohydric species which exhibit strong stomatal control on one end and anisohydric species which show little or no stomatal regulation on the other. This difference in behavior has physiological importance because prolonged stomatal closure (i.e., isohydry) can result in the over-depletion of labile carbon reserves caused by reductions in photosynthetic capacity, i.e., carbon starvation (Sala et al. 2012, Martínez-Vilalta et al. 2016), whereas anisohydric behavior can compromise the water column and result in catastrophic embolism and reduce xylem conductivity, i.e., hydraulic failure (Sperry et al. 2002, McDowell et al. 2008, Urli et al. 2013). Anisohydric species are typically considered to be more tolerant of drought than isohydric species (McDowell et al. 2008), but most species demonstrate some level of vulnerability to both carbon starvation and hydraulic failure due to their overlapping effects (Sevanto et al. 2013, Adams et al. 2017). Furthermore, a recent study found that plant vulnerability to drought is poorly predicted when using a singular plant hydraulic trait (Martínez-Vilalta and Garcia-Forner 2016), and it has been suggested that plant hydraulics should be studied and classified independently of the iso/anisohydry framework (Hochberg et al. 2018). It is thus important that ecologists measure multiple drought responses to understand and then predict the consequences of drought.

There are several indicators of hydraulic strategy that can be used to partially explain a plant's response to drought stress; these include regulation of internal water potentials (Thomas and Eamus 1999), regulation of photosynthetic capacity (Roman et al. 2015), depletion of non-structural carbohydrates (Sala et al. 2012, Quentin et al. 2015), and loss of xylem conductivity

(Sperry and Tyree 1990). Predawn leaf water potential (Ψ_{PD}) is a measure of plant hydraulic stress that is more representative of soil moisture conditions compared to midday leaf water potential, which is more strongly affected by hydraulic stress imposed by the atmosphere and is thus more negative (Cavender-Bares and Bazzaz 2000, Williams and Araujo 2002). Ψ_{PD} is especially sensitive to soil water availability in drought conditions for anisohydric species (Bréda et al. 1995) and is therefore useful as a metric of plant water status in stressful conditions. Water potential has strong effects on the regulation of stomatal conductance (Anderegg et al. 2017), and stomatal regulation in turn affects Ψ_{PD} by allowing a plant to maintain internal water pressures above critical thresholds (Sperry et al. 2002, McDowell et al. 2008), below which the plant's water column would snap, resulting in hydraulic failure. Tree species with strict stomatal regulation exhibit relatively narrow ranges of Ψ_{PD} that are maintained by reductions in stomatal conductivity until that threshold is surpassed and the plant dies (Breshears et al. 2009). In contrast, species that exhibit anisohydric behavior have much wider variation in Ψ_{PD} and can survive to much lower water deficits (Breshears et al. 2009). This strategy is common in species that have wide xylem conduits that can be refilled easily after water availability is reestablished (Ogasa et al. 2013) and species with physiological adaptations that prevent the spread of cavitation once it is initiated (Pittermann et al. 2006). Strict regulation of Ψ_{PD} tends to be associated with species which are more vulnerable to drought (McDowell et al. 2008), although there is recent evidence that this is not a fully generalizable rule (Martínez-Vilalta and Garcia-Forner 2016).

Plant photosynthetic capacity (i.e., A_{max}) is tightly linked to stomatal conductance, and thus plant water potential, during drought since stomatal closure limits CO_2 from entering leaves (Cowan and Farquhar 1977). This causes plants with strict stomatal regulation to reach net

negative photosynthetic rates at less extreme soil water potentials compared to species that exhibit a more anisohydric drought response (McDowell et al. 2008). There is evidence of a strong relationship between stomatal regulation and changes in photosynthetic capacity across a wide range of species and biomes (Reich and Hinkley 1989, Thomas and Eamus 1999, Wilson et al. 2000, Roman et al. 2015).

Without being able to rely on the assimilation of new photosynthate, isohydric species instead mobilize labile carbon sources in order to meet plant energy demands (Sala et al. 2012). This source of carbon, commonly referred to as non-structural carbohydrates (NSC), includes starch as well as soluble sugars such as glucose (Quentin et al. 2015). Reductions in NSC concentrations have been shown to be caused by drought (McDowell et al. 2008, Sala et al. 2012, O'Brien et al. 2014) and other stressful conditions such as shade (Maguire and Kobe 2015, Piper and Fajardo 2016), and extreme reductions would theoretically result in death via carbon starvation, although it is unlikely that plants would need to exhaust their carbon supply to experience negative effects (Sala et al. 2010, Sala et al. 2012). For example, refilling xylem following cavitation often requires the expenditure of energy (Trifilò et al. 2019) and soluble sugars are involved in plant osmoregulation such that reduced sugar content can lead to increased vulnerability to xylem cavitation (Sevanto et al. 2013, Adams et al. 2017). Despite the difficulty associated with quantifiably measuring carbon starvation, the ability to increase or maintain [NSC] during drought is associated with drought-tolerant species that can afford to maintain stomatal conductivity due to other physiological and morphological traits (Cavender-Bares et al. 2000, Martínez-Vilalta and Garcia-Forner 2016).

Xylem conductivity (or hydraulic conductivity) is the rate at which fluid passes through a given stem or branch segment, and decreases with the amount of cavitation (i.e., gas embolisms)

present within the segment (Sperry and Tyree 1990, Tyree et al. 1992). Plants that conserve hydraulic conductivity through the closure of stomata are typically classified as isohydric and experience steep drop-offs in conductivity past a certain threshold (McDowell et al. 2008). Anisohydric plants are typically characterized by their more gradual decrease in conductivity that occurs across a wider gradient of water availability (McDowell et al. 2008), a strategy that is commonly associated with drought tolerance. This strategy often coincides with wide xylem conduits (i.e., ring-porous anatomy), which are easier to refill following drought (Ogasa et al. 2013), and reduced stomatal regulation that provides the energy needed to expend in the refilling process (Trifilò et al. 2019).

Accurate classification of these traits is especially important for forest drought studies involving seedlings or saplings, which can substantially differ in hydraulic strategy compared to mature canopy trees. Cavender-Bares and Bazzaz (2000) showed that although adult *Quercus rubra* exhibit anisohydric behavior, seedlings were relatively isohydric, even when controlling for microenvironment differences between the two groups. The authors speculate that this is in part due to seedlings being unable to access deep water sources due to their shallow root profiles as well as to their higher vulnerability to environmental stress. Other recent research has also demonstrated that saplings received no tangible benefit from anisohydric behavior during drought and took longer to recover after the drought ended (Kannenberg et al. 2019), suggesting that small size classes will have different vulnerability to drought even if they follow the hydraulic strategies of adult trees. Together, results from these studies support the recent call for a full quantification of hydraulic responses to drought (Martínez-Vilalta and Garcia-Forner 2016, Hochberg et al. 2018) that is more robust in addressing suites of traits and within the context of ontogenetic differences.

Seedlings are the size class most likely to experience directional mortality effects (Harper 1977, Grubb 1977, Green et al. 2014), meaning that differences in species' response to environmental drivers should be strongest in this phase of recruitment. Therefore, improving our understanding of ontogenetic differences in drought response will be critical to forecast changes to forest systems. Predicting future seedling performance will then require an accurate estimation of hydraulic traits and behavior; if seedlings tend toward the same hydraulic strategies as their adult counterparts, climate change-related drought could accentuate differences in species performance based on these traits. However, if seedlings tend to be more isohydric than adult trees in general, as suggested by Cavender-Bares and Bazzaz (2000), drought effects could be more homogenous across species, increasing the relevance of other drivers of recruitment dynamics that affect community assemblage.

One such driver is light availability, which can severely limit photosynthetic rates even in species with high photosynthetic capacities (Farquhar et al. 1980). Shade-tolerant species, i.e., species that can withstand prolonged periods in full shade, typically have relatively lower respiration demands than shade-intolerant species that allow them to persist on limited resources (Boardman 1977). They may also exhibit phenological escape behavior that allows them to assimilate the resources they need in a short period of time when light availability is high (Jacques et al. 2015). Light limitations can lead to carbon deficits analogous to carbon starvation caused by stomatal limitations during drought (Piper and Fajardo 2016) and can strongly shape recruitment in forest understories (Coates 2002, Wright et al. 2003, Rüger et al. 2009).

Furthermore, light availability is likely to affect seedling drought response (Maguire and Kobe 2015, Piper and Fajardo 2016). Carbon starvation caused by deep shade can potentially compound with carbon starvation caused by stomatal limitations during drought (Holmgren

2003, Sevanto et al. 2013). However, there is also evidence that shading can ameliorate drought stress (Quero et al. 2006), particularly for drought-intolerant and shade-tolerant species (Holmgren et al. 2012). These positive effects of shading are projected to drive seedling recruitment in some systems (Dobrowski et al. 2015, Ibáñez and McCarthy-Neuman 2014), and should therefore be considered alongside drought when studying the effects of climate change on forest demography.

In order to evaluate the extent to which drought response in tree seedlings differs from their adult counterparts, we measured four ecophysiological drought responses (leaf water potential, photosynthetic capacity, non-structural carbohydrate concentration [NSC], and xylem conductivity) for seedlings of two temperate tree species that commonly occur throughout eastern North America: isohydric *Acer saccharum* and anisohydric *Quercus rubra*. We used a greenhouse experiment to combine artificial drought and shading treatments. Our research questions were 1) Does seedling hydraulic strategy differ between species where adult hydraulic strategies are different? 2) How is seedling hydraulic strategy affected by light availability? And, 3) what are the implications for seedling demographic performance under climate change? We hypothesize that if seedlings of these species have hydrologic strategies similar to those used by their adult counterparts then: 1) the range of leaf water potential experience by *A. saccharum* seedlings is much narrower than those observed in *Q. rubra* seedlings. 2) Under drought conditions, reductions in photosynthetic capacity are steeper in isohydric *A. saccharum* than in anisohydric *Q. rubra*. 3) The drop in NSC levels under drought is larger for *A. saccharum* seedlings. And, 4) the magnitude of the decrease in xylem conductivity when exposed to drought is higher for *A. saccharum*. Addressing these questions and hypotheses will contribute to our

knowledge on how climate change will affect the demographic processes that shape temperate forest communities.

METHODS

We studied two temperate deciduous tree species that commonly co-occur across eastern North America, and that differ in their respective tolerances to shade and drought: *Acer saccharum* (Marsh.) and *Quercus rubra* (L.). *Acer saccharum* is a strongly shade-tolerant species (Lei and Lechowicz 1990) that is intolerant of drought (Coble et al. 2017). It has relatively narrow xylem conduits (i.e., diffuse-porous xylem; Ellmore et al. 2006) and has been shown to exhibit isohydric stomatal behavior in response to drought (Roman et al. 2015). In contrast, *Q. rubra* is moderately shade-tolerant (Crow 1988) and moderately drought-tolerant (Coble et al. 2017). Trees of this species have large xylem conduits (i.e., ring-porous xylem; Ellmore et al. 2006) and exhibit anisohydric stomatal behavior in response to drought (Cavender-Bares & Bazzaz 2000). Although wider xylem conduits are more vulnerable to embolism, there is also evidence that they are easier to refill following drought (Ogasa et al. 2013), conferring the higher drought tolerance generally associated with this trait. Adult *Q. rubra* trees also develop deeper roots than *Acer* species (Thomsen et al. 2013), which may enhance their relative drought-tolerance by allowing them to access deeper water sources.

Seeds of both species (from two different sources) were cold-stratified beginning in December 2016 and sown in large plastic tubs filled with potting soil (SunGro Horticulture; Agawam, MA, USA) at the Matthaei Botanical Gardens greenhouse (42.2996° N, 83.6630° W) the following spring. Once seedlings developed their first true leaves, we carefully removed them from the tubs and transplanted them into individual pots (volume = 313 cm^3),

supplementing new potting soil as needed. Sixteen seedlings of each species x source combination were randomly assigned to each treatment group (control, shade, drought, shade and drought) for a total of 256 total seedlings; 191 of these seedlings survived to be used in our analyses. Initial height for each seedling was measured two weeks following transplantation in order to account for maternal effects (Ibáñez and McCarthy Neumann 2014).

Experimental Design

Following transplantation to individual pots, seedlings were immediately moved under moderate shade cloth (~40% ambient PAR) and allowed to grow for an entire growing season (summer of 2017) under well-watered conditions. This was done to minimize the effects of first-year transplant stress and to allow seedlings the ability to assimilate enough carbon to allocate photosynthate to storage tissue and other labile carbon pools. Seedlings were moved to an outdoor pit following the onset of leaf color change in fall in order to allow seedling foliar phenology to respond to natural climate conditions. The pit was used to help insulate seedling roots from frost conditions they would otherwise not experience, and seedlings were further insulated by surrounding the pots with potting soil.

Seedlings were removed from the pit and moved back into the greenhouse in early spring 2018 corresponding to when leaf bud expansion was noted for both species. All pots were moved under one layer of shade cloth and were regularly watered until treatments were implemented. Environmental sensors were added simultaneously with when the seedlings were moved back inside, measuring air temperature and relative humidity (HOBO U23 Pro v2 data loggers) and light (HOBO Pendant data loggers; Onset Computer Corporation; Bourne, MA, USA). Temperature, relative humidity, and light were all measured at 30-minute intervals. Soil moisture

was also measured at the individual (pot) level coinciding with harvesting or gas exchange measurement using a FieldScout TDR300 soil moisture meter (Spectrum Technologies; Aurora, IL, USA).

We took pre-treatment measurements of photosynthetic capacity and non-structural carbohydrate concentrations approximately four weeks following initial seedling leaf-out (June 14th), after which treatment conditions were initiated. Our four treatments were drought (D; no additional shade cloth added, seedlings are no longer watered), shade (S; extra shade cloth used to reduce PAR to 10% of ambient, seedlings remained well-watered), shade and drought (DS; extra shade cloth added, seedlings are no longer watered), and a control treatment (C; no additional shade cloth, seedlings remain well-watered).

All seedlings acclimated to the study treatments for two weeks before three harvests were made at weekly intervals. Seedlings in each treatment combination were randomly assigned to be harvested for measurement of either xylem conductivity or [NSC]. Each harvest included six seedlings from each group: two for measurement of xylem conductivity and four for measurement of [NSC]. Predawn leaf water potential (Ψ_{PD}) was measured on the morning of each harvest before sunrise as an approximation for soil water potential. Water potential was measured using excised leaves and a Scholander pressure chamber (PMS Instrument Company, Albany, OR, USA).

Gas exchange measurements (A_{max})

The day before each harvest, for each treatment, we measured gas exchange in two of the four seedlings selected for the NSC analyses. We used an LI-6400 Portable Photosynthesis System equipped with a CO_2 mixer assembly, LI-02B LED red/blue light source, and LI-06 PAR

sensor (Li-COR Biosciences, Lincoln, NE, USA). We constructed light curves (i.e., *A*-*Q* curves) for each plant by recording gas exchange at 1500, 1000, 750, 500, 250, 100, 50, 25, and 0 μmol photons m^{-2} s^{-1} at CO_2 concentrations of 400 ppm, ambient temperature, and ambient humidity. Maximum photosynthetic capacity (A_{max}) was calculated using equations published by Marshall and Biscoe (1980) and using the *nls* command in the *stats* package in *R* v3.5.3. This parameter represents the maximum photosynthetic rate that a leaf is capable of under saturating light conditions. Reductions in A_{max} indicate limitations on the photosynthetic machinery, such as from reduced stomatal conductance (Roman et al. 2015).

Non-structural carbohydrate concentrations [NSC]

After Ψ_{PD} measurement, tissue from seedlings selected for the NSC analysis were immediately separated into three pools: leaves (including petioles), stem (above root collar), and roots (below root collar). Leaves were microwaved for 180 seconds at 800 watts to stop leaf enzyme activity (Quentin et al. 2015) and then all tissues were transferred to a drying oven and dried for 48 hours at 70 °C. We weighed each sample, ground them using a ball mill, and then stored the samples at 20 °C in airtight containers. We measured out 50 mg of each sample in to screw-top conical tubes and soluble sugars were extracted according to Quentin et al. (2015) using repeated incubation and centrifuging in 80% ethanol. We measured glucose concentrations using a phenol-sulfuric acid colorimetric assay as described by DuBois et al. (1956). Glucose concentration was measured against a glucose standard curve using absorbance measured at 490 nm. Measurements were then converted to units of mg glucose per gram of dry tissue.

Xylem conductivity (k)

Following Ψ_{PD} measurement, seedlings harvested for xylem conductivity measurements were removed from their pots and their root balls were soaked in water for 10 minutes to alleviate stress on the water column. We then cut stem segments from each plant underwater, recording the length of each segment and its average diameter. Conductance was measured using protocol established by Kolb et al. (1996). We slightly modified this protocol by using 20 mM KCl solution filtered to 0.22 μm (used to prevent microbial growth within the system that could cause artificial xylem blockages). Flow rate of the solution through the stem segment was measured at pressures of 0, -8, -16, -24, and -32 KPa. Hydraulic conductance (*k*) was calculated as the slope of the relationship between flow rate and pressure (Sperry and Tyree 1990, Kolb et al. 1996). Flow rate was then standardized by segment length and cross-sectional area. Our vacuum source was not strong enough to forcefully remove embolisms from the stem segments and so we were unable to calculate the percent loss of conductivity.

ANALYSES

Analyses were performed for each species independently. For each analysis we addressed our specific questions by trying different types of relationships between the variables involved (e.g., linear, exponential, additive, interactions), and tried several combinations of additional explanatory variables (i.e., initial seedling height and seed source). We describe below the models with the best fits based on Deviance Information Criterion for the photosynthetic capacity model (DIC; Spiegelhalter et al. 2002) and based on residual sum of squares comparisons for the other two analyses. Analyses used data from all harvests where seedlings from all relevant treatments were alive to be measured, with the exception being xylem

conductivity measurements for *A. saccharum* where there was no data available for seedlings in the drought treatment.

Predawn leaf water potential

Leaf water potential measurements (Ψ_{PD}) taken over the span of the experiment (Fig. 1) were used to assess the range of water potentials experience by seedlings of each species. Measurements were pooled across all seedlings harvested for both NSC and xylem conductivity experiments. We conducted a one-way ANOVA in order to assess whether Ψ_{PD} differed significantly between the two species.

Photosynthetic capacity

We modeled maximum photosynthetic capacity (A_{max}) as a function of light treatment and of leaf water potential (our proxy for drought effects); thus we combined seedlings from the two shaded treatments (S and DS) as well as from the two unshaded treatments (C and D) to assess the two light treatments and then used the full range of observed water potentials to account for drought treatments. Photosynthetic capacity for seedling *i* was estimated from a normal likelihood:

$$A_{max,i} \sim N(\mu_i, \sigma^2)$$

And an exponential process model that described well the reductions in A_{max} observed in the data (Fig. 2a-b):

$$\mu_i = \beta 1_{shade(i)} * Exp(\beta 2_{shade(i)} * \Psi_{PD\,i})$$

Parameter β1 represents the maximum photosynthetic rate at water potential equal to zero (i.e., full water availability). Parameter β2 indicates the decay rate at which A_{max} changes in response to changes in Ψ_{PD}; we used this parameter to assess reductions in photosynthetic capacity. Both

parameters were estimated for each shade treatment. The model was also evaluated for the effects of seed source and initial height, but they did not improve model fit and so we did not include them in the final model.

Parameter β1 was estimated from non-informative normal priors constrained to be positive, $\beta 1_* \sim N(0,1000)$, and parameter β2 was estimated from non-informative uniform prior $\beta 2_* \sim Uniform(-1,1)$. Model variance was estimated from a non-informative gamma prior distribution $1/\sigma^2 \sim Gamma(0.01, 0.01)$. We ran the model using two Monte Carlo chains for 40,000 iterations following a 60,000-iteration burn-in period. Analyses were completed using OpenBugs statistical software v3.2.3 (Lunn et al. 2009) and model convergence was assessed using the Brooks-Gelman-Rubin statistic (Gelman and Rubin 1992). Parameter values (means, variances, and covariances) were estimated from their posterior distributions.

Non-structural carbohydrates

Since seedling glucose concentrations did not change significantly over the duration of the harvest periods (Fig. SI 4.5), data was pooled across harvest dates for which seedlings from all treatments were still alive (harvest 1 for *A. saccharum* and harvests 1 and 2 for *Q. rubra*). Non-structural glucose concentrations were analyzed using ANOVA that estimated the effects of treatment on values pooled by tissue type (leaf, stem, and root), or averaged across all pools (using averages weighted by the mass of each pool). Analyses were conducted separately for each pool x species combination. We only included data for seedlings that were recorded as alive at the time of harvest because most of the dead seedlings appeared to have died from hydraulic failure, and therefore could skew the results.

Xylem conductivity

For each species, we analyzed the differences in xylem conductivity between seedlings harvested before and after the initiation of drought and shade treatments. We limited our analysis to compare differences only using seedlings harvested in the second harvest period (three weeks after the initiation of treatments) because there were no surviving seedlings in either of the two drought treatments past this harvest. We used initially carried out an ANCOVA to estimate the effects of treatment (C, D, S, DS), maternal effects (initial height), and of seed source. The effects of initial height and seed source did not improve the model fits and were therefore excluded from the final analysis.

Seedling conductivity and [NSC] analyses were conducted in R (v3.5.3) using the *aov* and *anova* commands in the *stats* package to fit and compare models, respectively. Significant differences between treatments were estimated using Tukey's HSD test, performed using the *TukeyHSD* command in *stats*.

RESULTS

Average daytime light levels across the two light treatments (Fig. SI 4.6a) were consistent with light levels measured in related field experiments (Fig. SI 2.6). Light levels in the deep shade treatments were 30% (± 0.05% s.d.) of the light levels in the control light treatment. Average daily temperature (Fig SI 4.6b) was also consistent with field observations (Fig. SI 2.13a), although maximum hourly temperatures were much higher in the greenhouse than what has been observed in the field (Fig. SI 4.7), and well above the temperature increases predicted under extreme climate change conditions for the Great Lakes region (Handler et al. 2014). Temperatures were consistent across all treatments. We found some significant differences in

height and mass between populations for each species (see Supporting Information 4.2), but they did not significantly affect any of our analyses and are not included in the following results.

Predawn leaf water potential (Ψ_{PD})

Leaf water potential decreased under the drought treatments for both species (Fig. 4.1) with *Q. rubra* seedlings reaching more negative water potentials (-3.28 MPa) than *A. saccharum* seedlings (-1.76 MPa). However, we did not find any significant difference in Ψ_{PD} between the two species (Pr(>F) = 0.291). All *A. saccharum* seedlings in the D and DS treatments died before the second harvest (~21 days after treatments were initiated) and all *Q, rubra* seedlings died before the third harvest (~28 days after treatment initiation).

Photosynthetic capacity

Our model fit (r^2 of predicted vs observed) was 0.289 for *A. saccharum* and 0.305 for *Q. rubra*. Posterior parameter estimates can be found in Table SI 4.2. There were no significant differences in posterior estimates of intercept parameter β1 between light treatments for either species (Fig. 4.2c), although values were higher in the shade treatment for *Q. rubra*. Decay parameters β2 were statistically significant, different from zero, for both shade treatments for *Q. rubra* but was only significant for the unshaded treatment in *A. saccharum* (Fig. 4.2d). These decay parameters did not significantly vary between light treatments for either of the species. Predicted A_{max} decreased from 3.375 μmol m^{-2} s^{-1} (± standard deviation of 0.692) at Ψ_{PD} = 0 MPa to 1.309 ± 0.413 μmol m^{-2} s^{-1} at Ψ_{PD} = -1 MPa for unshaded *A. saccharum* seedlings, a decrease of 61.2% (Fig. 4.2a). This drop was proportionally smaller in the shade treatment, with A_{max} decreasing from 2.936 ± 0.568 to 2.577 ± 0.929 μmol m^{-2} s^{-1} (12.3% decrease). This trend

was the opposite for *Q. rubra* seedlings (Fig. 4.2b), where predicted A_{max} decreased in light conditions from 2.775 ± 0.383 to 1.893 ± 0.325 μmol m^{-2} s^{-1} (31.8% decrease) and in shade conditions from 4.934 ± 0.746 to 1.137 ± 0.411 μmol m^{-2} s^{-1} (77% decrease).

Non-structural carbohydrates

Non-structural glucose concentrations showed a general decrease over time across all treatments and pools for both species (Fig. 4.3), but there were no significant differences between treatments for any of the species x pool combinations (Table SI 4.3). Some carbon pools significantly decreased from the pre-treatment values (Fig. 4.3). There were no statistically significant drops in NSC between control and treatment seedlings in either of the two species, and in some cases mean NSC values were higher in the treatments than the control (particularly for *Q. rubra*, Fig. 4.3e-h).

Xylem conductivity

There were no significant differences in conductivity between any of the treatments for either species (Table 4.1a; Fig. SI 4.8). Average *A. saccharum* conductivity was 0.075 ± 0.016 g s^{-1} MPa^{-1} mm^{-1} (mean ± s.d.) in the control treatment and 0.073 ± 0.027 g s^{-1} MPa^{-1} mm^{-1} in the shade treatment (n = 4 in each treatment). There were no *A. saccharum* seedlings that survived in the drought treatments that could be used in this analysis. *Quercus rubra* average conductance was 0.076 ± 0.024 g s^{-1} MPa^{-1} mm^{-1} in the control treatment, 0.041 g s^{-1} MPa^{-1} mm^{-1} in the drought treatment, 0.082 ± 0.011 g s^{-1} MPa^{-1} mm^{-1} in the shade treatment, and 0.043 ± 0.021 g s^{-1} MPa^{-1} mm^{-1} in the combined drought and shade treatment (n = 3, 1, 4, and 3, respectively). We found a significant by drought treatment for *Q. rubra* seedlings when the different shade

treatments were grouped together (Table 4.1b, Fig. SI 4.9.b), with seedlings of this species exposed to drought having significantly lower hydraulic conductivity (0.043 ± 0.017 g s^{-1} MPa^{-1} mm^{-1}) compared to those in the well-watered treatments (0.079 ± 0.021 g s^{-1} MPa^{-1} mm^{-1}). *Acer saccharum* seedling conductivity in the combined well-watered treatments was 0.074 ± 0.021 g s^{-1} MPa^{-1} mm^{-1}.

DISCUSSION/CONCLUSION

There is wide variation in the hydraulic strategies that plants use to avoid, tolerate, and recover from drought, and these strategies can be more nuanced than what is represented by broad categorization such as iso/anisohydry (Hochberg et al. 2018). Previous research has demonstrated that common drought response indicators such as stomatal conductance regulation are often dependent on environmental context (Hochberg et al. 2018) and other trait axes (Martínez-Vilalta and Garcia-Forner 2016, Kannenberg and Phillips 2020), suggesting that adequate representation of drought tolerance requires the simultaneous quantification of multiple indicators. Furthermore, there is evidence that hydraulic strategy in tree species can vary substantially along ontogeny (Cavender-Bares and Bazzaz 2000), and there is a sizeable knowledge gap in the scientific literature for how seedling drought response differs from that of adults. Whether seedling hydraulic strategies differ from adult hydraulic strategies will affect our predictions of forest demography under climate change (McDowell et al. 2011).

In this experiment we measured the hydraulic strategies used by seedlings of two dominant tree species that commonly co-occur across a wide range of eastern North American forests, and that differ in their response to drought (as measured in adults). We quantified four commonly measured indicators of drought tolerance (leaf water potential, photosynthetic

capacity, non-structural carbohydrate concentrations, and hydraulic conductance) over the duration of a greenhouse dry-down experiment. We used two different light treatments to investigate the potential interaction effects between shade and drought on tree seedling performance, since shade can both exacerbate carbon starvation via low light levels and/or ameliorate drought stress via decreasing temperature. Our results indicate that, as predicted from adult characteristics, *A. saccharum* seedlings appear to be slightly more vulnerable to drought due to their relative inability to survive past relatively moderate levels of soil water potential (Fig. 4.1a), whereas *Q. rubra* were recorded to survive to considerably lower levels (Fig. 4.1b). *Quercus rubra* seedlings were also able to survive longer in the drought treatments by about a week. Still, we did not find statistically significant differences between species in any of the drought indicators, suggesting that seedlings of these two species are still similarly vulnerable to drought. However, due to the relatively small sample sizes used in this study, it is important to be cautious with these results and the conclusions drawn from them. Overall, our results suggest that the increased drought frequency predicted for the Great Lakes region (Handler et al. 2014) could negatively affect recruitment and demography of both species in approximately equal measure.

1) Does seedling hydraulic strategy differ between species where adult hydraulic strategies are different?

Tree performance during drought is strongly affected by stomatal regulation via two interacting processes (McDowell et al. 2008, Adams et al. 2017). Restricting stomatal conductance allows trees to avoid excessively low internal water pressures that can embolize xylem and lead to hydraulic failure (Sperry et al. 2002). However, reducing conductance comes

at the cost of reducing photosynthetic capacity, which makes it necessary for trees to consume labile carbon pools and increase the risk of dying from carbon starvation (Sala et al. 2012). Trees exhibit variation in other traits such as rooting depth (Loewenstein and Pallardy 1998, Lopez et al. 2005) and xylem pit anatomy (Pittermann et al. 2006) that can help mitigate the negative effects associated with one process or the other (e.g., by giving trees access to more resources or by helping them resist cavitation), but there is strong evidence that tree performance in drought conditions is strongly determined by tradeoffs between these two processes (Adams et al. 2017). Furthermore, juvenile trees may not be able to make use of the same mitigating strategies used by adults due their size and relative lack of access to resources (i.e., deep water sources; Cavender-Bares and Bazzaz 2000). Hydraulic outcomes at the seedling level may therefore be more similar among species than they are at larger size classes.

Our results do not fully support the idea that seedling hydraulic strategies are similar to those of the adults; while leaf water potentials reached lower levels in *Q. rubra* seedlings, as we expected, the other responses to drought we measured did not show a different pattern between the two species. First, while adult *Q. rubra* (as well as other *Quercus* species in general) respond to drought stress by maintaining photosynthetic capacity at the cost of reduced leaf water potential (Cavender-Bares and Bazzaz 2000, Roman et al. 2015), we found that seedlings of this species exhibited declines in photosynthetic capacity that began at $\Psi_{PD} < -1$ MPa (Fig. 4.2b). This was not significantly different from the trend found in *A. saccharum* seedlings (Fig. 4.2a), which matched the photosynthetic response demonstrated in adults of this species (Roman et al. 2015). This relatively isohydric response of *Q. rubra* seedlings agrees with previous work done by Cavender-Bares and Bazzaz (2000) and provides support for the idea that seedling hydraulic strategies will be more similar between species than they are in conspecific adults.

Adults of these two species have also been shown to have different wood densities, with *A. saccharum* having dense wood and diffuse-porous xylem and *Q. rubra* having ring-porous xylem and wood that is less dense (Ellmore et al. 2006). Diffuse-porous xylem can help trees avoid embolism formation due to the narrower conduits, but they are also more difficult to refill after embolism occurs (Ogasa et al. 2013). Narrow xylem conduits and strong stomatal control help *Acer* species maintain hydraulic conductance during drought (Sperry et al. 1988, Hoffman et al. 2011). In contrast, *Quercus* species are more prone to gradual but significant declines in conductivity (Tyree et al. 1992, Lo Gullo et al. 2005, Hoffman et al. 2011). We hypothesized that *A. saccharum* seedlings would demonstrate stricter control of internal water potentials compared to *Q. rubra*, and thus show little variation in the conductivity of living seedlings, whereas *Q. rubra* seedlings would show a gradual decline in conductivity associated with anisohydric stomatal regulation.

We found tentative support for this hypothesis with respect to *Q. rubra* seedlings, for which conductivity appeared to decrease gradually beginning at $\Psi_{PD} < -1$ (Fig. 4.4), which closely resembles the pattern seen in conspecific adults (Lo Gullo et al. 2005) and agrees with previous work done on seedlings of this species (Tyree et al. 1992). However, we were not able to fully quantify this trend in a more complex analysis because we did not measure percent loss in conductivity (*sensu* Kolb et al. 1996) and because we had limited survival in our seedlings. There was high mortality for this species past the -1 MPa threshold, suggesting these seedlings are still vulnerable to drought. *Acer saccharum* seedlings supported the hypothesis, with conductivity maintained at $\Psi_{PD} > -1$ and hydraulic failure past that point (Fig. 4.4), which agrees with the strategy used by adults. We observed seedlings of this species surviving to slightly more negative Ψ_{PD} in the NSC harvests (Ψ_{PD} =-1.76 MPa, Fig. 4.1), suggesting that reductions in

conductivity may follow a trend more similar to that of the *Q. rubra* seedlings, but conductivity was not quantified for these individuals and thus we lack the evidence needed to better support this conclusion.

Photosynthetic capacity and hydraulic conductivity are both strongly intertwined with changes to non-structural carbohydrate concentrations. Reductions in photosynthetic capacity limit the production of carbohydrates and make plants more dependent on labile carbon pools, reducing [NSC] to maintain metabolic rates (Sala et al. 2012). Conductivity directly affects a plant's ability to transport carbohydrates from source tissue (leaves) to tissues where sugars are needed (stems and roots). However, [NSC] also affects conductivity since energy is often required to refill xylem following cavitation (Trifilò et al. 2019) and because soluble sugars are necessary for osmoregulation processes (Sevanto et al. 2013); thus, reduced sugar content can lead to faster hydraulic failure.

We found no significant differences between non-structural glucose treatment conditions for *A. saccharum* in any of the tissue pools, and limited differences between treatment [NSC] and pre-treatment [NSC] (Fig. 4.3a-d). This suggests that seedlings were generally able to maintain their labile carbon pools throughout the experiment. This is consistent with a previous study that worked with *Acer rubrum* seedlings (which are closely related to *A. saccharum* and typically exhibit a similar hydraulic strategy; Davies and Kozlowski 1977), which found reductions in soluble sugar concentrations over time in similar treatments (Maguire and Kobe 2015). We also found no significant differences between treatments in any of the *Q. rubra* NSC pools (Fig. 4.3e-h), but there were more instances of [NSC] reductions relative to pre-treatment controls. This contradicts previous research by Maguire and Kobe (2015), which found general increases in soluble sugar concentrations for this species under similar drought and shade

treatments and suggests that seedlings of this species also experienced similar stress across all treatments.

The lack of a significant difference between our control treatments and the three stress treatments prevents us from being able to make strong conclusions about how drought will affect [NSC] for seedlings of either species. The difference between our results the results from other studies that have found significant effects in similar experiments (e.g., Maguire and Kobe 2015) could be due to the extremely high temperatures experienced by seedlings in the greenhouse environment (Fig. SI 4.7), which would have affected all seedlings equally and could have caused reductions in [NSC] associated with high respiration rates (Tjoelker et al. 2002). It is also possible that the trends we report do not tell the full story as we did not measure starch concentrations, nor did we measure the concentrations of other soluble sugars besides glucose. Recent evidence suggests that soluble sugar concentrations can be maintained through the conversion (and therefore reduction) of starch (Kannenberg and Phillips 2020), suggesting that measurement of total non-structural carbohydrate concentrations may tell a more complete story.

2) How is seedling hydraulic strategy affected by light availability?

There is experimental evidence for both the mitigating (e.g., Quero et al. 2006, Piper and Fajardo 2016) and exacerbating effects (e.g., Holmgren 2003, Sevanto et al. 2013, Maguire and Kobe 2015) that shade can have on tree performance during drought. In temperate North American forests, understory light availability under full canopies can be 2-3 orders of magnitude lower than light availability in open canopy conditions (Fig. SI 2.6), and access to light plays a significant role in tree seedling demographic performance in these systems (Canham

1988, Beckage et al. 2000). It is therefore important that projections of tree recruitment under climate change account for any interactions between drought and shade.

Contrary to other tree seedling studies (e.g. Piper and Fajardo 2016), we did not find any significant effects associated with light availability in any of our drought response indicators. Although including light treatments improved our photosynthetic capacity model's performance, there were no significant differences between light condition effects for either β1 (photosynthetic capacity at saturating water availability) or β2 (the decay rate parameter) (Fig. 4.2c-d). There were no significant shade effects in any of the glucose pools (Fig. 4.3) and hydraulic conductance was better predicted in an analysis that explicitly omitted light treatment and focused solely on differences in drought treatment (Fig. SI 4.9). The lack of a shade effect on glucose concentrations is consistent with previous research that found no significant change in soluble sugar concentrations over time in seedlings (Maguire and Kobe 2015) and saplings (Kannenberg and Phillips 2020) of temperate tree species common in our study region. However, both studies found significant reductions in starch concentrations that suggest that plants prioritize the mobilization of starch for use in metabolism over the consumption of soluble sugars, potentially due to the importance of soluble sugars in osmoregulation (Sevanto et al. 2013).We did not measure starch concentrations, so we can only speculate that this mechanism may have affected our results. The extreme temperatures experienced in the greenhouse could have also created respiration demands across all treatments that overwhelmed any signal that we might have otherwise observed with differences in light availability (Tjoelker et al. 2002). Still, our results do not support the existence of either mitigating or exacerbating effects of shade on hydraulic performance of temperate tree seedlings.

3) What are the implications for seedling demographic performance under climate change?

Altogether the results from our experiment suggest a convergence in the vulnerability of temperate tree seedlings to drought that is inconsistent with drought responses expected from previous evidence collected in adult trees of the same species. There were no drought treatment *A. saccharum* seedlings that survived longer than two weeks past the initiation of experimental treatments and no water-limited *Q. rubra* seedlings that survived past three weeks. Although our stress treatments were harsh (and also likely exacerbated by high temperatures) the lack of a significant difference between seedling responses is consistent with results from previous research (Maguire and Kobe 2015). Still, the relatively small sample size of seedlings surviving in this experiment could have affected our ability to pick up on differences between the two species at finer scales of time, temperature, and soil moisture, and it therefore prevents us from making stronger conclusions about seedling drought dynamics.

Even so, with no clear distinction in seedling vulnerability to drought, potential differences in seedling demography and recruitment between species within the context of climate change are more likely to be driven by other factors. For example, we have previously shown that access to spring light (Chapter 3) and the capacity to track climate change with spring leaf out phenology (Chapter 2) differs between species and that this mechanism can help account for carbon starvation dynamics expected under hotter and drier summers. The lack of a difference between species further indicates that seedling drought vulnerability is decoupled from adult vulnerability and suggests that future community assembly in temperate forests will not be strongly limited by the vulnerability of tree seedlings to drought. This puts a stronger importance on traits and behaviors that do differ between species and that could lead to differential outcome during climate change.

REFERENCES

Adams, H. A., M. J. B. Zeppel, W. R. Anderegg, and 59 other authors. 2017. A multi-species synthesis of physiological mechanisms in drought-induced tree mortality. *Nature Ecology & Evolution*, 1: 1285-1291. https://doi.org/10.1038/s41559-017-0248-x

Allen, C. D., D. D. Breshears, and N. G. McDowell. 2015. On underestimation of global vulnerability to tree mortality and forest die-off from hotter drought in the Anthropocene. *Ecosphere*, 6: 1-55. https://doi.org/10.1890/ES15-00203.1

Anderegg, W. R. L., T. Klein, M. Bartlett, L. Sack, A. F. A. Pellegrini, B. Choat, and S. Jansen. 2016. Meta-analysis reveals that hydraulic traits explain cross-species patterns of drought-induced tree mortality across the globe. *Proceedings in the National Academy of Science*, 113: 5024-5029. https://doi.org/10.1073/pnas.1525678113

Anderegg, W. R. L., A. Wolf, A. Arango-Velez, B. Choat, D. J. Chmura, S. Jansen, T. Kolb, S. Li, F. Meinzer, P. Pita, V. Resco de Dios, J. S. Sperry, B. R. Wolfe, and S. Pacala. 2017. Plant water potential improves prediction of empirical stomatal models. *PLoS ONE*, 12: e0185481. https://doi.org/10.1371/journal.pone.0185481

Bartlett, M. K., Y. Zhang, J. Yang, N. Kreidler, S.-W. Sun, L. Lin, Y.-H. Hu, K.-F. Cao, and L. Sack. 2016. Drought tolerance as a driver of tropical forest assembly: Resolving spatial signatures for multiple processes. *Ecology*, 97: 503-514. https://doi.org/10.1890/15-0468.1

Beckage, B., J. S. Clark, B. D. Clinton, and B. L. Haines. 2000. A long-term study of tree seedling recruitment in southern Appalachian forests: The effects of canopy gaps and shrub understories. *Canadian Journal of Forest Research*, 30: 1617-1631. https://doi.org/10.1139/x00-075

Boardman, N. K. 1977. Comparative photosynthesis of sun and shade plants. *Annual Review of Plant Physiology*, 28: 355-377. https://doi.org/10.1146/annurev.pp.28.060177.002035

Bréda, N., A. Granier, F. Barataud, and C. Moyne. 1995. Soil water dynamics in an oak stand: I. Soil moisture, water potentials and water uptake by roots. *Plant and Soil*, 172: 17-27. https://doi.org/10.1007/BF00020856

Bréda, N., R. Huc, A. Granier, and E. Dreyer. 2006. Temperate forest trees and stands under severe drought: A review of ecophysiological response, adaptation processes and long-term consequences. *Annals of Forest Science*, 63: 625-644. https://doi.org/10.1051/forest:2006042

Breshears, D. D., O. B. Myers, C. W. Meyer, F. J. Barnes, C. B. Zou, C. D. Allen, N. G. McDowell, and W. T. Pockman. 2008. Tree die-off in response to global change-type drought: Mortality insights from a decade of plant water potential measurements. *Frontiers in Ecology and the Environment*, 7: 185-189. https://doi.org/10.1890/080016

Canham, C. D. 1988. Growth and canopy architecture of shade-tolerant trees: Response to canopy gaps. *Ecology*, 69: 786-795. https://doi.org/10.2307/1941027

Cavender-Bares, J. and F. A. Bazzaz. 2000. Changes in drought response strategies with ontogeny in *Quercus rubra*: Implications for scaling from seedlings to mature trees. *Oecologia*, 124: 8-18. https://www.jstor.org/stable/4222661

Coates, K. D. 2002. Tree recruitment in gaps of various size, clearcuts and undisturbed mixed forest of interior British Columbia, Canada. *Forest Ecology and Management*, 155: 387-398. https://doi.org/10.1016/S0378-1127(01)00574-6

Coble, A. P., M. A. Vadeboncoeur, Z. C. Berry, K. A. Jennings, C. D. McIntire, J. L. Campbell, L. E. Rustad, P. H. Templer, and H. Asbjornsen. 2017. Are northeastern U.S. forests vulnerable to extreme drought? *Ecological Processes*, 6. https://doi.org/10.1186/s13717-017-0100-x

Cowan, I. R. and G. D. Farquhar. 1977. Stomatal function in relation to leaf metabolism and environment. *Symposia of the Society for Experimental Biology*, 31: 475-505.

Crow, T. R. 1988. Reproductive mode and mechanisms for self-replacement of Northern Red Oak (*Quercus rubra*) – A review. *Forest Science, 34*: 19-40. https://doi.org/10.1093/forestscience/34.1.19

Davies, W. J. and T. T. Kozlowski. 1977. Variations among woody plants in stomatal conductance and photosynthesis during and after drought. *Plant and Soil*, 46: 435-444. https://doi.org/10.1007/BF00010099

Dobrowski, S. Z., A. K. Swanson, J. T. Abatzoglou, Z. A. Holden, H. D. Safford, M. K. Schwartz, and D. G. Gavin. 2015. Forest structure and species traits mediate projected recruitment declines in western US tree species. *Global Ecology and Biogeography*, 24: 917-927. https://doi.org/10.1111/geb.12302

DuBois, M., K. A. Gilles, J. K. Hamilton, P. A. Rebers, and F. Smith. 1956. Colorimetric method for determination of sugars and related substances. *Analytical Chemistry* 28: 350-356.

Ellmore, G. S., A. E. Zanne, and C. M. Orians. 2006. Comparative sectoriality in temperate hardwoods: Hydraulics and xylem anatomy. *Botanical Journal of the Linnean Society*, 150: 61-71. https://doi.org/10.1111/j.1095-8339.2006.00510.x

Farquhar, G. D., S. von Caemmerer, & J. A. Barry. 1980. A biochemical model of photosynthetic CO2 assimilation in leaves of C3 species. *Planta*, 149: 78-90. https://doi.org/10.1007/BF00386231

Fisher, R., N. McDowell, D. Purves, P. Moorcroft, S. Sitch, P. Cox, C. Huntingford, P. Meir, and F. I. Woodward. 2010. Assessing uncertainties in a second-generation dynamic vegetation model caused by ecological scale limitations. *New Phytologist*, 187: 666-681. https://doi.org/10.1111/j.1469-8137.2010.03340.x

Gelman, A. and D. B. Rubin. 1992. Inference from iterative simulation. *Statistical Science*, 7: 457-511. https://doi.org/10.1214/ss/1177011136

Green, P. T., K. E. Harms, and J. H. Connell. 2014. Nonrandom, diversifying processes are disproportionately strong in the smallest size classes of a tropical forest. *Proceedings of the National Academy of Sciences*, 111: 18649-18654. https://doi.org/10.1073/pnas.1321892112

Grubb, P. J. 1977. The maintenance of species-richness in plant communities: The importance of the regeneration niche. *Biological Reviews*, 52: 107-145. https://doi.org/10.1111/j.1469-185X.1977.tb01347.x

Guo, J. S. and K. Ogle. 2019. Antecedent soil water content and vapor pressure deficit interactively control water potential in *Larrea tridentata*. *New Phytologist*, 221: 218-232. https://doi.org/10.1111/nph.15374

Handler, S., M. J. Duveneck, L. Iverson, and 42 other authors. 2014. Michigan forest ecosystem vulnerability assessment and synthesis: A report from the Northwoods Climate Change Response Framework. US Department of Agriculture, Forest Service, Northern Research Station, General Technical Report NRS-129, Newtown Square, PA. https://doi.org/10.2737/NRS-GTR-129

Harper, J. L. 1977. *Population Biology of Plants*. Academic Press. London, UK. ISBN 13: 9780123258502

Hochberg, U., F. E. Rockwell, N. M. Holbrook, and H. Cochard. 2018. Iso/Ansiohydry: A plant-environment interaction rather than a simple hydraulic trait. *Trends in Plant Science*, 23: 112-120. https://doi.org/10.1016/j.tplants.2017.11.002

Hoffman, W. A., R. M. Marchin, P. Abit, and O. L. Lau. 2011. Hydraulic failure and tree dieback are associated with high wood density in a temperate forest under extreme drought. *Global Change Biology*, 17: 2731-2742. https://doi.org/10.1111/j.1365-2486.2011.02401.x

Holmgren, M. 2003. Combined effects of shade and drought on tulip poplar seedlings: Trade-off in tolerance or facilitation? *Oikos*, 90: 67-78. https://doi.org/10.1034/j.1600-0706.2000.900107.x

Holmgren, M., L. Gómez-Aparicio, J. L. Quero, and F. Valladares. 2012. Non-linear effects of drought under shade: Reconciling physiological and ecological models in plant communities. *Oecologia*, 169: 293-305. https://doi.org/10.1007/s00442-011-2196-5

Ibáñez, I. and S. McCarthy-Neumann. 2014. Integrated assessment of the direct and indirect effects of resource gradients on tree species recruitment. *Ecology*, 95: 364-375. https://doi.org/10.1890/13-0685.1

Jacques, M.-H., L. Lapointe, K. Rice, R. A. Montgomery, A. Stefanski, & P. B. Reich. 2015. Responses of two understory herbs, *Maianthemum canadense* and *Eurybia macrophylla*, to experimental forest warming: Early emergence is the key to enhanced reproductive output. *American Journal of Botany*, 102: 1610-1624. https://doi.org/10.3732/ajb.1500046

Kannenberg, S. A., K. A. Novick, and R. P. Phillips. 2019. Anisohydric behavior linked to persistent hydraulic damage and delayed drought recovery across seven North American tree species. *New Phytologist*, 222: 1862-1872. https://doi.org/10.1111/nph.15699

Kannenberg, S. A. and R. P. Phillips. 2017. Soil microbial communities buffer physiological responses to drought stress in three hardwood species. *Oecologia*, 183: 631-641. https://doi.org/10.1007/s00442-016-3783-2

Kannenberg, S. A. and R. P. Phillips. 2020. Non-structural carbohydrate pools not linked to hydraulic strategies or carbon supply in tree saplings during severe drought and subsequent recovery. *Tree Physiology* 40: 259-271. https://doi.org/10.1093/treephys/tpz132

Kolb, K. J., J. S. Sperry, and B. B. Lamont. 1996. A method for measuring xylem hydraulic conductance and embolism in entire root and shoot systems. *Journal of Experimental Botany*, 47: 1805-1810. https://doi.org/10.1093/jxb/47.11.1805

Lebrija-Trejos, E., E. A. Pérez-García, J. A. Meave, F. Bongers, and L. Poorter. 2010. Functional traits and environmental filtering drive community assembly in a species-rich tropical system. *Ecology*, 91: 386-398. https://doi.org/10.1890/08-1449.1

Lei, T. T., & M. J. Lechowicz. 1990. Shade adaptation and shade tolerance in saplings of three *Acer* species from eastern North America. *Oecologia*, 84: 224-228. https://doi.org/10.1007/BF00318275

Lo Gullo, M. A., A. Nardini, P. Trifilò, and S. Salleo. 2005. Diurnal and seasonal variations in leaf hydraulic conductance in evergreen and deciduous trees. *Tree Physiology*, 25: 505-512. https://doi.org/10.1093/treephys/25.4.505

Loewenstein, N. J. and S. G. Pallardy. 1998. Drought tolerance, xylem sap abscisic acid and stomatal conductance during soil drying: A comparison of canopy trees of three temperate deciduous angiosperms. *Tree Physiology*, 18: 431-439. https://doi.org/10.1093/treephys/18.7.431

Lopez, O. R., T. A. Kursar, H. Cochard, and M. T. Tyree. 2005. Interspecific variation in xylem vulnerability to cavitation among tropical tree and shrub species. *Tree Physiology*, 25: 1553-1562. https://doi.org/10.1093/treephys/25.12.1553

Lunn, D., D. Spiegelhalter, A. Thomas, and N. Best. 2009. The BUGS project: Evolution, critique and future directions. *Statistics in Medicine*, 28: 3049-3067. https://doi.org/10.1002/sim.3680

Maguire, A. J. and R. K. Kobe. 2015. Drought and shade deplete nonstructural carbohydrate reserves in seedlings of five temperate tree species. *Ecology and Evolution*, 5: 5711-5721. https://doi.org/10.1002/ece3.1819

Markesteijn, L. and L. Poorter. 2009. Seedling root morphology and biomass allocation of 62 tropical tree species in relation to drought- and shade-tolerance. *Journal of Ecology*, 97: 311-325. https://doi.org/10.1111/j.1365-2745.2008.01466.x

Marshall, B. and P. V. Biscoe. 1980. A model for C3 leaves describing the dependence of net photosynthesis on irradiance. *Journal of Experimental Botany*, 31: 29-39. https://doi.org/10.1093/jxb/31.1.29

Martínez-Vilalta, J. and N. Garcia-Forner. 2016. Water potential regulation, stomatal behaviour and hydraulic transport under drought: Deconstructing the iso/anisohydric concept. *Plant, Cell & Environment*, 40: 962-976. https://doi.org/10.1111/pce.12846

Martínez-Vilalta, J., A. Sala, D. Asensio, L. Galiano, G. Hoch, S. Palacio, F. I. Piper, and F. Lloret. 2016. Dynamics of non-structural carbohydrates in terrestrial plants: A global synthesis. *Ecological Monographs*, 86: 495-516. https://doi.org/10.1002/ecm.1231

McDowell, N., W. T. Pockman, C. D. Allen, D. D. Breshears, N. Cobb, T. Kolb, J. Plaut, J. Sperry, A. West, D. G. Williams, and E. A. Yepez. 2008. Mechanisms of plant survival and mortality during drought: Why do some plants survive while others succumb to drought? *New Phytologist*, 178: 719-739. https://doi.org/10.1111/j.1469-8137.2008.02436.x

McDowell, N. G., D. J. Beerling, D. D. Breshears, R. A. Fisher, K. F. Raffa, and M. Stitt. 2011. The interdependence of mechanisms underlying climate-driven vegetation mortality. *Trends in Ecology & Evolution*, 26: 523-532. https://doi.org/10.1016/j.tree.2011.06.003

Meehl, G. A. and C. Tebaldi. 2004. More intense, more frequent, and longer lasting heat waves in the 21st century. *Science*, 305: 994-997. http://doi.org/10.1126/science.1098704

Múnne-Bosch, S. and L. Alegre. 2004. Die and let live: Leaf senescence contributes to plant survival under drought stress. *Functional Plant Biology*, 31: 203-216. https://doi.org/10.1071/FP03236

O'Brien, M. J., S. Leuzinger, C. D. Philipson, J. Tay, and A. Hector. 2014. Drought survival of tropical tree seedlings enhanced by non-structural carbohydrate levels. *Nature Climate Change*, 4: 710–714. https://doi.org/10.1038/nclimate2281

Ogasa, M., N. H. Miki, Y. Murakami, and K. Yoshikawa. 2013. Recovery performance in xylem hydraulic conductivity is correlated with cavitation resistance for temperate deciduous tree species. *Tree Physiology*, 33: 335-344. https://doi.org/10.1093/treephys/tpt010

Piper, F. I., and A. Fajardo. 2016. Carbon dynamics of *Acer pseudoplatanus* seedlings under drought and complete darkness. *Tree Physiology*, 36: 1400-1408. https://doi.org/10.1093/treephys/tpw063

Pittermann, J., J. S. Sperry, U. G. Hacke, J. K. Wheeler, and E. H. Sikkema. 2006. Inter-tracheid pitting and the hydraulic efficiency of conifer wood: the role of tracheid allometry and cavitation protection. *American Journal of Botany*, 93: 1265-1273. https://doi.org/10.3732/ajb.93.9.1265

Quentin, A. G., E. A. Pinkard, M. G. Ryan, D. T. Tissue, L. S. Baggett, and 55 other authors. 2015. Non-structural carbohydrates in woody plants compared among laboratories. *Tree Physiology*, 35: 1146-1165. https://doi.org/10.1093/treephys/tpv073

Quero, J. L., R. Villar, T. Marañón, and R. Zamora. 2006. Interactions of drought and shade effects on seedlings of four *Quercus* species: Physiological and structural leaf responses. *New Phytologist*, 170: 819-834. https://doi.org/10.1111/j.1469-8137.2006.01713.x

Reich, P. B. and T. M. Hinckley. 1989. Influence of pre-dawn water potential and soil-to-leaf hydraulic conductance on maximum daily leaf diffusive conductance in two oak species. *Functional Ecology*, 3: 719-726. https://www.jstor.org/stable/2389504

Roman, D. T., K. A. Novick, E. R. Brzostek, D. Dragoni, F. Rahman, and R. P. Phillips. 2015. The role of isohydric and anisohydric species in determining ecosystem-scale response to severe drought. *Oecologia*, 179: 641-654. https://doi.org/10.1007/s00442-015-3380-9

Rüger, N., A. Huth, S. P. Hubbell, and R. Condit. 2009. Response of recruitment to light availability across a tropical lowland rain forest community. *Journal of Ecology*, 97: 1360-1368. https://doi.org/10.1111/j.1365-2745.2009.01552.x

Sala, A., F. Piper, & G. Hoch. 2010. Physiological mechanisms of drought-induced tree mortality are far from being resolved. *New Phytologist*, 186: 274-281. https://jstor.org/stable/27797547

Sala, A., D. R. Woodruff, and F. C. Meinzer. 2012. Carbon dynamics in trees: Feast or famine? *Tree Physiology*, 32: 764-775. https://doi.org/10.1093/treephys/tpr143

Sevanto, S., N. G. McDowell, L. T. Dickman, R. Pangle, and W. T. Pockman. 2013. How do trees die? A test of the hydraulic failure and carbon starvation hypotheses. *Plant, Cell & Environment*, 37: 153:161. https://doi.org/10.1111/pce.12141

Sperry, J. S., J. R. Donnelly, and M. T. Tyree. 1988. Seasonal occurrence of xylem embolism in sugar maple (*Acer saccharum*). *American Journal of Botany*, 75: 1212-1218. https://doi.org/10.1002/j.1537-2197.1988.tb08834.x

Sperry, J. S., and M. T. Tyree. 1990. Water-stress-induced xylem embolism in three species of conifers. *Plant, Cell & Environment*, 13: 427-436. https://doi.org/10.1111/j.1365-3040.1990.tb01319.x

Sperry, J. S., U. G. Hacke, R. Oren, and J. P. Comstock. 2002. Water deficits and hydraulic limits to leaf water supply. *Plant, Cell & Environment* 25, 251-263. https://doi.org/10.1046/j.0016-8025.2001.00799.x

Spiegelhalter, D. J., N. G. Best, B. P. Carlin, And A. Van Der Linde. 2002. Bayesian measures of model complexity and fit. *Journal of the Royal Statistical Society: B*, 64: 583-639. https://doi.org/10.1111/1467-9868.00353

Thomas, D. S. and D. Eamus. 1999. The influence of predawn leaf water potential on stomatal responses to atmospheric water content at constant C_i and on stem hydraulic conductance and foliar ABA concentrations. *Journal of Experimental Botany*, 50: 243-251. https://doi.org/10.1093/jxb/50.331.243

Thomsen, J. E., G. Bohrer, A. M. Matheny, V. Y. Ivanov, L. He, H. J. Renninger, and K. V. R. Schäfer. 2013. Contrasting hydraulic strategies during dry soil conditions in *Quercus rubra* and *Acer rubrum* in a sandy site in Michigan. *Forests*, 4: 1106-1120. https://doi.org/10.3390/f4041106

Tjoelker, M. G., P. B. Reich, and J. Oleksyn. 2002. Changes in leaf nitrogen and carbohydrates underlie temperature and CO_2 acclimation of dark respiration in five boreal tree species. *Plant, Cell & Environment*, 22: 767-778. https://doi.org/10.1046/j.1365-3040.1999.00435.x

Trifilò, P., N. Kiorapostolou, F. Petruzzellis, S. Vitti, G. Petit, M. A. Lo Gullo, A. Nardini, and V. Casolo. 2019. Hydraulic recovery from xylem embolism in excised branches of twelve woody species: Relationships with parenchyma cells and non-structural carbohydrates. *Plant Physiology and Biochemistry*, 139: 513-520. https://doi.org/10.1016/j.plaphy.2019.04.013

Tyree, M. T., J. Alexander, and J.-L. Machado. 1992. Loss of hydraulic conductivity due to water stress in intact juveniles of *Quercus rubra* and *Populus deltoides*. *Tree Physiology*, 10: 411-415. https://doi.org/10.1093/treephys/10.4.411

Urli, M., A. J. Porté, H. Cochard, Y. Guengant, R. Burlett, and S. Delzon. 2013. Xylem embolism threshold for catastrophic hydraulic failure in angiosperm trees. *Tree Physiology*, 33: 672-683. https://doi.org/10.1093/treephys/tpt030

Williams, L. E. and F. J. Araujo. 2002. Correlations among predawn leaf, midday leaf, and midday stem water potential and their correlations with other measures of soil and plant water status in *Vitis vinifera*. *Journal of the American Society for Horticultural Science*, 127: 448-454. https://doi.org/10.1093/jxb/50.331.243

Wilson, K. B., D. D. Baldocchi, and P. J. Hanson. 2000. Quantifying stomatal and non-stomatal limitations to carbon assimilation resulting from leaf aging and drought in mature deciduous tree species. *Tree Physiology*, 20: 787-797. https://doi.org/10.1093/treephys/20.12.787

Wright, S. J., H. C. Muller-Landau, R. Condit, and S. P. Hubbell. 2003. Gap-dependent recruitment, realized vital rates, and size distributions of tropical trees. *Ecology*, 84: 3174-3185. https://doi.org/10.1890/02-0038

Table 4.1 – Xylem conductivity ANOVA statistics

ANOVA statistics describing the differences in xylem conductivity between all four factorial treatments (a) and the differences between drought treatments (b) for seedlings of both species. Drought treatment *A. saccharum* seedlings were not available to be used in this analysis and are thus excluded.

(a)	**Df**	**Sum Sq.**	**Mean Sq.**	**F value**	**Pr(>F)**
A. saccharum	1	$7.5*10^{-6}$	$7.5*10^{-6}$	0.015	0.906
Q. rubra	3	$3.45*10^{-3}$	$1.15*10^{-3}$	3.307	0.087
(b)	**Df**	**Sum Sq.**	**Mean Sq.**	**F value**	**Pr(>F)**
A. saccharum	-	-	-	-	-
Q. rubra	1	$3.37*10^{-3}$	$3.37*10^{-3}$	12.1	*0.007*

Figure 4.1 – Leaf water potential over course of experiment

Predawn plant water potential (Ψ_{PD}) plotted over the duration of the experiment for *A. saccharum* (a) and *Q. rubra* seedlings (b).

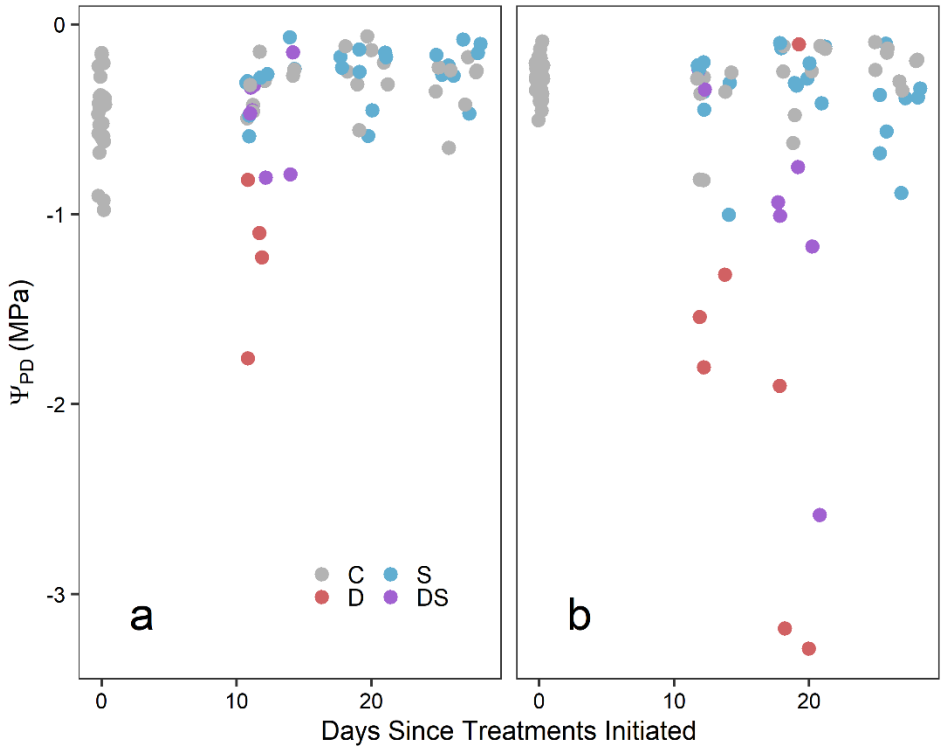

Figure 4.2 – Changes in Amax over gradient of leaf water potential

a-b) Observed (points) and modeled (lines) relationship between Ψ_{PD} and maximum photosynthetic capacity (A_{max}) for *A. saccharum* (a) and *Q. rubra* seedlings (b). Dashed lines represent 95% predictive intervals. c-d) Posterior estimated means (± 95% credible intervals) for the intercept parameter β1 (c) and the decay parameter β2 (d) relating Ψ_{PD} to A_{max}. Parameters β2 are considered significantly positive if the 95% credible intervals (CI) do not overlap with zero. Light treatments are considered different from each other (c-d) if their 95% CI do not overlap.

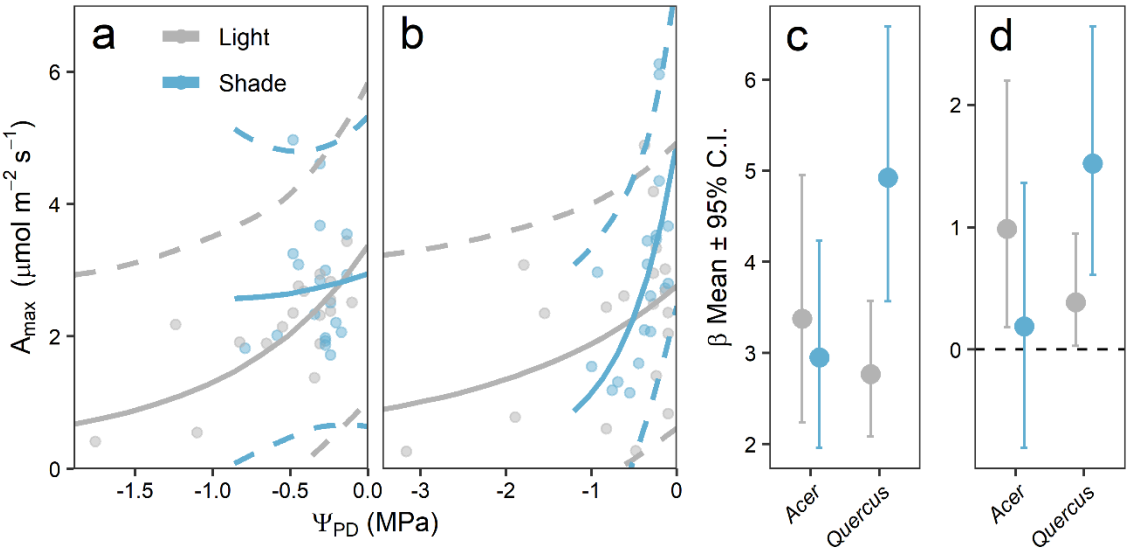

Figure 4.3 – Differences in NSC glucose concentrations between treatments

NSC (Non-structural carbohydrate) glucose concentrations (means + 2 s.d.) for *A. saccharum* (a-d) and *Q. rubra* seedlings (e-h) across the four experimental treatments. Rows show concentrations of NSC_{Glu} in leaf (a, e), stem (b, f), and root (c, g) pools as well as concentration of NSC_{Glu} averaged across all pools and weighted by dry mass of each pool (d, h). Horizontal lines indicate means (solid) ± 2 s.d. (dashed) of NSC_{Glu} in seedlings harvested prior to the initiation of treatments.

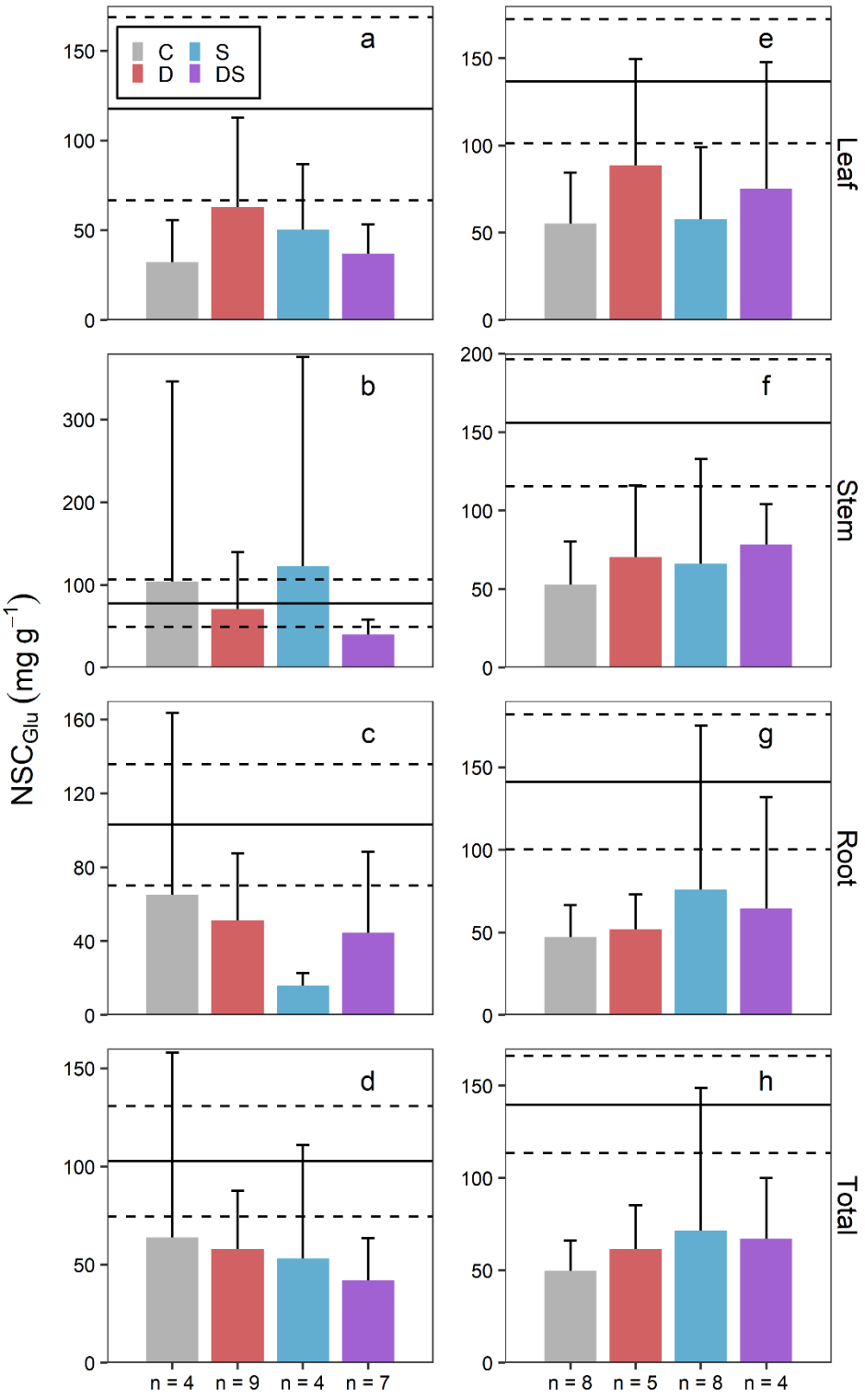
C
S
D
DS
a
b
c
d
e
f
g
h
Leaf
Stem
Root
Total
NSC$_{Glu}$ (mg g^{-1})
n = 4
n = 9
n = 4
n = 7
n = 8
n = 5
n = 8
n = 4

Figure 4.4 – Xylem conductivity over gradient of leaf water potential

Xylem conductivity (k) for *A. saccharum* (a) and *Q. rubra* seedlings (b) plotted by pre-dawn plant water potential (Ψ_{PD}). These plots show data from across all three harvests for seedlings that were recorded as alive at time of harvest.

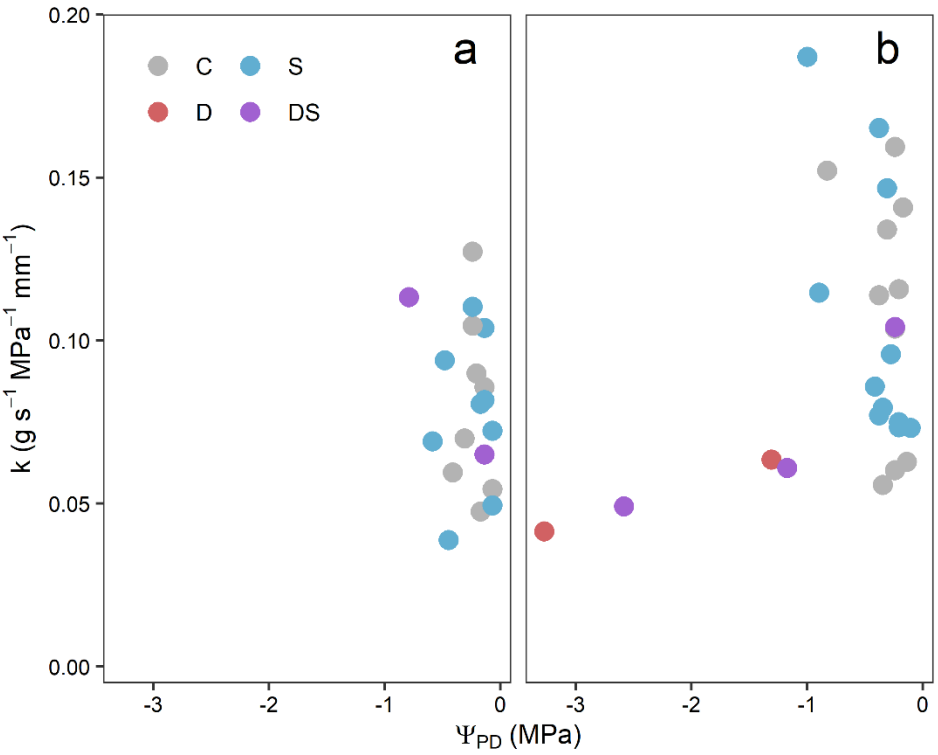

SUPPORTING INFORMATION

Supporting Information 4.1 – Seed source information

Initial seedling height of seedlings from the northern seed sources was significantly greater than initial height of seedlings from southern seed source for both species (Fig. SI 4.10; $Pr(>F) < 0.05$ for one-way ANOVAs ran separately for each species). However, there were no significant maternal effects in any of our analyses, suggesting that these differences in initial height do not play a large role in hydraulic strategies. Seedling dry mass at time of harvest was significantly greater for *A. saccharum* from northern seed sources, but there was no significant difference between *Q. rubra* seed sources (Fig. SI 4.11). *Quercus* seedling mass was more heavily concentrated in the roots whereas *A. saccharum* seedling mass was evenly distributed between leaves and roots (Fig. SI 4.11). Stem mass made up the least amount of the total mass for both species.

Supporting Information 4.2 - Supplemental Tables and Figures

Table SI 4.2 – Amax model parameter estimates

Posterior parameter estimates of means and 95% credible intervals in the exponential A_{max} models.

		A. saccharum		*Q. rubra*	
		mean	**95% CI**	**mean**	**95% CI**
β1	Light	3.38	2.24, 4.95	2.77	2.09, 3.57
	Shade	2.95	1.96, 4.23	4.92	3.56, 6.58
β2	Light	0.987	0.184, 2.20	0.387	0.0298, 0.949
	Shade	0.190	-0.802, 1.36	1.52	0.609, 2.64
$\tau = 1/\sigma^2$	(total model)	0.952	0.656, 1.30		

Table SI 4.3 – ANOVA summary statistics for differences in NSC

ANOVA statistics for treatment effects on NSC pools for *A. saccharum* (a) and *Q. rubra* seedlings (b).

(a)	**Df**	**Sum Sq.**	**Mean Sq.**	**F value**	**Pr(>F)**
Leaf	3	3844	1281	0.677	0.576
Stem	3	21009	7003	0.661	0.586
Root	3	5342	1780	0.831	0.492
Combined	3	1521	507.1	0.342	0.795
(b)	**Df**	**Sum Sq.**	**Mean Sq.**	**F value**	**Pr(>F)**
Leaf	3	4413	1471	0.74	0.54
Stem	3	2029	676.4	0.246	0.863
Root	3	3764	1255	0.243	0.865
Combined	3	2068	689.2	0.223	0.879

Figure SI 4.5 – NSC concentration plotted over time

Non-structural glucose concentrations averaged across all tissue pools for *A. saccharum* (a) and *Q. rubra* seedlings (b), plotted by days since the initiation of treatment.

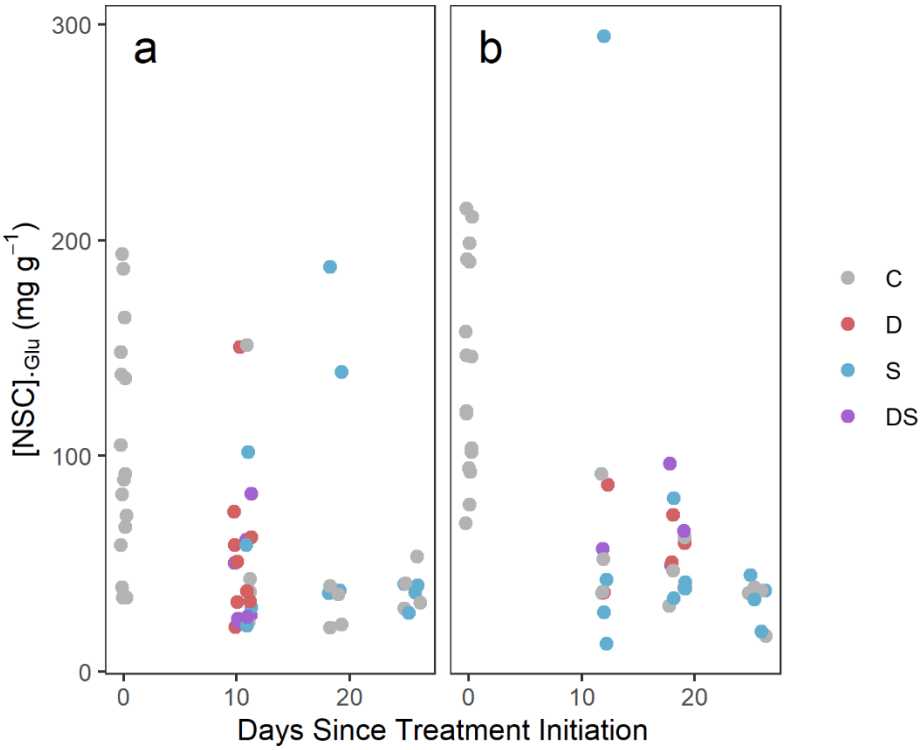

Figure SI 4.6 – Greenhouse environmental conditions

Average daytime light levels (a) and average daily temperature (b) experienced by tree seedlings. The vertical line represents the day the treatments were initiated, with line colors representing control (C), drought (D), shade (S), and drought + shade (DS) treatments.

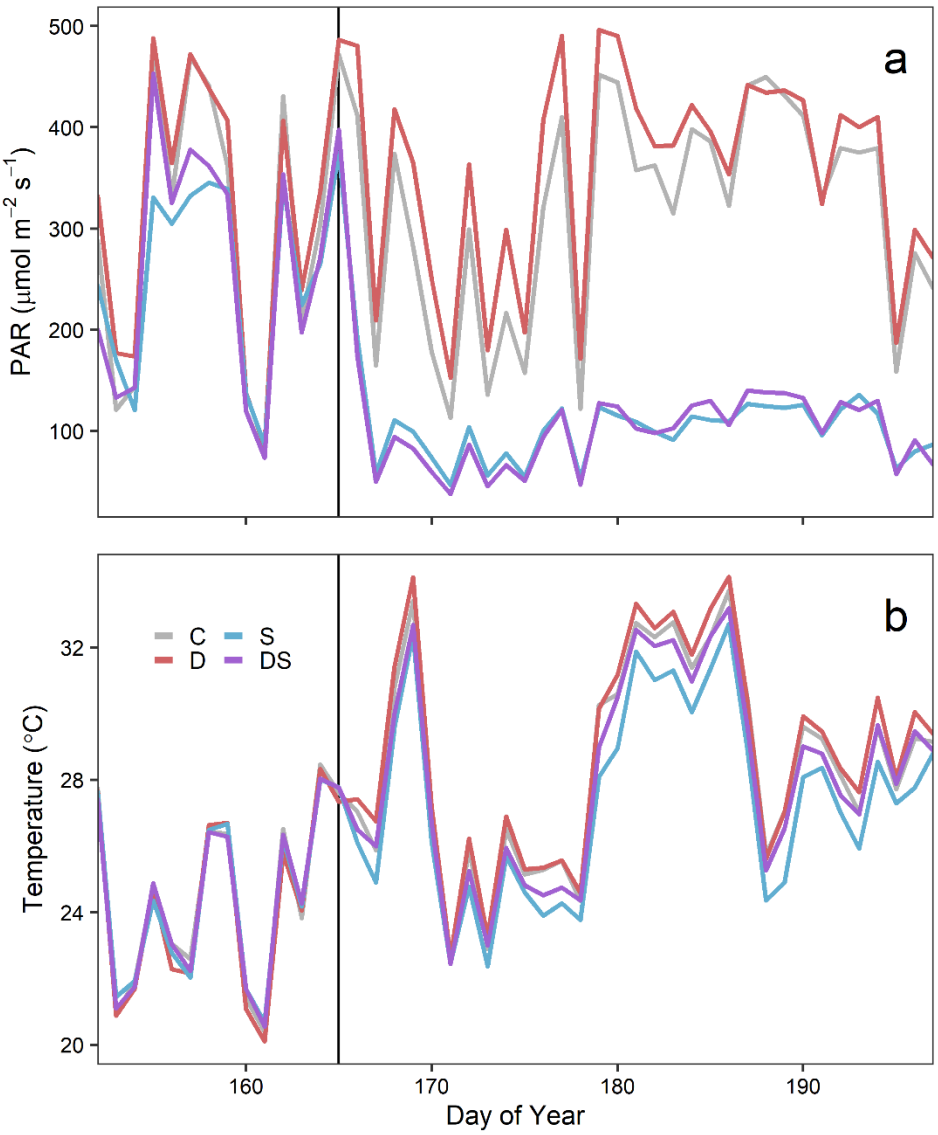

Figure SI 4.7 – Greenhouse temperature variability

Average daily temperature (solid lines) measured over the course of the experiment with dashed lines showing the minimum and maximum daily temperatures. Colors represent different drought and shade treatments and the vertical line shows the day of treatment initiation.

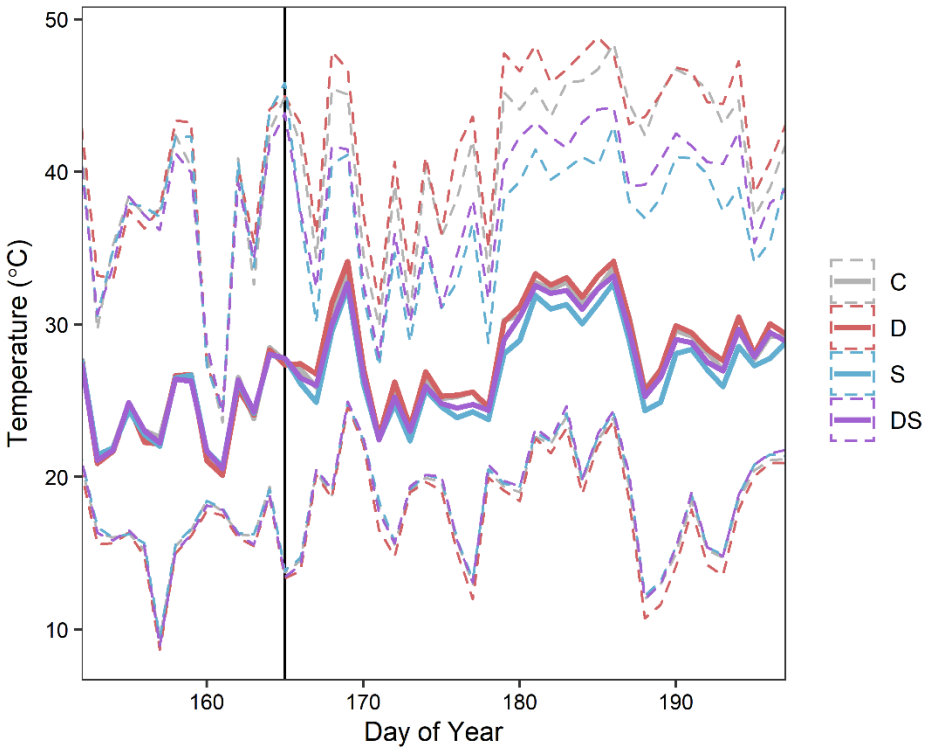

Figure SI 4.8 – Differences in xylem conductivity by treatment

Boxplots showing the xylem conductivity for *A. saccharum* (a) and *Q. rubra* seedlings (b) that were recorded as alive at the time of the second harvest (n = 4, 0, 4, 0 for *A. saccharum* seedlings and n = 3, 1, 4, 3 for *Q. rubra* seedlings in treatments C, D, S, and DS, respectively). Colors indicate experimental treatment: control (C; grey), drought (D, red), shade (S, blue), and combined drought and shade (DS, purple).

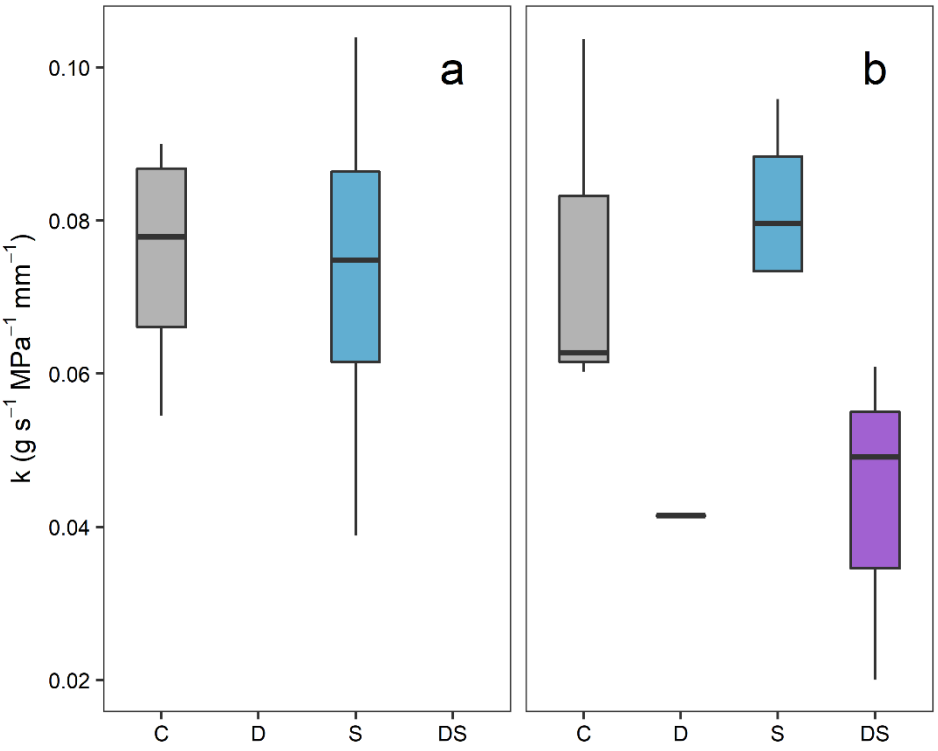

Figure SI 4.9 – Differences in xylem conductivity by drought

Boxplots showing the xylem conductivity for *A. saccharum* (a) and *Q. rubra* seedlings (b) that were recorded as alive at the time of the second harvest (n = 8 and 0 for *A. saccharum* seedlings and n = 7 and 4 for *Q. rubra* seedlings in combined C and S or D and DS treatments, respectively).

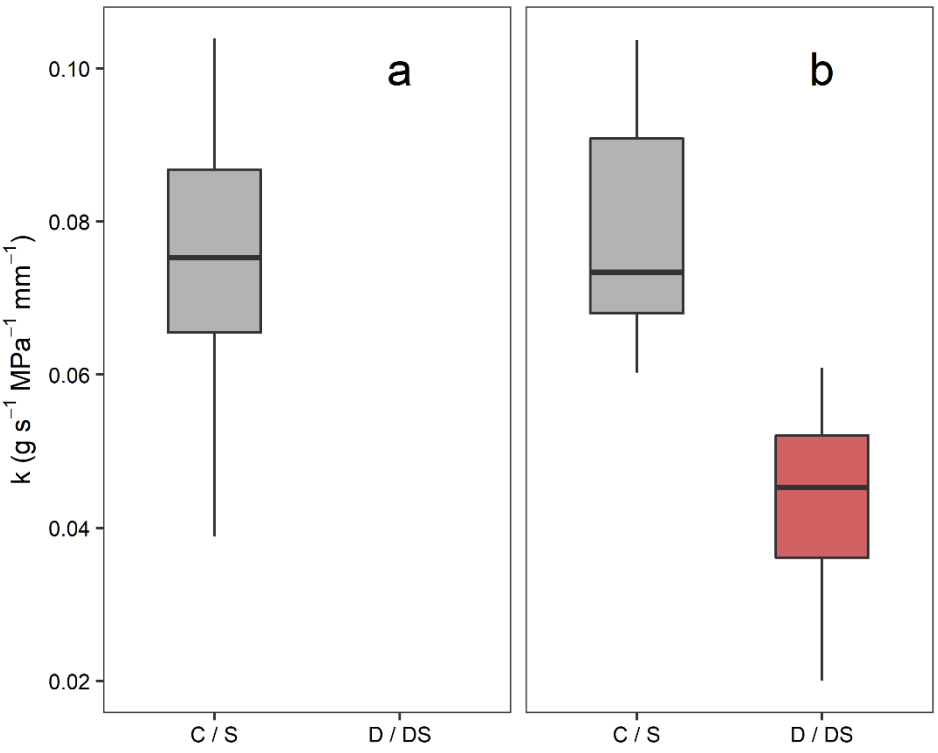

Figure SI 4.10 – Seedling initial height by seed source

Initial height of *A. saccharum* and *Q. rubra* seedlings at time of harvest, separated by mass of leaves, stem, and roots. Dry mass is shown for seedlings of both species that were grown from either northern (N) or southern (S) seed sources.

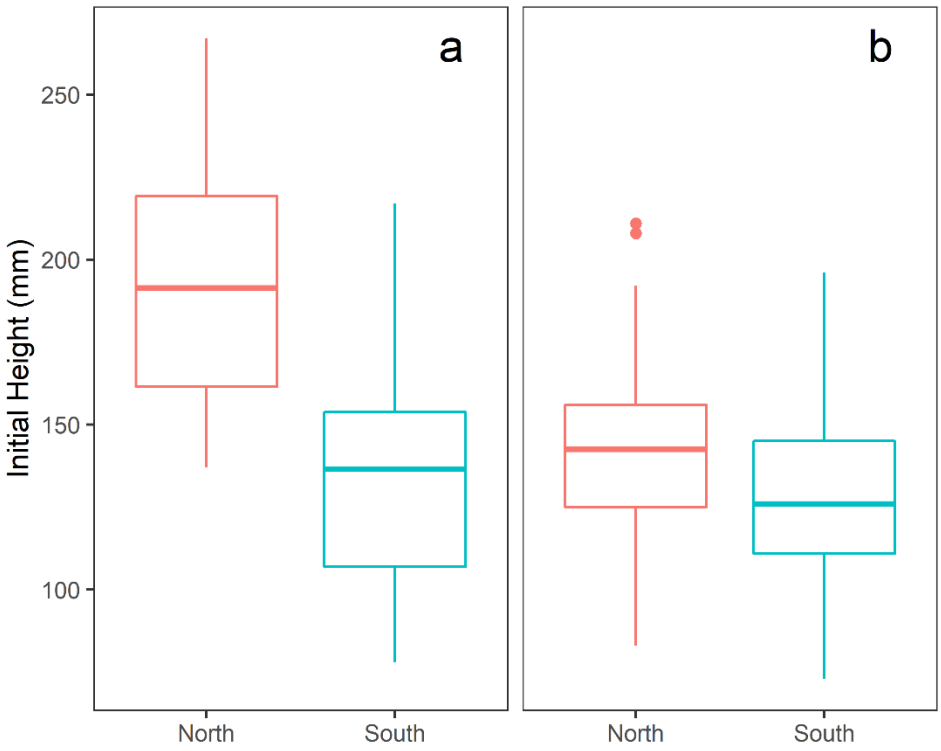

Figure SI 4.11 – Dry mass at time of harvest by seed source

Dry mass of *A. saccharum* and *Q. rubra* seedlings at time of harvest, separated by mass of leaves, stem, and roots. Dry mass is shown for seedlings of both species that were grown from either northern (N) or southern (S) seed sources.

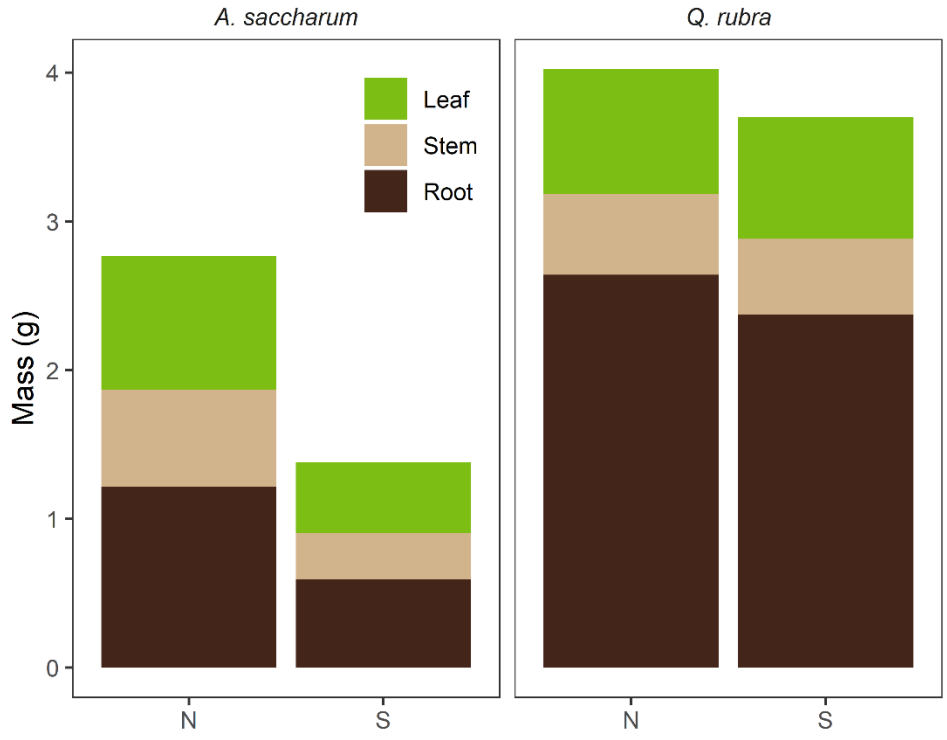

Chapter 5 Conclusions

In this dissertation, I used a combination of field and greenhouse experiments to investigate and predict the effects that climate change may have on temperate tree recruitment for two species that commonly co-occur across a wide range of eastern North America. In Chapter 2, I investigated the relationship between climate drivers and leaf-out phenology of seedlings and of the surrounding canopy and found that seedlings may track climate better than adult trees and are therefore likely to gain access to spring light availability under climate change scenarios. I found that, despite the increase in spring carbon assimilation associated with this increase in access to light, seedlings of both species are projected to assimilate less carbon in the future due to high respiration costs caused by predicted hotter and drier summers. This chapter emphasizes the importance of phenological escape in maintaining positive carbon status for these seedlings. In Chapter 3, I combined phenology and leaf area measurements collected for individual seedlings with the photosynthetic model parameters calculated in Chapter 2 and detailed microclimate data to estimate annual carbon assimilation at the individual level and use it to predict seedling demographic performance (growth and survival). I found that carbon assimilation was significantly associated with both processes, suggesting that the reduced assimilation predicted in Chapter 2 will cause reductions in seedling recruitment performance under climate change. Importantly, the results from this chapter showed that predicted changes in performance may be less dire when phenology shifts are accounted for, highlighting the potential importance of this mechanism in mitigating some of the negative effects of climate change. Finally, in Chapter 4, I conducted a greenhouse dry-down experiment to quantify the hydraulic

response of seedlings to drought to estimate whether species will experience differential performance as a result of climate change predicted in my study region. I found little to differentiate between species responses, despite the differences observed for adults of these two species in the literature. This suggests that recruitment of these two species may not be as different as expected given their adults' hydraulic performance under drought and implies that differences in performance of these two species under climate change will be driven by other mechanisms such as those covered in Chapters 2 and 3.

The results of my dissertation demonstrate the importance of phenological escape in the recruitment of temperate deciduous tree species, a novel mechanism that has only recently been studied in spring ephemeral wildflowers (Heberling et al. 2019). Furthermore, my research contextualizes phenological escape with respect to climate change and provides the model parameterization needed to predict seedling recruitment under a wide range of possible climate change scenarios.

The core contribution of my work is in demonstrating that climate change will likely affect species differently depending on their ability to maintain phenological escape in spring, but other findings of mine are of potential interest to other areas of plant ecology. In Chapter 2 I found that the performance of my photosynthesis model was improved by the inclusion of soil moisture and vapor pressure deficit as covariates, demonstrating the importance of water availability to seedling carbon assimilation. I then demonstrated in Chapter 3 that reductions in carbon assimilation associated with reduced water availability will likely have profound effects on seedling demography that are only partially ameliorated by projected increased access to spring light.

In Chapter 4, however, I found few differences between species with respect to the strategies they use to respond to drought, despite the hypothesized differences suggested by hydraulic strategies used by adults. Together, these results suggest that seedlings are equivalently susceptible to death from hydraulic failure and that, therefore, the most important drought effects with respect to differential seedling performance may involve reductions in carbon assimilation and depletion of non-structural carbohydrates that exacerbate the negative effects of mid-seasonal shade. Specifically, my results suggest that access to light will be the primary driver of temperate seedling mortality for these two species (Chapter 3), but the effects of shading will likely be affected by drought controls on photosynthetic activity during the middle of the growing season (Chapter 2). This is an important finding that may explain some of the variability in the importance of non-structural carbohydrate reductions found in a recent meta-analysis that evaluated global patterns of tree mortality in response to drought (Adams et al. 2017).

My results also suggest that the interactions between biological and environmental drivers of tree mortality will be important in predicting future tree recruitment. In Chapter 2 I found strong reductions in carbon assimilation for seedlings of both species when planted next to *Quercus rubra* canopy tree compared to when planted next to *Acer saccharum* adults. I speculate that this result is caused by differences in leaf nitrogen content arising from higher N mineralization rates (Finzi et al. 1998, Phillips and Fahey 2006) and higher organic N content (McCarthy-Neumann and Ibáñez 2012) that have been previously documented in soils collected from beneath *Q. rubra* trees. Soil nitrogen has recently been linked to leaf nitrogen content (Tang et al. 2019), and in turn leaf nitrogen concentration has been found to correlate with respiration rates (Reich et al. 1998, Cannell and Thornley 2000), so it is possible that increases in respiration costs observed in our study are evidence of this dynamic. However, I did not measure

soil or leaf nitrogen content and further research is therefore required to provide more substantial support to this speculation.

Finally, and perhaps most importantly, my results showcase the negative consequences that climate change will have on temperate tree recruitment irrespective of phenological escape or hydraulic response to drought. In Chapters 2 and 3 I found strong projected reductions in carbon assimilation and seedling performance for both species under an extreme climate change scenario that represented predicted climate conditions in the year 2100 if there is no change to current global carbon emissions (the A1FI scenario used by the IPCC Global Assessment). Our conservative climate change scenario assumes the invention and utilization of green energy sources and a global reduction in carbon emissions by 2100 (IPCC B1 scenario). Although realized climate conditions are likely to fall somewhere in between these two scenarios (Hausfather and Peters 2020), the increasing frequency at which previous climate change forecasting has been recently proved correct (Hausfather et al. 2019) causes concern that these two species will have difficulty recruiting into temperate forests. Without immediate and dramatic reductions in global carbon emissions, temperate forests could look very different than they do today.

REFERENCES

Adams, H. A., M. J. B. Zeppel, W. R. Anderegg, and 59 other authors. 2017. A multi-species synthesis of physiological mechanisms in drought-induced tree mortality. *Nature Ecology & Evolution*, 1: 1285-1291. https://doi.org/10.1038/s41559-017-0248-x

Cannell, M. G. R. and J. H. M. Thornley. 2000. Modelling the components of plant respiration: Some guiding principles. *Annals of Botany*, 85: 45-54. https://doi.org/10.1006/anbo.1999.0996

Finzi, A. C., N. Van Breemen, and C. D. Canham. 1998. Canopy tree-soil interactions within temperate forests: Species effects on soil carbon and nitrogen. *Ecological Applications*, 8: 440-446. https://doi.org/10.1890/1051-0761(1998)008[0440:CTSIWT]2.0.CO;2

Hausfather, Z., H. F. Drake, T. Abbott, and G. A. Schmidt. 2019. Evaluating the performance of past climate model projections. *Geophysical Research Letters*, 47: e2019GL085378. https://doi.org/10.1029/2019GL085378

Hausfather, Z. H. and G. P. Peters. 2020. Emissions – the 'business as usual' story is misleading. *Nature*, 577: 618-620. https://10.1038/d41586-020-00177-3

Heberling, J. M., C. M. MacKenzie, J. D. Fridley, S. Kalisz, and R. B. Primack. 2019. Phenological mismatch with trees reduces wildflower carbon budgets. *Ecology Letters*, 22: 616-623. https://doi.org/10.1111/ele.13224

McCarthy-Neumann, S. and I. Ibáñez. 2012. Tree range expansion may be enhanced by escape from negative plant-soil feedbacks. *Ecology*, 93: 2637-2649. https://doi.org/10.1890/11-2281.1

Phillips, R. P. and T. J. Fahey. 2006. Tree species and mycorrhizal associations influence the magnitude of rhizosphere effects. *Ecology*, 87: 1302-1313. https://doi.org/10.1890/0012-9658(2006)87[1302:TSAMAI]2.0.CO;2

Reich, P. B., M. B. Walters, D. S. Ellsworth, J. M. Vose, J. C. Volin, C. Gresham, and W. D. Bowman. 1998. Relationships of leaf dark respiration to leaf nitrogen, specific leaf area and leaf life-span: A test across biomes and functional groups. *Oecologia*, 114: 471-482. https://doi.org/10.1007/s004420050471

Tang, J., B. Sun, R. Cheng, Z. Shi, D. Luo, S. Liu, and M. Centritto. 2019. Effects of soil nitrogen (N) deficiency on photosynthetic N-use efficiency in N-fixing and non-N-fixing tree seedlings in subtropical China. *Nature Scientific Reports*, 9: 4604. https://doi.org/10.1038/s41598-019-41035-1